URBAN GROWTH SIMULATION USING REMOTE SENSING, GIS, AND SLEUTH URBAN MODEL IN GELEPHU CITY, BHUTAN.

LOBZANG TOBGYE

A Thesis Submitted to the Graduate School of Naresuan University
in Partial Fulfillment of the Requirements
for the Master of Science in (Geographic Information Science)
2019

URBAN GROWTH SIMULATION USING REMOTE SENSING, GIS, AND SLEUTH URBAN MODEL IN GELEPHU CITY, BHUTAN.

LOBZANG TOBGYE

A Thesis Submitted to the Graduate School of Naresuan University
in Partial Fulfillment of the Requirements
for the Master of Science in (Geographic Information Science)
2019

Thesis entitled "Urban growth simulation using remote sensing, GIS, and SLEUTH urban model in Gelephu City, Bhutan."

By LOBZANG TOBGYE

has been approved by the Graduate School as partial fulfillment of the requirements for the Master of Science in Geographic Information Science of Naresuan University

Oral Defense Committee

..... Chair
(Dr. Chudech Losiri, Ph.D.)

..... Advisor
(Assistant Professor Kampanart Piyathamrongchai, Ph.D.)

..... Internal Examiner
(Assistant Professor Sittichai Choosumrong, Ph.D.)

Approved

.....
(Professor Paisarn Muneesawang, Ph.D.)

for Dean of the Graduate School

Title URBAN GROWTH SIMULATION USING REMOTE SENSING, GIS, AND SLEUTH URBAN MODEL IN GELEPHU CITY, BHUTAN.

Author LOBZANG TOBGYE

Advisor Assistant Professor Kampanart Piyathamrongchai, Ph.D.

Academic Paper Thesis M.S. in Geographic Information Science, Naresuan University, 2019

Keywords Cellular automata, Gelephu city, SLEUTH model, Urban growth

ABSTRACT

Urbanization is one of the most evident global changes. Gelephu city under Sarpang Dzongkhag has experienced rapid urbanization over the past decades. The number of people living in urban areas has drastically increased mainly arising from natural population growth and rural-urban migration along with socio-economic development. This ultimately leads to the unplanned and uncontrolled urban expansion causing an irreversible change of urban landscape posing great threats to natural environments.

The primary objective of the research was to apply remote sensing and geographic information system technology with the integration of cellular automata (CA) based SLEUTH urban growth model to simulate the urban expansion and evaluate the urban growth factors through the development of future growth scenarios. The model was calibrated with historical data for the period 1990-2017, extracted from a time series of satellite images. The dataset consists of four historical urban extents (1990, 2000, 2010, and 2017), two land-use layers (1990, 2017), two transportation layers (1990, 2017), slope layer, hillshade layer, and urban excluded layers.

Three specific scenarios were designed to simulate the spatial growth consequences of urban growth under different land-use conditions. The first scenario is to simulate the unmanaged growth in business as usual (BAU) scenario with no

restriction on land use categories except water bodies. The second scenario is to project the managed growth scenario (MGS) trend by taking into consideration of moderate environmental protection, specifically for forest land and open spaces. The last scenario is to simulate the compact growth scenario (CGS) with maximum protection. It was found that altering the level of growth protection in the urban exclusion layer for different land-use types patently affects the growth changes in the region. In the BAU scenario, it is estimated to gain approximately 26 sq.km of urban land by 2047, which is twice the current urban area in 2017. Approximately, 9 sq.km of the resources could be saved by the third scenario, compact growth with maximum growth protection of (80 percent) was applied. However, the growth seems to be highly underestimated in the areas which have high growth probability. The second scenario was found to be the ideal growth scenario in the current study area where moderate growth protection (50 percent) was applied. Though the scenario consumes 23 sq.km of urban land by 2047, it attempts to save the limited agriculture land and facilitate future growth in a much-sustained manner considering the topography of the region.

Findings suggest that the SLEUTH model can be applied successfully and produce a realistic projection of urban growth that it can assist urban planner and policymakers to establish proper urban planning as a decision-support tool for sustainable development.

ACKNOWLEDGEMENTS

This is a great opportunity to express my deep and sincere gratitude to all the people who have supported me and contributed to my research.

Firstly, I would like to acknowledge the Royal Government of Bhutan (RGoB) and Thailand International Cooperation Agency (TICA) under Royal Thai Government for awarding me the scholarship in M.Sc Program in Geographic Information Science.

My deepest respect and immense thanks to my Advisor Dr. Kampanart Piyathamrongchai, Assistant Professor, Faculty of Agriculture Natural Resources and Environment, who has supervised this research. I would not have completed my research without his constant guidance and support at various stages. His patient and meticulous guidance and suggestions are indispensable to the completion of my research.

I would like to extend my gratitude to the thesis committee members: Dr. Chudech Losiri (Chairperson), Assistant Professor, Dr. Kampanart Piyathamrongchai and Assistant Professor, Dr. Sittichai Choosumrong (Committee members) for their valuable comments and suggestions that improved my research.

I thank all the relevant agencies and departments of RGoB for sharing the spatial data required in my research. In particular, I would like to thank my agency National Land Commission Secretariat (NLCS) for support and encouragement to pursue the study.

Last but not the least, I would like to thank all my family members for their unwavering support throughout my study period, especially my wife who constantly gave moral support and shoulder the family responsibilities in my absence. Finally, I also would like to thank the Naresuan University for facilitating necessary resource materials during my entire study period.

LOBZANG TOBGYE

TABLE OF CONTENTS

Page

List of tables

Page

List of figures

Page

ABBREVATION AND DEFINITIONS

SLEUTH	Slope, Land use, Exclusion, Urban extent, Transportation, and Hillshade
LULC	Land use Land cover
UGM	Urban growth model
LCD	Land Cover Deltatron. It is the sub-component of the SLEUTH model that attempts to change the land use/cover class of the immediate neighborhood. Deltatron is an artificial “agent” of change that has “life” in change space whenever land cover transition takes place.
HGS	Historical Growth Scenario or Business as usual (BAU) scenario. It is the scenario developed for future urban growth of the city. This scenario assumes the urban growth and development that would continue along historical trends without applying any restrictions in current growth trend apart from water bodies and agriculture land which acts as a constraints.
MGS	Managed Growth Scenario. This scenario defines the future urban growth through moderate protection on environment and open space area which are available for urban growth.
CGS	Compact Growth Scenario. This scenario represents the maximum growth constraints applied compared with previous two growth scenarios.
CA	Cellular Automata
UN	United Nations
IHDP	International Human Dimensions Programme
IGBP	International Geosphere-Biosphere Programme

GIS	Geographic Information System
TM	Thematic Mapper (LANDSAT's sensor)
ETM +	Enhanced Thematic Mapper plus (LANDSAT's sensor)
OLI/TIR	Operational Land Imager & Thermal Infrared Sensor (LANSAT 8 sensors)
GIF	Graphics Interchange Format
USGS	United States Geological Survey
OSM	Optimal SLEUTH metrics

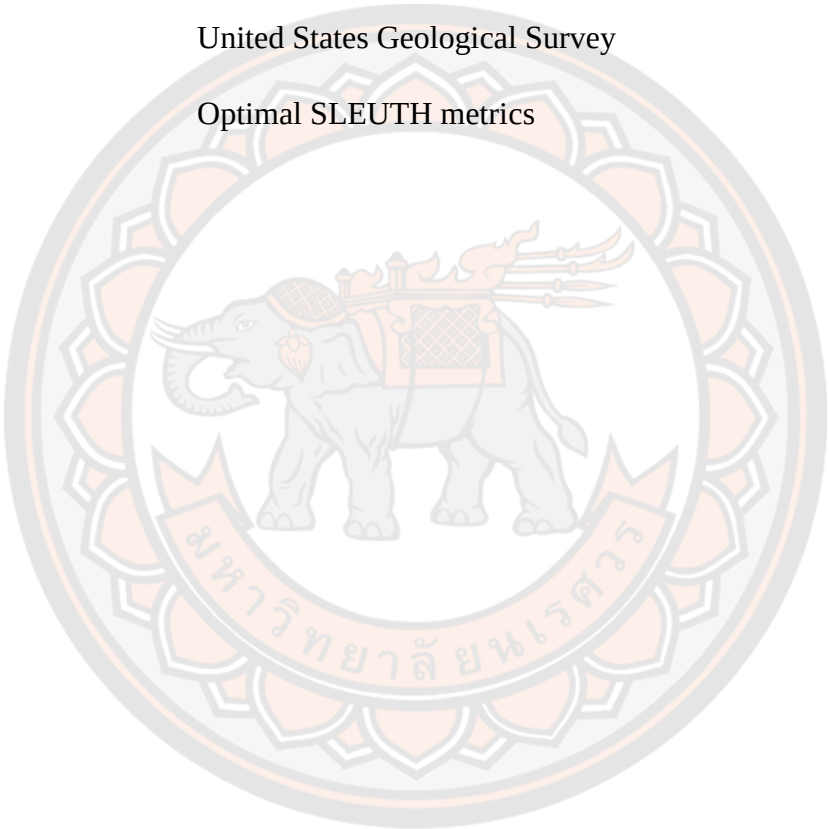

มหาวิทยาลัยนเรศวร

CHAPTER I

INTRODUCTION

This research seeks to explore the simulation of urban growth phenomenon using the cellular automata (CA) based SLEUTH urban growth model. SLEUTH is the acronym for the input data required to run the model: Slope, Land use, Exclusion, Urban extent, Transportation , and Hillshade (Dietzel & Clarke, 2006). The model is a well-known CA-based urban growth model coupled with land cover change model (Clarke et al., 1997), which can simulate urban growth on historical trends with urban and non-urban data under different development conditions. The main purpose of this study is to evaluate the future urban growth scenarios using remote sensing satellite images and SLEUTH urban growth model. It also seek to examine the urban growth parameters and assess the results obtained from the model calibration and prediction. Moreover, the study drives to demonstrate the effectiveness of model in a different geographical urban setting like Bhutan. It was anticipated that the information generated from this research would mitigate the urban development and approach to plans and policies of the city. This chapter begins with a background and significance that frames the study. Following this is the Statement of the problem, Research questions, Aims and objectives of the study, Scope, and Limitation of the study. The chapter concludes with outlining the succeeding research chapters.

Background and significance of the study

The number of people living in urban areas has drastically increased over the past few decades. According to a recent world urbanization prospects report by the United Nations (UN), over more than half of the world's population (55 percent) live in urban areas, and this number is expected to increase to 68 percent by 2050. The rapid growth of urban population from 751 million in 1950 to 4.2 billion in 2018 underscore the need to understand the key trends in urbanization for effective management of urban growth mainly in developing countries where the pace of urbanization is projected to be the fastest (United Nations, 2018).

It is important to know the urban growth and change which is critical to both city planners and decision-makers in this rapidly changing environments (Oguz et al., 2007). Recently the study on urban growth has gained attention among many researchers not only in a global context but at regional and local levels. This is mainly due to irreversible changes in the landscape, especially the natural vegetation. The rapid urban growth mostly depends upon the city requirement, facilities available and industrialization in the area (KantaKumar et al., 2011).

Urbanization in Bhutan is not a recent phenomenon. It started since 1961 with the implementation of the first five-year development plan in the country. Since then considerably growth has happened especially in urban area. Currently, Bhutan has a total population of over seven lakh, of which 37.8 % constitutes the urban population. It has been predicted that the total population will cross 800,000 by 2047, while the half of the population will be living in urban areas by 2037 (National Statistics Bureau, 2018). This means the urbanization level will continue to grow in the country and reported to have an over 7% increase in the current study area of Sarpang District by 2047. Currently, Bhutan occupies an area of over 38,000 square kilometers of which only 0.2% of built-up and 2.75 % of cultivated agriculture land available in the country. The constitution of the Kingdom of Bhutan mandates that a minimum of 60% of Bhutan's total land should be maintained under forest cover for all the times (*The Constitution of the Kingdom of Bhutan*, 2008).

According to UN (2014), urban living is often associated with higher levels of literacy and education, better health facilities, more access to social and economic services, and greater opportunities for cultural and political participation (United Nations, 2014). Roy and Saha (2011), identified the major factors exhibiting city growth: self-induced process, spreading functions from the center, market-oriented location, expansion and merging factors, geostrategic importance and socio-culture factors (Roy & Saha, 2011). However, key problems associated with the expansion of the city such as infiltration, land use, transportation, drinking water, social, and problems of slums were highlighted in the study. With this rapid growth, cities exert heavy pressure on land and natural resources on the outskirts of the city. Extensive growth of urban areas happened due to several factors, most notably population growth via rural-urban migration, development of city infrastructures, job

opportunities, and education attributed the city grew over time. This urban expansion, indeed at a rapid rate in which it is occurring, presents a formidable challenge to urban planners and managers (Masser, 2001).

Land cover and land-use change models are helpful tools to understand the urban dynamics and their consequences (Rafiee et al., 2009). In this context, remote sensing and Geographical Information System can make extensive use to map and manage the rapid urban change areas in the city. Nowadays, satellite data become inevitable for mapping and monitoring the urban growth change for municipal planning and enhance an emphasis on applications on urban planning (Treitz & Rogan, 2004). Constant, historical, and precise information about the urban land use land cover change is a prerequisite to further analysis of urban growth and scenarios. However, urban models using this information was not utilized in Bhutan by any researchers in the past to study urban growth.

The use of the Cellular automata (CA) model could be the first of its kind in Bhutan to study the urban growth scenarios. The previous research efforts and information on urban growth in the country according to the relevant literature reviews found that the study was done in Thimphu city to quantify the amount of forest cover and human processes involved and its adverse effect of cultural, political, and economic frameworks (Gosai, 2009). Yangzom et.al (2017) had conducted a temporal study of the urban expansion of Thimphu city from the year 2001 to 2017 and found that urban growth has almost tripled within these sixteen years. Moreover, the study identified the impact of urban expansion through socio-cultural, economic, and environmental impact in the city (Yangzom et al., 2017).

The urban growth models coupled with GIS can be useful to study the urban growth patterns through model simulations (Batty et al., 1999). In their study, many strategies have been identified for linking models to a GIS from loosely coupled to a strong couple. One such model of the Loose-coupling of cellular automaton and GIS has been studied by Clarke & Gaydos (1998) to predict the long term urban growth for San Francisco and Washington/Baltimore. Though the GIS is loosely coupled with the model, it was found to be a valuable enriching source of GIS data layers, and layers that have real value for planning and GIS application. According to Batty, Xie, & Sun (1999), urban models are developing rapidly which are at first sight, strongly

consistent with GIS. All models are based on the principles of cellular automata (CA) where temporal processes of change are represented through local interaction that take place in the immediate neighborhood of the various objects (Batty et al., 1999).

In recent years, the study of urban growth modeling and Land cover change in Asian countries such as China, Thailand, and India has been documented and studied using the CA-based SLEUTH urban growth model (Huanga et al., 2008; Maithani, 2011; Sangawongse, 2006). The model was gaining its popularity due to its effectiveness of the urban simulation and future growth scenario results obtained from the model. The model based on cellular automata is probably the most notable among all the documented dynamic models in terms of their technical progress in connection to urban applications. SLEUTH model has been tested more than 60 cities all over the world (Dietzel & Clarke, 2006). Using these models, city urban planners, decision and policymakers can analyze the different scenarios of the urban land use land cover change and can evaluate the effects in land use planning and policy (Veldkamp & Lambin, 2001). The current study involving model simulation would add spatial information's towards urban growth which is a prerequisite for urban planners and decision-makers to understand both current and future growth scenarios of the city. This study will also serve as a basis to mitigate the urban development and approach to plans and policies of the city.

Therefore, the ultimate aim of this research was to simulate future urban spatial development under different scenarios of SLEUTH models for the next 30 years. With the reliable prediction model and growth scenarios, the impact of urban growth can be minimized through proper planning and management. Besides, the findings of the study will also have the potential to implement the model to other Districts where similar growth would happen in the future.

The Problem Statement

The accelerated urban growth with an increase in population in the urban areas has led to various socio-economic demands in the country. Bhutan's total land area is approximately over 38,000 square kilometers of which limited area of land is available for human settlements due to the rugged mountainous region. More than 70

percent is reported to have under forest cover (Ministry of Works and Human Settlement, 2016). Gelephu is the third-largest urban city in the country and over the period, tremendous change in growth scenario was found both in the urban and peri-urban region. The city today has evolved to be one of the major commercial and business centers in central Bhutan.

The growth of the city has become more prominent due to the identification of the area as a viable economic hub of the country. It is also due to the construction of the domestic airport, vocational training institute and the industrial estate in the peri-urban region. The demand for land and other necessary amenities within the city has become high. On another hand, there is a lack of a proper system for urban land use planning and implementation which exerts heavy pressure on the city planners and decision-makers for sustainable future urban growth (Ministry of Works and Human Settlement, 2016).

It was found that there is little evidence of the research conducted to tackle the urban growth issues in future though the subject was widely research and highly used as a decision-making tool in both global and local setting of the area. From the above argument, it is imperative that the impact of the city upon surrounding areas is noticeably high and it is likely to be even more soon. Given such urban growth, the detailed study of past to present and future prospects of the city scenarios has become necessary for urban planners and policymakers to manage the city under the country development policy (Yang & Lo, 2003).

Research Questions

1. How can we understand the urban growth system through urban modelling and Simulation?
2. How do different types of urban growth can represent future urban development through the design of model scenarios?

Purpose of the study

The overall purpose of this research is to understand the urban growth phenomena through urban modeling and simulation. After the study of complex urban

growth systems and models behind the urban growth, Cellular Automata (CA) based SLEUTH urban growth model was applied in different growth scenarios of the city. Therefore, to achieve the overall result and ensure the research process remained on track, three specific research objectives were set;

1. To simulate the urban expansion using remote sensing data and SLEUTH model.
2. To evaluate the urban growth factors through management of three different growth scenarios of SLEUTH model: a) Business as usual scenario (BAU), b) Managed growth scenario (MGS), and c) Compact growth scenario (CGS).
3. To explore the model's effectiveness and suggest most appropriate scenario for future urban growth in a mountainous country like Bhutan.

Scope of the study

This study was focused on the future urban growth of the Gelephu city under the Sarpang Dzongkhag (District). The area consists of four sub-district including the District head quarter and the core municipal area which envisages the future urban growth in the region. This research makes use of the SLEUTH urban growth model which is a Cellular Automaton (CA) based urban growth tied with Land cover change model (Silva & Clarke, 2002). The model required six input layers; Slope, Land use, Exclusion, Urban extent, Transportation, and Hillshade layers derived from various data sources such as satellite images and topographical base map of the country.

Detailed functioning of the SLEUTH model through its four predefined grow rules and five growth coefficients will be examined. Moreover, model calibration in three phases: coarse, fine, and final spatial resolution will be carried out to narrow down the growth coefficient for the model prediction phase. The model simulation results will have a great potential to inform both city urban planners and decision makers to minimize the impact of future urban growth. Besides, the model can show the usefulness with the combined approach of remote sensing and geographical information system.

Limitation of the study

The accuracy and reliability of the predicted urban growth model will ultimately depend on the historical input data and the model calibration based on the urban growth scenarios. The high spatial resolution of remote sensing data interpretation is required to obtain better simulation results (Chaudhuri & Clarke, 2013). In this study, 30 meter Landsat satellite images obtained from USGS earth explorer website (https://earthexplorer.usgs.gov/) has been used. Generating accurate land use the land cover map was a challenge from such images due to a coarse resolution. It was difficult to make a clear distinction between different land use features classes.

Some extent of the visual interpretation of the model results might impact the actual urban growth results compared to the real growth. This study was located relatively flat terrain compared to other cities, and the results obtained may not demonstrate or reflect the same behavior to other cities.

Since urban growth and land-use change is a complex and complicated process, the growth is also influenced by other subjective factors such as social, economic, and political aspects which are not considered in this study because of the model's ability. This research mainly considered the historical data sets and land use land cover information to explore the potential urban growth through different management scenarios using the SLEUTH urban growth model.

Organization of the research

This research is presented in 5 chapters in total. The first chapter includes the background and significance of the study with its purpose, research questions and the statement of the problem for conducting this research. The scope and limitations of the study were also highlighted.

Chapter 2 discussed the theoretical and practical views on land use land cover and urban growth detection through remote sensing and GIS. Detailed urban growth modeling and the model functions of SLEUTH are presented in this chapter.

In the third chapter, materials and methodology of the study were presented which consist of data collection and preparation, land use land cover mapping, SLEUTH model calibration, model simulation, and validation processes.

The results obtained from the model calibration and prediction scenarios are presented in Chapter 4. Finally, chapter 5 presented the detailed discussion of results followed by a conclusion and recommendations of the study.

Study area

Gelephu is located about 30 kms to the east of Sarpang Dzongkhag (District) Headquarter, located in the Southern foothills of central Bhutan. Gelephu is one of the gateways to Bhutan from neighboring border town India. Due to the geographical setting of the area with relatively flat terrain and the proximity to the border city, the Royal Government of Bhutan had identified the Dzongkhag as one of the preferred locations for future development.

The proposed development corridor of along the Sarpang-Gelephu highway will serve as the backbone for a Special Economic Zone (Ministry of Works and Human Settlement, 2010a). Gelephu region is planned as a growth center for the central parts of the Bhutan, serving a series of smaller settlements, or service centers, like Sarpang, Tsirang, Zhemgang and other Dzongkhags.

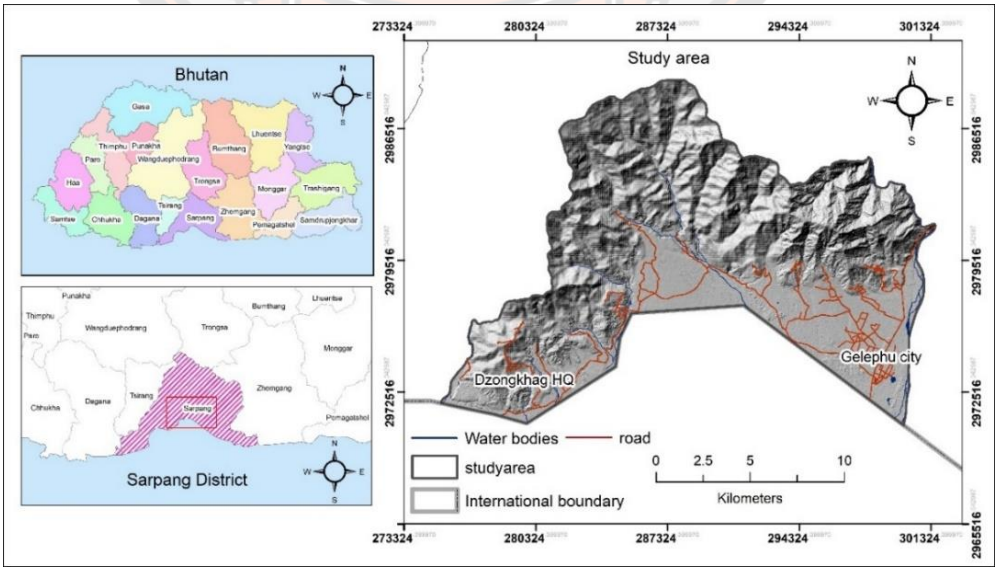

Figure 1 Map showing the study area

The current study area covers the entire Sarpang-Gelephu development corridor including the Dzongkhag Headquarter where major infrastructure development has been carried out and observed rapid urban growth in recent decades. Study area covers approximately 244 sq.km bounded with geographic coordinates of Longitude 90° 15' 16" to 90° 31' 09" East and Latitude 26° 50' 49" to 27° 00' 46" North. The altitude of the area ranges from 200 to 1500 meters above the MSL. The total population in the Dzongkhag is 46,004 persons recorded in 2017 (National Statistics Bureau, 2017), and projected to 65,774 persons by 2047.

With experiencing pressure on urban development, it is timely to do the study and understand both current and future prospects of urban growth scenarios for the management of future urban growth.

CHAPTER II

LITERATURE REVIEW

Introduction

This chapter presents a review of the theories, models and techniques that are used for urban simulation. Since this study explore the CA based SLEUTH urban growth model, this chapter deals in depth in SLEUTH model. It is important to introduce readers about model concepts and techniques that helps to understand the model calibration and prediction phases in later stages. Basically, this chapter has divided into four parts: Land use land cover dynamics, urbanization and urban expansion, urban growth modelling, and SLEUTH urban growth model. Before dwelling into the urban growth modeling concepts, we first introduce the basic theories and background of Land use land cover dynamics and urbanization process which is one of the main factors for urban expansion. Then review of the recent progresses in urban models, and detailed functioning of SLEUTH urban growth models and its applications will be highlighted in detail which in later chapter deals with model calibration and prediction.

Land use Land cover (LULC) dynamics

Urbanization is one of the main factors of LULC in the cities. It is a common worldwide trend that is caused by population growth and economic development. The rapid urban growth triggered by population growth and economic development has caused numerous problems, such as the loss of open space, agricultural land, and degradation of the forest. With the limitation of land resource, not all the land-use changes are from rural to urban; more and more land-use changes are occurring within the urban area. These variations are generally caused by mismanagement of agricultural, urban, and forest lands which lead to major environmental problems such as landslides, floods, etc. (Liu et al., 2017).

According to Lambin, Geist, & Lepers (2003), LULC change consist of two different terms: Land cover and land use. Land cover refers to a biophysical cover

over the earth's land surface and immediate subsurface which includes water, vegetation cover, bare soil, and manmade structures (Lambin et al., 2003). Foody (2002) defined the land cover change as a fundamental variable that affects and links many parts of the human and physical environments. Understanding the importance of the land cover and predicting the effects of land cover change is mainly limited by the lack of accurate land cover data and up-to-date information on land cover and land cover change are therefore required for many applications (Foody, 2002).

Land use is a more complicated term. It is the intended human employment and management of the land, the ways and means of its misuse to meet human resource demands (Meyer & Turner, 1996). They proposed three ways of land cover change due to land use activity; firstly conversion of the whole land into a different state, changing condition without full conversion, and preserving its condition against natural agents of change. As per the Lambin, Geist, & Lepers (2003), land use is defined by the purpose for which humans exploit the land cover. They identified various factors of land-use change such as economic and technological factors, demographic, institutional, cultural, and globalization.

Over the last few decades, the number of researchers have improved the measurements of land cover change and the understanding of its causes, and land cover modelling, in part under the supports of the LULCC Project conducted by International Geosphere-Biosphere Programme (IGBP) and International Human Dimensions Programme (IHDP) on Global Environment Change (Lambin et al., 2003).

Land use land cover is crucial for any kind of natural resource and action planning be it in global, national, & local planning. Timely and accurate land use land cover information is vital for better management and decision making. Firdaus (2014) highlighted the importance and prior advantage of LULC which is one of the most precise techniques to understand what types of changes had happened and to be expected in the future. It states that the LULC serves as one of the major input criteria for any kind of sustainable development program (Firdaus, 2014).

Satellite remote sensing technology has been widely applied to detecting LULC changes (Firdaus, 2014; Lambin et al., 2003; Rongqun & Daolin, 2011; Veldkamp & Lambin, 2001) especially the urban expansions (Li, 2014; Masser, 2001;

Sangawongse, 2006). Singh (1989) highlighted several techniques of land cover change detection using digital data such as image differencing, vegetation index differencing, principal components analysis, post-classification comparison, and change vector analysis. Among these methods, post-classification change detection was a commonly used method for detecting the land-use change and also used in various areas effectively (Fan et al., 2007; Singh, 1989).

LULC analysis using satellite remote sensing

One of the main objectives of digital image analysis is to classify the land cover types from satellite images. Lu and Weng (2007) identified the major steps of image classification which includes the selection of suitable classification system, training samples, image preprocessing, feature extraction, post-processing, and accuracy assessment (Lu & Weng, 2007). According to Shalaby & Tateishi (2007), the accurate change detection from satellite imagery will depend on the nature of change involved and the correctness of the image preprocessing and classification procedures (Shalaby & Tateishi, 2007). However, Erasu (2007) argues that whatever the classification methods and techniques developed by the scientist and authors, classifying the remotely sensed data into thematic map remains a challenge (Erasu, 2017). Various factors such as the nature of chosen study area, selection of remotely sensed data, choice of classification techniques, and spatial resolution of the different data sets and the availability of the classification software attributed the challenge in the image classification system.

A variety of classification algorithms have been proposed to conduct the remote sensing image classification and it was documented two main spectral recognition methods; Supervised and unsupervised multispectral classification (Li, 2014). Many efforts have been made to improve urban land cover classification accuracy and Li (2014) proposed three methods as per the existing works of literature: Making more efficient use of spectral information. This information is readily available in satellite images and the number of spectral indices was developed to help the interpretation of remote sensing images. For example, the widely used Normalized Difference Vegetation Index, Principal Component Analysis (PCA) (Rongqun &

Daolin, 2011). Incorporation of multi-sensor data and ancillary spatial information; this technique is the fusion of two types of data to enhance the accuracy of classification. The third one is the increasing use of spatial information. Generally, classification accuracy refers to the extent of correspondence between the remotely sensed data and reference information (Congalton, 1991). Accuracy assessment is necessary to validate the classification results.

Stehman & Czaplewski (1998) proposed three basic components of classification accuracy assessment: sampling design, responsive design, and estimation and analysis procedures (Stehman & Czaplewski, 1998). The collection of sample size and choosing the sampling scheme is another important consideration when assessing the accuracy of the remotely sensed data (Congalton, 1998). It is critical to generate the error matrix that is representative of the entire classified image. Congalton (1998) pointed out that the poor choice in sampling schemes can result in significant biases being introduced into the error matrix which may over or underestimate the true accuracy. The overall accuracy of image classification was calculated using the following formula:

$$\text{Overall accuracy (\%)} = \frac{\text{Total number of correct sample}}{\text{Total number of sample}} * 100 \qquad (1)$$

Besides overall accuracy, two other classification accuracy of the individual classes were also calculated similarly: User's accuracy and Producer's accuracy. The user's accuracy is calculated by dividing the number of correctly classified pixels in each category by the total number of pixels that were classified in that category. The Producer's accuracy is obtained from the number of corrected pixels in a particular class divided by the number of corrected pixels obtained from reference data. It measures how well a certain area has been classified. These two accuracies can also be expressed in terms of commission and omission errors. The errors of commission indicate pixels that were placed in a given class when they belong to another, while the error of omission indicates the percentage of pixels that should have been put into a given class (Congalton, 1991).

$$\text{Proceducer's accuracy (\%)} = 100\% - \text{error of ommision (\%)} \qquad (2)$$

$$\text{User's accuracy } (\%) = 100\% - \text{error of commission } (\%) \quad (3)$$

The type of error used to evaluate the overall accuracy of the classified images is also known as the kappa coefficient. It is generally known as a precision measure since it is considered as a measure of agreement in the absence of chance (Congalton, 1991). The kappa statistic is calculated from the error matrix by using the following mathematical formula. (Congalton, 1991).

$$K = \frac{N\sum_{i=1}^{r} X_{ii} - \sum_{i=1}^{r} (X_{i+} * X_{j+})}{N^2 - \sum_{i=1}^{r} (X_{i+} * X_{j+})} \quad (4)$$

Where;

K: Kappa coefficient

X: Pixel

r: the number of rows

N: the total number of observed pixels

i: is the number of observations in row i

j: column in error matrix

+: total of rows and column sum

Urbanization and urban expansion

Bhutan is a small landlocked country situated between two giant neighbors China and India. Geographically characterized by steep mountains and deep valleys which led to scattered population settlements patterns. In recent decades, the population of the country has been increasing and rural-urban migration remains the highest among other factors which it played an important role in driving the growth of Bhutan's towns and cities. According to the report on leveraging urbanization in Bhutan by World Bank, 2014, the growth rate of Bhutan's urban population was the highest (at 5.7 percent per year) among the eight South Asian countries from year 2000-2010.

Urbanization is defined as a spatial and social process resulting in a change in the relationship between human societies and social behaviors in various dimensions (Li, 2014). Li et al. (2003) defined urban growth as a dynamic process of land-use change that is associated with details of the earth's surface such as topography, road network, and socio-economic in a city (Li et al., 2003). According to them, urban expansion was implemented in the area which is under the pressure of the population growth which triggered the land-use change of the city from natural vegetation and agricultural land into urban built up. Dramatic urbanization, especially in the developing countries will continue to be one of the central issues of global change influencing the human dimensions (Li, 2014). Though the change of urbanization promotes socio-economic development and improves quality of life, urban growth inevitably results in a significant decrease in vegetation cover in urban areas such as converting forest and agricultural land into urban built-up.

According to Sebastain, Jayaraman, & Chandrasekher (1998), the urbanization process has been characterized by increased in built-up areas due to industrial expansion, economic and social development activities, consuming the natural resources in large (Sebastain et al., 1998). Wilson et al. (2003) have identified three categories of urban growth: infill, expansion, and outlying. Infill growth is characterized by a non-developed pixel being converted to urban pixel surrounded by existing developed pixels. This type of growth is usually occurs in the existing developed infrastructure. An expansion growth represents an expansion of the existing urban patch. Outlying growth is also characterized by a change from non-developed to developed land cover occurring beyond existing developed areas which is further divided into three classes: isolated, linear branch, and clustered branch. (Wilson et al., 2003).

The same transition has been visibly seen in Bhutan's urbanization process from past to present. Urbanization in Bhutan started in 1961 with the start of the first five-year development plan by late King Jigme Dorji Wangchuck (Giri & Singh, 2013). According to the research article by Chand (2017), the urban landscape in Bhutan was nearly absent in the 1960s and until the 1980s, the pace of development has been very slow.

It was noted that urban settlement in Bhutan was limited to a few traditional clustered villages which were later being replaced by new urban buildings (Chand, 2017). Thimphu being the capital city of the country, the infrastructure development started at a rapid pace which led to the migration of people from rural areas to the Thimphu urban area. Slowly, the development of small towns across the country led to the urbanization and expansion of urban areas. As per the history of the development of Gelephu town, it dates back to 1961 when the original settlement was moved from the banks of Mou Chhu to the present location (Gelephu Thromde, 2019, August 2).

It was found that the pace of urbanization was very slow until the late 1990s. This perhaps due to the repopulation of landless people in the rural part of the region, land whose former settlements were deemed of unsuitable political loyalty (Walcott, 2009). However, it was presumed that the location being in the mid-country envisages future development such as an airport and a major transportation depot for the export of goods and services. It is only after the commencement of the resettlement program in 1997 by His Majesty the Fourth King started granting the land to the landless people in the country (National Land Commission Secretariat, 2016). The Sarpang Dzongkhag being one among the five Dzongkhag under this program had seen major socio-economic development with increased in population growth and ultimately leading to the growth of urban area.

Today, Gelephu became the third-largest city in the country and many development plans have been laid down in Structural Plan which envisages the further growth of the city. Rapid urbanization is responsible for many environmental and social changes in the urban environment and its effects are strongly related to global change issues. The huge growth in urban population may force to cause uncontrolled urban growth resulting in sprawl. The rapid growth of cities gives pressure to provide various services such as energy, education, health care, transportation, and clean sanitation and the direct implication of urbanization is attributed to spatial growth of towns and cities, which is referred to as urban growth.

The recent report on Comprehensive Development Plan for Bhutan 2030 (Ministry of Works and Human Settlement, 2019), identified that due to increase rate of out-migration, where people tend to migrate to urban area in search of better

opportunities in terms of higher education and jobs, as well as better conditions of employment than farming, the limited natural resources available in urban area are put on pressure. Currently, Bhutan's environmental problems had not reached at a serious stage, but importance has to accord in advance accordingly to the plans and policy, as stated in the report.

Recently, study on assessment of land use/cover change and urban expansion was carried out in two major cities; Phuntsholing and Thimphu. The study conducted in Phuntsholing Municipality shows the decline of vegetation cover of approximately 6.3 percent in last ten years due to considerable increase in urban built-up, which is about 7 percent. The study also projected the huge change of vegetation cover which will be decreased to 32 percent with expected increase of urban settlement to 26 percent by year 2026 (Chimi et al., 2017). According to the study conducted by Yangzom (2017), urban expansion is one of the significant driver of dynamics of landscape, degrading the natural system and emergence of different social issues. The study revealed that the urban settlement in Thimphu city had been increased tripled the size from 2001 to 2017 mainly along the transportation routes with more expansion towards the south of the city.

Easy access to the various facilities, employment opportunities and ease of city life were cited as the driving force for urban expansion. Rural-urban migration was cited as another factor causing increase in urban settlements encroaching into the forest and agricultural land (Yangzom et al., 2017). Such study could be one area to analyze the impact of urban growth and its consequences keeping in view the country's development plans and policies be it in the regional or in local municipal planning process.

Urban growth modelling

Urban growth modeling was introduced in the late 1950s. Since then the number of analytical and statistical urban model has been evolved based on diverse theories and applications such as urban geometry and size, relationships of cities and economic development functions. These models are used to explain the urban forms and growth patterns rather than forecasting future urban growth. In order to

understand the spatial consequences of urban growth, dynamic urban growth model is preferred (Rafiee et al., 2009).

With growing applications in remote sensing and geographic information system, advance modelling approaches such as CA models (Clarke et al., 1997), artificial neural network (Pijanowskia et al., 2002), Fractal model (Batty et al., 1989), multi-agent model (Benenson, 1998), and Statistical model (Cheng & Masser, 2003) has been applied. According to Torrens (2000), among those modeling approaches, the CA model is the most widely used in urban growth modeling. This may be due to their flexibility, simplicity in application, and due to tightly coupled remote sensing data and with GIS (Torrens, 2000).

History of the development of urban models was captured by Batty and colleagues (1997), in their study of urban systems as cellular automata. Urban modeling is generally aimed at urban design, building and operation of the mathematical models particularly for the cities and areas to help researchers understand urban phenomena (Batty et al., 1997). The first attempts to build mathematical CA models of urban systems of spatial diffusion models have been initiated by Hägerstand in 1965 (Hägerstrand, 1965). The work was followed by Tobler (1970), formulating a demographic model that describes the geographical location distribution of the population growth in the Detroit Region (Tobler, 1970).

Later in 1997, Couclelis followed the CA concept to explore theoretical problems such as complexity and formation of urban systems (Couclelis, 1997). Starting from the early 1990's number of studies were done with the CA model to practical problems in urban modeling and land-use planning. CA model was used to examine the principles of urban dynamics, evolution, and self-organization of urban land use patterns (White & Engelen, 1993). Batty et al. (1997) established a common framework for the urban simulation using CA in their studies of urban system as cellular automata. They defined CA as a lattice of cells, where each cell can exist in any number of finite allowed states that will change its state accordingly to the states of the change of neighboring cells, which are influenced by a uniform applied transition rules.

Basically CA system consists of four elements which are defined as cells, states, neighborhood, and transition rules (Li & Yeh, 2000). Cells are the smallest

objects in any dimensional space that appear in proximity to one another. A cell's state will change with its neighboring cells when a set of transition rules is applied. A neighborhood consists of a CA cell itself and any number of cells in a given configuration around the cell. In CA, transition rules are considered as the main component of the change of states (Torrens, 2000). They specify the behavior of cells between time-step evolutions, deciding the future conditions of cells based on a set of fixed rules that are evaluated on input from neighborhood cells. A Transition rule in the context of urban CA is responsible for explaining how the city works. Depending upon the transition rules, and calibration methods the CA model developed for many modeling purposes has been popularly applied in the area of modeling urban studies and growth processes (Al-shalabi et al., 2012).

According to Torrens & O'Sullivan (2001), CA is defined as an array of regular spaces or cells that change their states iteratively and synchronous through the repeated application of the transition rules. Apart from the four elements, they considered the fifth element called a temporal component in the CA framework due to the inadequacy of the model to represent the real objects (Torrens & O'Sullivan, 2001). CA models have been used in the study of the diverse field of urban phenomena, including from traffic simulation, regional-scale urbanization to land-use dynamics, historical urbanization, and urban development. New CA models such as URBANISM, UPLAN, and SLEUTH have been evolved in recent years to forecast future changes trends of urban development both current and future, and to explore the potential impacts of different policy scenarios (Al-shalabi et al., 2012).

SLEUTH urban growth model

Clarke and colleagues developed an urban growth model called SLEUTH based on cellular automata for simulating historical urban and land-use change (Clarke et al., 1997). The initial application of SLEUTH was successfully implemented in the San Francisco Bay area in simulating historical urban development (Clarke & Gaydos, 1998). The name of the model came from the six input data layers, namely Slope, Land cover, Exclusion, Urban extent, Transportation, and Hillshade. It is a program written in programming language C under UNIX that

uses the standard GNU C compiler (gcc) and runs under Unix, Linux and Cygwin, a Windows-based Unix emulator (Project gigalopolis, 2003).

The model works in a grid space of homogeneous cells, with a neighborhood of eight cells, two cell states (urban/non-urban) with five transition rules that applied in consecutive time steps. The model can classify urban/non-urban dynamics as well as urban land use dynamics. These capabilities led the model to the development of two subcomponents within the model; an urban growth model (UGM), and a LULC change model or Land Cover Deltatron (LCD) (Dietzel & Clarke, 2007). Each subcomponent uses the same calibration phase, however, if only urban growth is analyzed, then Land Cover Deltraton is not stimulated by the model. It was only activated when land use/land cover is being analyzed by the model.

The model functions with predefined growth rules and uses the five factors to calibrate the model to a particular city. The rules of the model are complex than those of a typical cellular automaton (CA) and involve the use of multiple data sources such as transportation networks, topography, and existing land use details (Clarke et al., 1997). The growth rules are applied on a cell by cell basis and the cell is updated at the end of every year.

The complete documentation and downloadable code of this model are available at the Project Gigalopolis website: (http://gigalopolis.geog.ucsb.edu/).

Model operation

SLEUTH requires a minimum of five input maps if land use is not modeled: urban layers, transportation, exclusion layers, slopes, and hillshade layers. All the layers should have the same number of rows and columns, standard naming format, and are correctly geo-referenced to one coordinate system since the model is sensitive to layer misregistration (Silva & Clarke, 2005). These raster layers are then converted to 8 bit GIF images. Once input layers are fed to the model, a predefined number of interactions takes place and every iteration of the model was unique and corresponds to the same number of years. Clarke et al. (1997) demonstrated the operation of the model through simulation program function as follows;

Read data layers

Initialized random numbers & control parameters

For n iterations {

For t time period {

Apply change rules

Apply self-modification rules

}

} Write images

An outer loop executes repeatedly in each growth history and retains statistical and cumulative data for each Monte Carlo iterations. An inner loop executes the growth rules for a single year and each iteration sets of descriptive statistics are retained for model calibration. The basic concept of model implementation is shown in Fig 2.

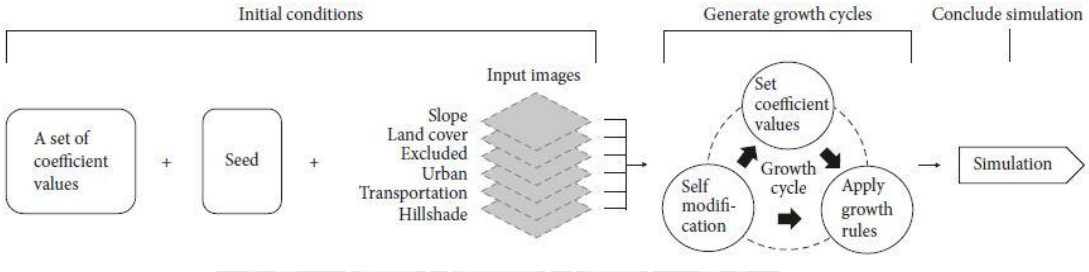

Figure 2 Basic concepts of the SLEUTH model implementation

Source: Adopted from (Chaudhuri & Clarke, 2013)

SLEUTH model parameters

Urban growth in SLEUTH is modeled in a spatial two-dimensional grid and the basic growth procedure is a cellular automaton. The model simulates four types of urban land-use change: a spontaneous growth, a new spreading center growth, edge growth and road-influenced growth (Jantz et al., 2003). These growth types or rules are applied sequentially during each growth cycle, or year, and are controlled through

the interactions of five growth coefficients: Diffusion (dispersion) coefficient, Breed coefficient, Spread coefficient, Slope coefficient, and Road gravity coefficient.

Spontaneous growth randomly selects potential new growth cells for urbanization. This means that any non-urbanized cell on the matrix has less probability of becoming an urbanized cell in any time step. This growth rules determined by the dispersion coefficient and slope coefficient which determines the weighted probability of the local slope. The stochasticity of the process is indicated by random. The cell state will not change if the cell is already urbanized or omitted from urbanization, and the ability to change also depends on the current cell value. (Project gigalopolis, 2003).

Diffusive/new spreading center growth determines the occurrence of new urbanizing centers by generating up to two neighboring urban cells around areas that have been urbanized through spontaneous growth. The breed coefficient determines the likelihood of newly generated urban pixels along with the road networks which begin its growth cycle.

Edge or Organic growth dynamics define the part of the growth that twigs from existing spreading centers. Edge growth is controlled by the spreading coefficient which stimulates the probability that nonurban cell with at least three neighbors will also become urbanized. Road-influenced growth is determined by the existing transportation networks on growth patterns by generating new spreading centers adjacent to roads.

Newly urbanized cells are randomly selected which is determined by the breed coefficient. The accessibility of road locations attracts urban development. According to Clarke et al. (1997), the most prevalent type of urban growth during the model run is recorded as an organic growth type, followed by spontaneous growth. It was noted that road-influenced growth increases as road layers from different historical periods are read in at the correct time.

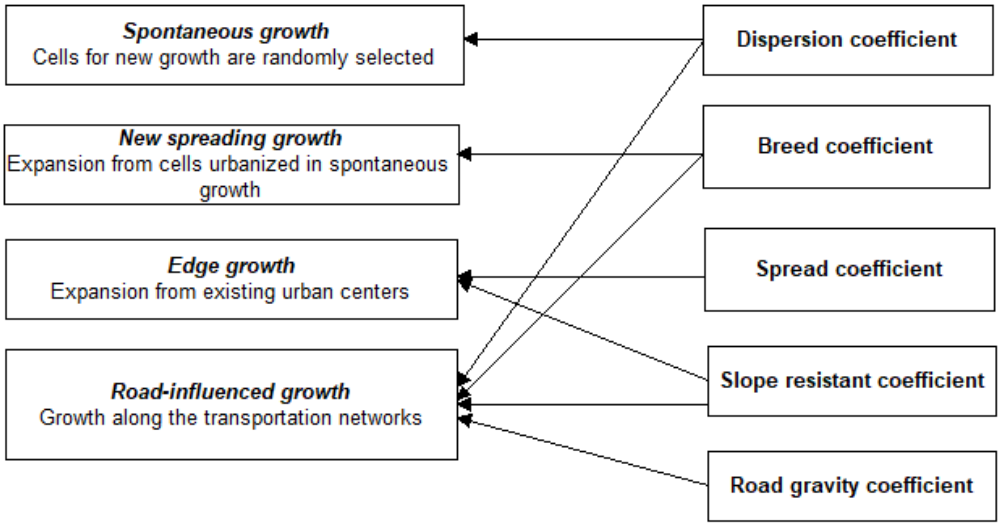

Figure 3 Relationship between growth types and growth coefficients in SLEUTH

Source: Adopted from (Ding & Zhang, 2007)

The above growth rules are influenced by the five growth factors applied in the SLEUTH model as represented in Fig 2. These controlled values are calibrated by comparing simulated land cover change to a study area's historical data (Project gigalopolis, 2003). The diffusion factor controls the depressiveness of isolated urban pixels which was generated by spontaneous growth. A breed factor controls the new spreading growth and the road gravity growth by monitoring the probability to become another newborn urbanized pixel of urban growth center and along the road influenced growth.

A spread factor controls the edge/organic growth type whether additional growth can be offspring from old or new urban centers. The breed coefficient controls the new spreading growth and likelihood of growth occurring along with the road networks. The slope resistance coefficient influences the likelihood of settlement development on steep slopes. A high slope coefficient value will decrease the likelihood of urban development that will occur on steep slopes. Road gravity factor attracts new settlement towards and along with the existing road system. The coefficient determines the maximum probing distance of a selected urban cells.

Table 1 summarizes the types of urban growth that can be simulated by SLEUTH. It encompasses various growth cycles with various growth types with specific growth coefficients that control the growth types.

Table 1 Summary of growth types simulated by the SLEUTH model

Growth cycle	Growth type	Growth coefficients	Summary description
1	spontaneous	dispersion	Randomly selects potential new growth cells.
2	new spreading center	breed	Growing urban centers from spontaneous growth.
3	edge (organic)	spread	Old or new urban centers spawn additional growth.
4	road-influenced	Road-gravity	Newly urbanized cell spawns growth along transportation network.
Throughout	slope resistance	slope	Effect of slope on reducing probability of urbanization.
Throughout	excluded layer	user-defined	User defined area resistant or excluded to development.

Source: Adopted from (Jantz et al., 2003)

Model self-modification

The SLEUTH model has a functionality called “self-modification” (Clarke et al., 1997). This self-modification allows the growth coefficients to change in the entire course of a model run and it simulates more realistically the different growth rates which occur in an urban system over time. This modification will either increase or decrease the growth parameters of dispersion (diffusion), spread and breed.

The growth rate is compared to two factors in the scenario file, namely critical high and critical low. When the rate of growth exceeds critical high values, the growth parameters diffusion, spread, and breed are multiplied by a factor greater than one simulating the development "boom" cycle. Likewise, when the rate of growth falls below a specified critical threshold value, the growth coefficients dispersion, spread, and breed factors are multiplied by a factor less than one which results in

stagnation showing the ‘bust" cycle like a depressed or saturated system (Project gigalopolis, 2003).

The self-modification is important to consider in the SLEUTH model because it estimates the typical S-curve growth which is common in urban expansion. Without which the form of urban growth would be either linear or exponential growth (Clarke et al., 1997).

Model applications

This section examines various research projects in which the SLEUTH model has been applied to supplement the rationale behind selecting this model in this research. The first application of the SLEUTH model was implemented in the San Francisco Bay area by Clarke et al. (1997). The historical urban extent was determined using cartographic and remote sensing data extracted from 1850 to 1990. With this information coupled with the road network and topographic, animation of the spatial growth patterns were created and statistics describing the spatial growth were calculated, and it was used for future prediction of urban growth.

The application of the SLEUTH model outside the USA was first carried out by Silva & Clarke (2002) for Porto and Lisbon metropolitan cities in Europe. The two cities present very different environmental and geographic characteristics but the rigorous model calibration has well captured both the city characteristics that best describe the actual reality. Four key findings were presented in their application: SLEUTH is a universally portable model that may not only be applied to North American cities but Europe and other international cities as well.

The model was sensitive to the local conditions with an increased spatial resolution and input datasets. They found using multistage ‘Brute force' calibration method, more refine model parameters that best replicate the historical growth patterns of an urban system, and lastly they highlighted the parameters that derived from model calibration may be compared between different system and the interpretation may provide a good background for understanding the urban growth processes (Silva & Clarke, 2002).

Yang & Lo (2003) used the SLEUTH model to simulate future urban growth in the Atlanta metropolitan city under three different policy scenarios. They found that SLEUTH as an effective tool to test, visualize and have options of different policy scenarios for the future urban growth. The number of reasons was cited for choosing the SLEUTH urban growth model in their study: First, it was being the model scale-independent, Model dynamic, and future-oriented (Yang & Lo, 2003). Jantz, Goetz, and Shelley (2004) applied the SLEUTH model to study the declining water quality in the Chesapeake Bay estuary. The model was calibrated using three different policy scenarios: Current trends, Managed growth and ecologically sustainable growth. The current trend allows urban fringe that are currently under rural or forested to be developed which would have implications for water quality. The managed and ecologically sustainable scenarios were put under constraints which affect less natural resource land. The study found that SLEUTH has the ability to visualize and quantify outcomes spatially from those interactive scenario developments and found to be useful tool for assessing the impacts of alternative policy scenarios, but spatial accuracy and scale sensitivity must be considered for practical application (Jantz et al., 2003).

Oguz et al. (2007) applied the SLEUTH urban growth model to simulate future urban growth in the Houston metropolitan area in the United States during the past three decades. The model was calibrated with historical data extracted from a time series of satellite images and three specific scenarios of future urban growth were designed and simulated. The simulation results are encouraging, but more accurate simulation could be achieved if more growth constraints were considered (Oguz et al., 2007). Before the work of Oguz et al. (2007), Sangawongse et al. (2006) had used the SLEUTH model with the integration of remotely sensed images and the Geographical Information System (GIS) data to analyze land-use/land cover dynamics in Chiang Mai city. The results showed increased in urban areas from 13 sq.km in 1952 to 339 sq.km in 2000 which has the potential to increase over time. The road & slope layers were considered as important variables for capturing the urban growth and it was found that the urban development in Chiang Mai was best captured by Xmean and edge growth regression score. However, the author assumes that the combination of remote sensing, GIS, & SLEUTH model can be best applied to study

urban growth and land-use change if some consideration for spatial accuracy and scale sensitivity are made to the model.

Rafiee et al. (2009) simulated the urban growth in Mashad City, Iran with the SLEUTH urban growth model. They designed to simulate the spatial pattern of urban growth under three different scenarios. The first scenario with historical urban growth which allows the continual urban expansion like existing condition. The second scenario was environmentally-oriented where urban growth has a limitation. The third represents similar to the first scenario, but the limitation was applied to construction on steeper slopes. The study concluded that the environmental scenario is preferable for Mashad City development (Rafiee et al., 2009). Sakieh et al. (2014) adopted the SLEUTH model to simulate urban expansion of Karaj city. The city was predicted under its historical trend as well as the other two different scenarios including compact and extensive growth up to the year 2040. The results of model prediction under a compact growth scenario demonstrate the least amount of increase in urban extent compared to the historically based scenario and extensive growth scenario. It was concluded that Karaj city under the compact growth scenario would minimize the utilization of vacant lands and agriculture lands (Sakieh et al., 2014).

SLEUTH model was applied in the Isfahan Metropolitan area in Iran to simulate urban growth expansion with two growth scenarios. The first scenario continues the historical growth and second estimated compact growth. Their calibration results showed a high value for the spreading coefficient, which means the future growth of Isfahan city will be experiencing more of organic or edge growth (Bihamta et al., 2014).

Leao et al. (2004) applied the SLEUTH urban growth model to test the applicability of the model to a developing country urban area in Porto Alegre City, Brazil. Calibration of the model in the specific case of their study area obtained satisfactory results which is an indication of model applicability to be used in less developed countries. A few reasons were cited for choosing the SLEUTH model for their study of urban growth in developing nations. It is due to the model sensitivity that able to depict different patterns of urban growth, due to the availability of datasets in government and research institutions, unlike other CA model, it does not increase model complexity where it uses only two classes urban and non-urban, the

model is freely available and easy to execute, and the model produces reliable urban growth patterns (Leao et al., 2004).

Bihamta et al. (2014) & Abedini & Azizi (2016) have modeled urban growth using SLEUTH model to simulate future urban expansion of the Isfahan metropolitan area and Urmia city, Iran. They had obtained high coefficient values of 77 and 67 in Urmia city and 52 and 94 in Isfahan metropolitan city indicating road and slope influenced growth in the region. Urban growth in Tehran metropolitan city has also reported the high road gravity coefficient and slope resistance coefficients among others and considered as most important factors to form different types of urban growth. (Dadashpoor & Nateghi, 2015).

Abedini & Azizi (2016) and Osman et al. (2016), also cited similar reasons for selecting the SLEUTH model in their study. Due to model's application over 66 different cities and regions worldwide (Chaudhuri & Clarke, 2013), compatible to integrate remote sensing and raster GIS, and it's dynamic are some reasons among others (Abedini & Azizi, 2016; Osman et al., 2016). All of the above SLEUTH model calibrations and scenarios were found to be adopted one of the following approaches for future model prediction;

1. Assigning different values to the exclusion layer to indicate different levels of cell's potential for urbanization. e.g. (Bihamta et al., 2014).
2. Manipulating the self-modification constraints. e.g. (Yang & Lo, 2003).
3. Changing the growth parameter values which affect the growth rule and type of urban growth. e.g. (Leao et al., 2004; Rafiee et al., 2009).

Model Calibration Approach

In SLEUTH, the model calibration process is known as “brute force calibration”, which relies on the high computing power and benefits highly from parallel processing and high-performance computing methods (Silva & Clarke, 2002). The process has been automated and model runs with every possible combination of growth coefficients and performs multiple runs from seed year to the present date.

The model generates 11 different metrics of the goodness of fit between the modeled and the real data sets. Brute force calibration reduces the number of solution

sets but it still searches the range of solutions through Monte Carlo iterations. Instead of executing every permutation and combination of possible coefficients sets, each model parameter range is examined incremental phase. For example, the range (0-100) may be used with an increment of 25 step values. In this way, the model may be calibrated to the data in steps which may successively narrow down the range of coefficient values through calibration phases.

Determining "Goodness of Fit" metrics

Outputs from each of the calibration phases are examined to determine the goodness of fit for each parameter set. A log file is created in the output file which captures the different statistical values which determine the accuracy of the combination of growth variables to the real urban change between the consecutive recorded input years. These matrices are used to narrow down the model parameters in subsequent calibration phases. It was noted that despite numerous applications of SLEUTH worldwide, there is no clear consensus as to which metrics are most appropriate to use during the calibration phases (Dietzel & Clarke, 2007). Narrowing of the parameter set can be based on a variety of different goodness of fit measures or their combinations and different researchers had used different metrics of statistical measures to compare the characteristics of urban growth in different scenarios.

In their application of SLEUTH to the Isfahan Metropolitan area in Iran, Bihamta et al. (2014) used Optimum SLEUTH Metric (OSM) which is the product of compare, population, edges, clusters, slopes, X mean and Y mean matrices generated by the model. Jantz et al. (2004) used the compare, population, and Lee-Sallee metrics in their application of SLEUTH to the Washington-Baltimore metropolitan area. Yang and Lo (2003) used a weighted sum for all the metrics, Silva & Clarke (2002), Abedini & Azizi (2016), & Osman et al. (2016) all used only Lee-Sallee to calculate the spatial fit in modelling Lisbon and Porto metropolitan area, Urmia city, Iran, and Giza Governorate in Greater Cairo metropolitan region.

In past Lee-Sallee matric was often used to describe the parameter sets that best define the reproduction of the historical datasets. It is the ratio of the intersection and the union of the simulated and actual urban area (Silva & Clarke, 2002). It states

that achieving the high values for this index is challenging. A perfect spatial match would result in a value of 1. Table 2 shows the overall metrics generated from the model calibration.

Model validation & simulation accuracy

To assess the model accuracy is an important component of the predictive modeling especially if the models are to be used for the decision-making purposes (Abedini & Azizi, 2016). Different methods were used to assess the simulation accuracy. Sakieh et al. (2014) had used two separate validation indices; the receiving operator characteristic (ROC), and the Kappa index of agreement. Serasinghe Pathiranage et al. (2018) validated model performance by comparing the number of simulated pixels to the number of urban pixels in the urban extent layers, which was derived from satellite images using the maximum likelihood classification method. (Serasinghe Pathiranage et al., 2018).

Similar validation was carried out by Oguz et al. (2007) and Abedini & Azizi (2016) through comparison of the simulated urban extent with the observed urban extent with the construction of error matrix and evaluating the overall classification accuracy and kappa coefficient (Oguz et al., 2007). Visual interpretation of the modeled urban growth with actual urban growth has been also used for judging the model prediction accuracy (KantaKumar et al., 2011). Other than graphic interpretation serving as a confirmation for the accuracy of the model, it also provides a historical perception of urban development and landscape change in the particular region (Yang & Lo, 2003).

Limitation of SLEUTH model

SLEUTH model being open-source has attracted many researchers and applied all around the world in various application over the past few decades. The model has been used to simulate land-use change and predict future urban growth. However, several limitations were observed apart from its wide applications.

i) The computation of the model was very extensive, especially in the calibration phase. It takes days to complete the one calibration phase with a normal or low-end processor computer.

ii) The preparation of model input data was found subjective since it needs to adhere to the same set of layers in scenario files. The model would not run if we try to fit the model with different resolutions of datasets in one scenario. They need the same extents (number of row and columns), same spatial resolutions, and also need to follow standard naming format of the files.

iii) The accuracy of model predictability depends on the period of the historical data sets used. Better results were observed with short time series (Jantz et al., 2003).

iv) Scale sensitivity is another drawback of the model. Jantz et al. (2004) found that the model provides a high level of accuracy at regional level than applied at the local level.

Table 2 Metrics for evaluation of calibration in the SLEUTH model.

Metrics	Descriptions
Product	All other scores multiplied together
Compare	Comparison of modeled final population to real data final population
Population	Least squares regression score for modeled urbanization compared to actual urbanization for the control years
Edges	Least squares regression score for modeled urban edge count compared to actual edge count for the control years
Cluster Size	Least squares regression score for modeled average urban cluster size compared to known average cluster size for the control years
Lee-Sallee	A shape index, a measurement of spatial fit between the model's growth and the known urban extent for the control years
Slope	Least squares regression of average slope for modeled urbanized cells compared to average slope of known cells for the control years
% Urban	Least squares regression of percent of available pixels urbanized compared to the urbanized pixels for the control years

Metrics	Descriptions
X-Mean	Least squares regression of average x-values for modeled urbanized cells compared to average x-values of known urban cells for the control years
X-Mean	Least squares regression of average x-values for modeled urbanized cells compared to average x-values of known urban cells for the control years
Y-Mean	Least squares regression of average y-values for modeled urbanized cells compared to average y-values of known urban cells for the control years
Rad	Least squares regression of standard radius of the urban distribution, i.e. Normalized standard deviation in x and y
F-Match	A proportion of goodness of fit across land use classes.

Source: Adopted from (Dietzel & Clarke, 2007)

CHAPTER III

RESEARCH METHODOLOGY

Introduction

This chapter highlights the research framework methodology adopted to conduct the study. In general, the four major components were used to derive the outcome of the research. (1) Data collection and preparation, (2) Land use land cover (LULC) change analysis, (3) SLEUTH model implementation, and (4) Model calibration and prediction outputs. A Geographic Information System (GIS) was used to compile the model's required input data and convert to the raster layers required by SLEUTH. The input layers included the known urban extents, road networks, slope, excluded area, and hillshade layer which is use as a background for the display of the model's output. Three data sets were created through resampling to the ground resolutions of 120m, 60m, and 30m respectively. These data sets were used to calibrate the model from 1990 to 2017. Once the model calibration is completed, the growth was simulated from past to present scenario and analyzed their accuracy by comparing them to the known urban extent of 2017 land use map. Finally, the SLEUTH was calibrated to predict the urban growth from 2017 to 2047 and visualize the output image files and statistical results of future urban growth scenarios. The details of each component with sub-components are described in the succeeding sections.

Data collection and preparation

Data Collection

The details of the data sets are described in Table 3. This study utilized data from various sources, including GIS digital data, satellite images, and topographic maps of 1:25000 obtained from the Department of Survey and Mapping under the National Land Commission of Bhutan. The land cover data for 2010 and 2016 from the Ministry of Agriculture, Bhutan. The Landsat satellite images were downloaded

from the USGS earth explorer web portal (https://earthexplorer.usgs.gov/) in GeoTIFF format with 30 meters spatial resolutions.

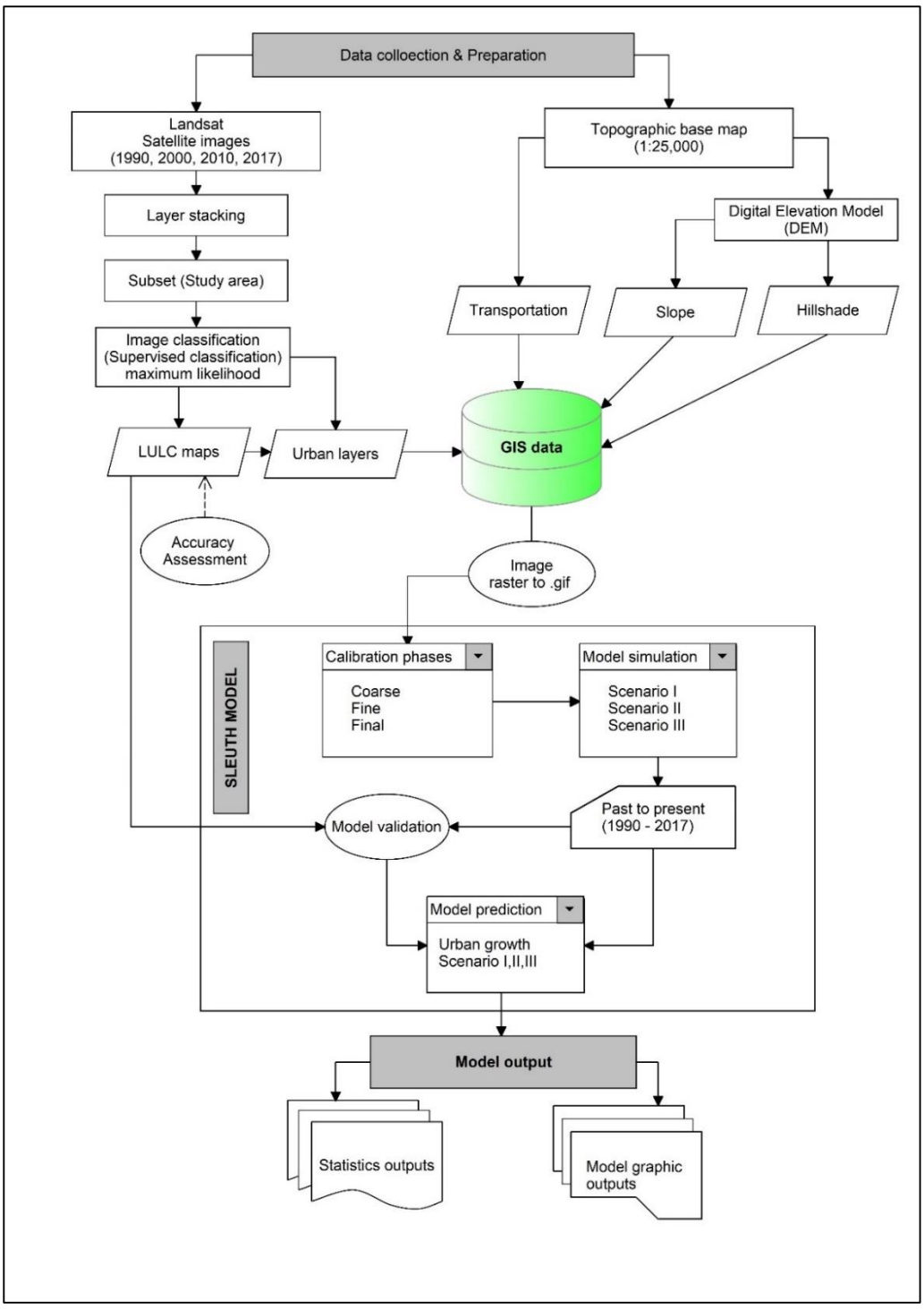

Figure 4 Detailed work methodology of the research

Table 3 Input data for SLEUTH model

Input layer	Source	Path/Row	Acquisition date	Format	Year
Urban	Landsat 5 TM	138/41	6/12/1990 & 05/11/2010	Raster	1990, 2000, 2010, & 2017
	Landsat 7 ETM+	137/41	28/12/2000		
	Landsat 8 (OLI/TIRS)	138/41	26/12/2017		
Transportation	Digitization/Topo map			Rasterized from vector	1990, 2017
Slope	DEM			Raster	
Hillshade	DEM			Raster	
Excluded	Landsat			Rasterized from vector	
Land use	Landsat & MoAF*			Raster & Vector	(1990, 2000, 2010, & 2017)
Google Earth	Google			Image	2017

*Ministry of Agriculture and Forest, Bhutan.

The Table 3 shows the detailed input data sets used in the study. Different sources were used to derive the model input layers. Landsat satellite images of year 1990, 2000, 2010, and 2017 was used to derive the land use maps and urban extent layers. All the four satellite images over the study area were free of clouds and distortion. The satellite data used were acquired approximately the same season of the year in order to minimize the seasonal difference either in sun angle or vegetation cover, that would affect the change detection (Al-Dail, 1998). The used of different image scene (Path/Row) for the same study area was due to the cloud cover. The choice of image year till 2017 was made due to the availability of existing land use maps of 2016 from Ministry of Agriculture and Forest (MoAF), Bhutan to validate the land use map derived from the satellite image. Moreover, the most recent demography data of the country was available till 2017. High resolution Google satellite images was also used in the study for validation of land use maps.

Spatial data creation

SLEUTH model required at least five input datasets (or six, if land use is included). Slope layer, Land use, Exclusion layer, urban extent, Transportation network, and Hillshade layer. For statistical calibration of the model, at least four temporal urban extents, Minimum of two transportation layers from two different years and land-use layers from at least two periods along with each slope, excluded and hill shade layers are required on three spatial resolutions with the same coordinate system and extent.

Data preparation depends greatly on GIS and remote sensing techniques such as data conversion, data import/export, and reclassification (Sangawongse, 2006). The software used for preparing the input data included ERDAS Imagine version 2014 and ArcGIS version 10.4.1. The model also requires a special naming format for the input datasets (Project gigalopolis, 2003).

Slope layers

The topography act as one of the important factors in urban development. Regions with low lying areas are more suitable for urban growth. In this research, the slope layer was prepared from the 30 meter spatial resolution of Digital Elevation Model (DEM) obtained from the topographic base map of 1:25000 scale using the contour and spot heights of the area. The layer was prepared in percentage values and then changed into integer value through reclassification from 0 to 100.

For example, the slope above 100 percentage value is more than the 45-degree slope which is not feasible for development. The integer value after reclassification will assign a value of 100 to it and zero to those below 100 percent slope value. Since the topography will not change dramatically in the short term, the same slope layer was used for model calibration and prediction scenarios.

According to Watkiss, 2008, the SLEUTH cells on a slope greater than 21 percent are called critical slope (Watkiss, 2008). However, in this research we have assigned 70 percent to be a critical slope due to the nature of topography in the region. The 70 percent of slope correspond to maximum of 35 degree slope.

Land use Land cover (LULC) layers

An optional input layer to the SLEUTH model is a LULC. Landsat images were first classified into five land classes: Forest, Urban/Built-up, Agriculture land, Open space, and Water bodies. LULC with consistent classification for at least two periods is needed for the model. Each pixel value contained in the grayscale land use images should represent a unique land class (Project gigalopolis, 2003). For example, the LULC class Urban is encoded by integer assigned as 1 and class Agriculture as 2 in order.

Exclusion layers

This constraint layer has an important role in urban growth by setting up resistant factors of urbanization (Qi, 2012). It shows the region whose urban growth is undesired or restricted. In this study, all water bodies are taken as the exclusion layer. However, to what extent the excluded regions would be protected from the growth was indicated by assigning the numeric value (0 – 100). For example, while a value of 100 indicates that the area should be excluded from urban growth (100 % protection), 50 shows that only 50% of that area should be protected. Locations that are available for urban development have a value of zero. Concerning the areas designated by the policy plans, such as protected areas, wetlands, and open spaces, the values can be assigned based on the importance or priority of the development policy in the region. (http://www.ncgia.ucsb.edu/projects/gig).

In this study, we have prepared urban exclusion layers from the land use classified images for different scenario. For instants, in Business as Usual scenario, the urban exclusion layer includes the water bodies and agriculture land with fully protected from the urban growth. Similarly, different level of growth protection was applied to other land use classes from future development. Therefore, the excluded layer plays a significant role in SLEUTH modeling and by adjusting this constraint layers, a SLEUTH model can integrate urban planning and policy with other macro elements to forecast urban development from both regional and local perspectives.

Urban layers

For this study, four temporal datasets of urban the area from 1990, 2000, 2010, and 2017 have been extracted from satellite images. Urban layers is the base layer for running the SLEUTH model. The beginning year known as a 'seed' layer is used to initialize the model and other years called controlled layers are applied during model calibration phase for the least square calculation to obtain the goodness of fit statistic results. The model requires the binary classification of urban or non-urban data with a value of 1 indicating the urban and 0 implies non-urbanized area. The land use layer is optional for SLEUTH model and was excluded from our modeling process.

Transportation layers

Transportation network has a great influence on urban development as the city tends to develop to the directions along with the transportation networks. The SLEUTH model requires more than one-year transportation data to simulate dynamic effects in the model. Since 1990 is a base year, we obtained the 1990 road layer from 1:50000 scale base map and it was validated through satellite image.

For the year 2017, it was obtained from a recent updated 1:25,000 scale topographic base map of the country. The layers were categorized into three categories. 1) The National highway, 2) Secondary road, and 3) Tertiary road accordingly to their importance and accessibility. The layers can be categorized in binary numbers, relative weight values, or the relative accessibility of the road (high, medium, low, none). In this research, relative weight values are used to categorize the importance of the roads. For example, the national highway being the primary transportation network it was assigned with a relative weight of 4 and the Secondary road with 3 and etc.

Hillshade layers

This layer has no impact on the model simulation. It is used for better visualization as a background image to the spatial data generated by the model output

files. This layer can be embedded with water bodies such as rivers and lakes to enhance the visual effects.

To run the SLEUTH model, input data need to be standardized in terms of data format, same spatial resolution, and same extents (rows x columns). Firstly, we need to convert all the layers into a single raster format in ArcGIS environment, then resample each layer into three spatial resolution of 120 meter, 60 meter, and 30 meter respectively using the nearest neighbor algorithm. Then covert these images into an 8-bit GIF format and rename the files according to the naming convention followed to run the model (Project gigalopolis, 2003).

Land use Land cover change (LULC) analysis

The LULC change which serves as one of the important input criteria for urban growth analysis needs constant, historical, and accurate information. The land cover change information can be obtained from remote sensing data by applying a variety of techniques such as visual interpretation, land cover classification, and change detection (Li, 2014). In this study, pixel-based supervised classification using a maximum likelihood algorithm was applied to classify the images.

Selection of LULC classification system

For this study, LULC classification was extracted and modified from the LULC categories of the Ministry of Agriculture and Forest, Bhutan. The detailed land classes and its description was described in Table 4.

Table 4 Land use land cover class details

Major class	Sub-class name	Class Description
Urban	Built-up areas	Includes artificial constructions covering the land with an impervious surface. (e.g. concrete, CGI sheet, urban areas, schools & institutes, industrial areas and transportations)
Non-urban	Forest	Class incudes different types of forest cover such as Broadleaf and Mixed conifers.

Major class	Sub-class name	Class Description
Non-urban	Agriculture land	Cultivated agricultural land includes Orchards, dry and wet land.
	Open space	Bare soils, bushes, dry land, meadows.
	Water bodies	Includes both natural and artificially created water bodies such as Rivers, Streams and Ponds, side flood plain area and sands.

Source: Adopted from LULC, 2016

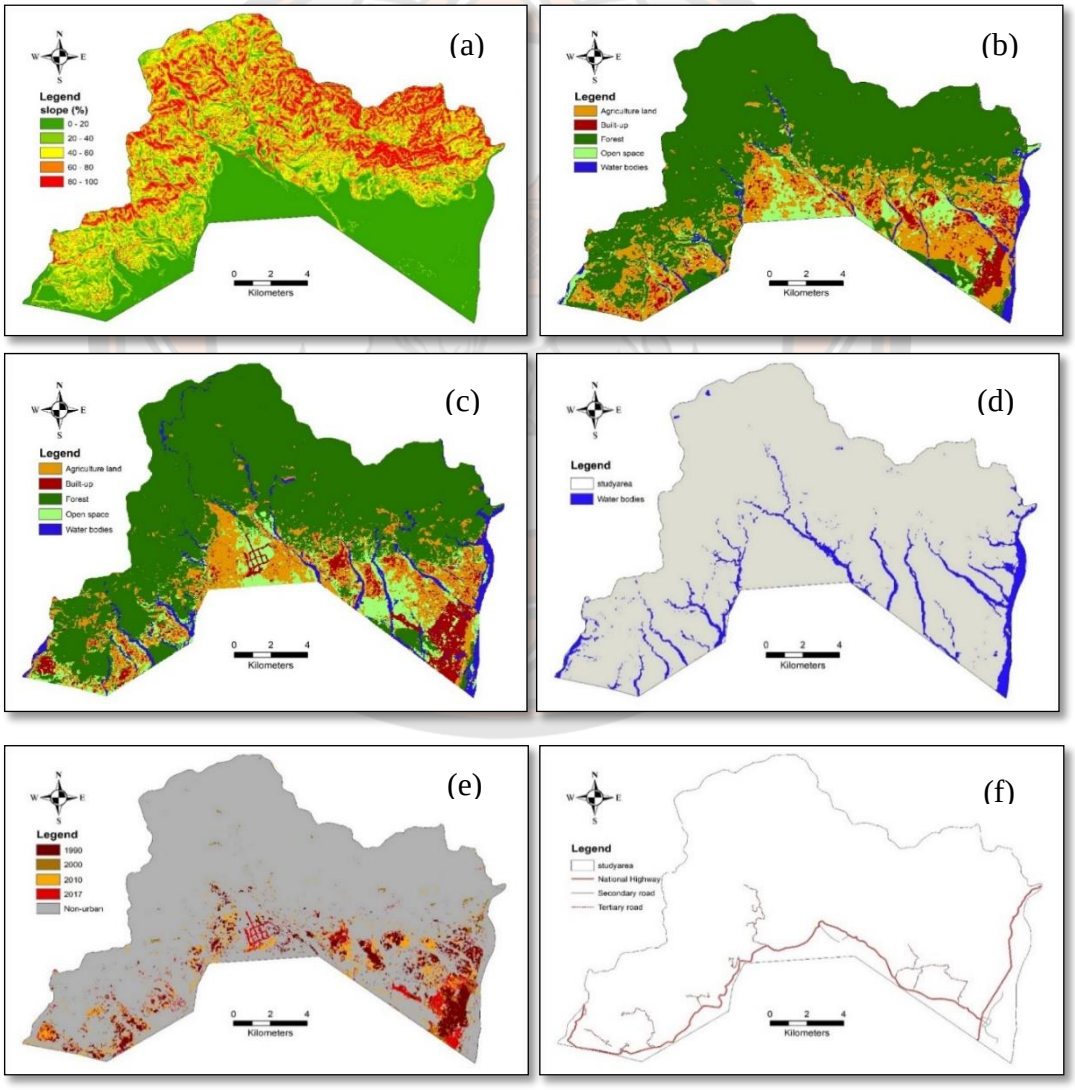

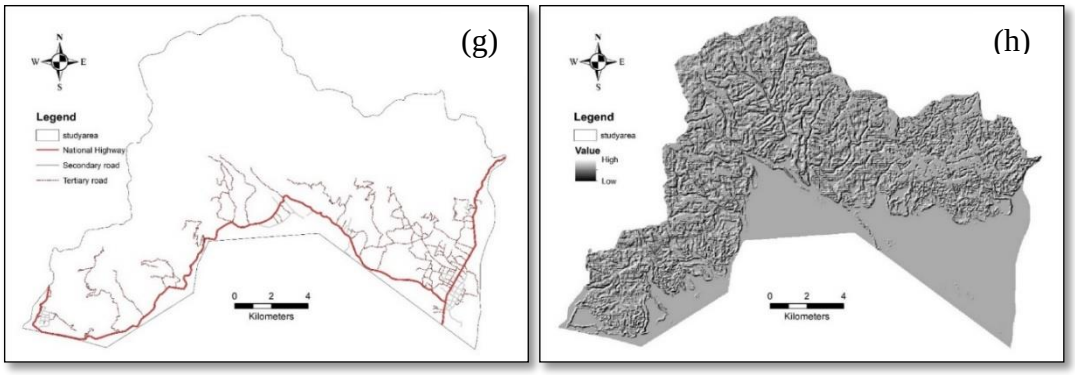

Figure 5 Input layers for the SLEUTH model.

(a) Slope layer, (b) Land use 1990, (c) Land use 2017, (d) Excluded layer, (e) Urban extent, (f) Road layer 1990, (g) Road layer 2017, & (h) Hillshade layer

LULC classification

Image classification aims to automatically classify all pixels in an image into land cover classes (Alphan, 2003). The basic of remote sensing image classification is the spectral characteristics of the earth's surface features. While it is relatively easy to generate a land cover map from a remote sensing image but it is difficult to generate inaccurate as desired (Rongqun & Daolin, 2011). In this study, a supervised classification technique which is the most popular method for assessing remote sensing images was used and the maximum likelihood classifier algorithm was applied. Thermal band (band 6) was removed from the Landsat 5 Thematic Mapper and bands 1 to 7 and 9 were used for Landsat 8 (OLI/TIRS) for classification. ERDAS Imagine 2014 program was used for image classification.

Accuracy assessment

Image accuracy assessment are necessary to validate the results obtained from the image classifications. It also allows a degree of confidence to be attached to the classification results. The method of accuracy assessment used in this study is based on the pixel scale to derive the accuracy of classification in the remotely sensed data which is resulted from the calculation of the error matrix. It contains information

on a classification result of both user and producer accuracies of classification carried out by the classification system.

The pixels that have been categorized from the image was compared to the same area in the ground. The sample size of the test point/pixels was derived based on the thumb rule that, it should be at least be ten times the number of classes for each land use class. With five Land use land cover classes, the total sample size was computed as 5*10*5 = 250 points/pixels. The number of points/pixels for each class were determined by using the ratio calculation, where the classes are assigned a rank in the ascending order of their area and each rank is divided by the total rank multiplied by the total number of sample points/pixels. Stratified random sampling strategy was used to create a points that are randomly distributed within each class, where each class has a number of points proportional to its relative area.

The result of an accuracy assessment provides the users with overall accuracy, User's accuracy and Producer's accuracy of the map. Among many measurements proposed to improve the interpretation of the meaning of error matrix, the Kappa coefficient is one of the most popular measures in addressing the difference between the actual agreement and chance agreement (Fan et al., 2007). The value greater than 0.80 represents good classification; the value between 0.40 and 0.80 as moderate and value less than 0.40 represents the poor agreement.

SLEUTH model implementation

Model calibration

Model calibration was done with SLEUTH version 3.0 beta with patch 1 obtained from the Project Gigalopolis web page. The model calibrate through Cygwin command which is a Linux based emulator that runs inside windows. Before running the calibration mode, test run is done in order to check if input data sets were correctly prepared as per the model requirement. The purpose of calibration is to obtain the best set of parameters to make the model capable of simulating a city with the best similarity with the real world scenario (Oguz et al., 2007). The calibration was performed in three phases; coarse, fine and final phases. Input data in 30 meters resolution were resampled into 120 meters to be used in the coarse calibration phase,

into 60 meters to be used in the fine calibration phase. Data sets with 30 meters (full resolution) were used in the final calibration phase. These resolutions were applied due to the model's extensive computational demands, which are directly proportionated to the resolution of the data and the size of the area to be modeled (Watkiss, 2008).

In this study, the calibration phase encompassed the years from 1990 to 2017 and four urban extent map of the year 1990, 2000, 2010 and 2017 was utilized. In each phase, the coefficient range, increment size, and resolution of the input layers were changed. To find the best fit model, 11 different metrics were calculated for each run of the model. In this study, the shape factor called LeeSallee metric was used for choosing the best parameters set. The output statistics file was sorted by descending order using LeeSallee metric and the six highest scoring values and respective parameter values were selected.

Coarse phase

The first phase of model calibration starts from the coarse resolution of the input data sets. In this phase model parameters are widely defined. It is recommended to set to (0-100,25), where the 0 is the start vale, 100 is the stop value, and 25 is the step (Project gigalopolis, 2003). This gives 3,125 (5^5) different parameter sets that are tested to determine which range of parameter sets that best describes the data located within the calibration phase. To reduce the computation time, a value of 4 is used for the number of Monte Carlo computations.

Fine phase

In the fine calibration phase, it further narrow down the parameter ranges to about 10 or less (± 5) and it takes steps of 5 or 6 units through the coefficient space (Project gigalopolis, 2003) and more times of Monte Carlo iterations (number_of_times) was used to reduce the level of error. It was increased to 8 and the unit computation time also increases with a larger number of Monte Carlo iteration.

Final phase

Using the best-fit values found in the control_stats.log file produced in the fine calibration phase, the range of possible coefficient values is narrowed. The range is narrowed so that the increment of 1-3 may be used while using about 5-6 values per coefficient (eg, for a single coefficient, value = (4,6,8,10,12) and a larger number of Monte Carlo iterations (number_of_times) to 10 is used.

Deriving forecasting coefficients

The best coefficients obtained from the final calibration was the starting values of the control coefficients. Due to SLEUTH's self-modification, these starting values (Start_date) tend to change when the model run is complete (stop_date). To initialize the forecasting, the end date values form the best-calibrated coefficients are preferred. However, due to the random variability of the model, averaged parameter results of many Monte Carlo iterations will result in more robust forecasting parameters (Rafiee et al., 2009). The best coefficient values in 100 Monte Carlo iterations were used with one step increment to derived and average values for each parameter.

Model simulation

The urban growth and landscape change from past to present was simulated and project the future changes for different scenarios. The model simulation from past to present (1990 – 2017) would serve as a visual confirmation for the model calibration. It would also provide a historical view of urban growth and landscape change. For model simulation, the final derived coefficients value are used as the starting values for model simulation. In order to minimize the uncertainty in model simulation. Higher value of 100 Monte Carlo iterations is used. The model simulation produce various statistical measures apart from the simulated images which will represent the general trend of urban growth.

Model validation

In this study, the model validation was conducted by comparing the simulated results generated from the SLEUTH model with observed maps through the evaluation of fit metrics. As discussed in previous chapter, there are many ways to assess the model simulation accuracy and choosing an appropriate method is its ability to represent the perfect match between the modeled and actual urban growth patterns. It is learned that visual interpretation is also one of the important validation of model accuracy since it gives a visual idea about the different growth patterns and different land-use types if the land use land cover map is modeled. The accuracy of the models is judged by their predictive power (Silva & Clarke, 2002).

Model prediction

The model prediction phase simulates the future urban growth of the city using historical growth trends from the past to present (Yang & Lo, 2003). It is the last step of the modeling phase of the SLEUTH model implementation (Bihamta et al., 2014). The result of executing the prediction mode is a probabilistic map which shows the probability of each cell being urbanized in the future. In this study, we used the first approach of the model prediction through assigning different level of protection values to the excluded layers as reflected in chapter two. Based on the model calibration results, the future urban growth trend was predicted to year 2047 with three different management scenarios, each of which is linked with different conditions for future urban development. The excluded layer served as the main tool to differentiate between those management scenarios. The values of the excluded area layers under these three different scenarios are shown in table 5.

Table 5 The growth scenario and level of protection

Growth Scenarios	Excluded from development (in percent)					
	Agriculture	Forest	open space	urban built-up	Water bodies	Unclassified
Business as usual (BAU)	100	0	0	0	100	100

Growth Scenarios	Excluded from development (in percent)					
	Agriculture	Forest	open space	urban built-up	Water bodies	Unclassified
Managed growth scenario (MGS)	100	50	50	0	100	100
Compact growth scenario (CGS)	100	80	80	0	100	100

These growth scenarios and level of protection dictates the future urban growth. The model scenario can be designed in line with the policy framework or with plans and priority for the development of the particular area. In this study, the development of scenarios and level of urban growth protection were designed based on the major land use classification system and accordance with the existing acts and policies of the country. According to Oana et al., (2011), the design of scenarios ('What If?') in the context of policy option for both regional and local planning has been considered very important and it has inspired the discussion among researchers more than other forms of reports such as graphs and text (Oana et al., 2011).

Three possible scenarios for future urban growth are considered in this study. The first scenario which we called as Business as Usual (BAU) scenario assumes that the present growth trend would remain when developmental activities do not change. Model prediction was carried out with the same initial conditions used for the model simulation from past to present. The scenario has excluded the agriculture land from future development in accordance with the existing laws and regulations of the country. According to the Land Act of Kingdom of Bhutan, 2007, development has been strictly prohibited in such land category. Some study suggest that the business as usual scenario could be defined based on its own developmental process and would represent a continuation of the current development policy and used the existing interventions (Zhu et al., 2019). Two aspects were accounted for the design of such scenarios: Protective level, location and size of different land use types, and if there are urban development zones defined by planning project, industrial zones, and policy zones that are influenced by national, regional, and local policies (Xi et al., 2009).

The second scenario considers more managed form of urban growth. We called it Managed growth scenario (MGS). While the level of growth in Agriculture land are still valid as first scenario, this managed growth scenario gives the options of growth strategy in which level of protection value in natural environment and other land category is emphasized in hope of creating more livable city. The protection level was defined 50% for both the forest and open space (a 50% urban growth probability) within the boundary.

The third form of growth scenario is term as Compact growth scenario. In this scenario, more growth constraint are applied compared to other two scenarios and kept only 20 percent probability for urban development. (See Table 5). Designing and developing such scenario would help planners and decision makers for management of city growth in future. The results of the model calibration and prediction from these growth scenarios will be discussed in the next chapter.

CHAPTER IV

RESULTS

In the previous chapters, the attempt was made to illustrate the SLEUTH model functions that can study the urban growth using the historical datasets and how urban growth can be analyzed by adopting related methods. In order to evaluate the performance of the proposed methods described in previous chapter and for better understanding of the urban growth scenarios in the current study area, the methods have been applied and the findings of the study was discussed in this chapter in detail.

Urban growth change from 1990 to 2017

The main idea of using satellite images to prepare data for this study is to define the initial state of the urban simulation at actual year 1990 and to use the results from images to detect the urban growth and to validate the model for future growth scenarios. Four time series images at different dates, 1990, 2000, 2010 and 2017 were used to derive the actual urban extent and then analyzed the urban change from 1990 to 2017. Figure 6 depicts the actual distribution of land use land cover from which comparable changes can be extracted. The 1990 image from a Landsat5 TM with 30-metre resolution, and the 2017 image from a Landsat8 (OLI/TIRS) with 30-metre resolution is used. Both images are represented with false colour composite with band 5 as red, band 4 as green and band 3 as the blue colour in Landsat5 TM and band 7 as red, band 5 as green and band 3 as blue colour in Landsat8 image. In order to detect the land use/cover change, both images need to be classified. Five land use classes which comprise built-up areas, agriculture land, forest, open space, and water bodies were used for the classification. The method used was a supervised classification based on the Maximum Likelihood Classification as described in the previous chapter.

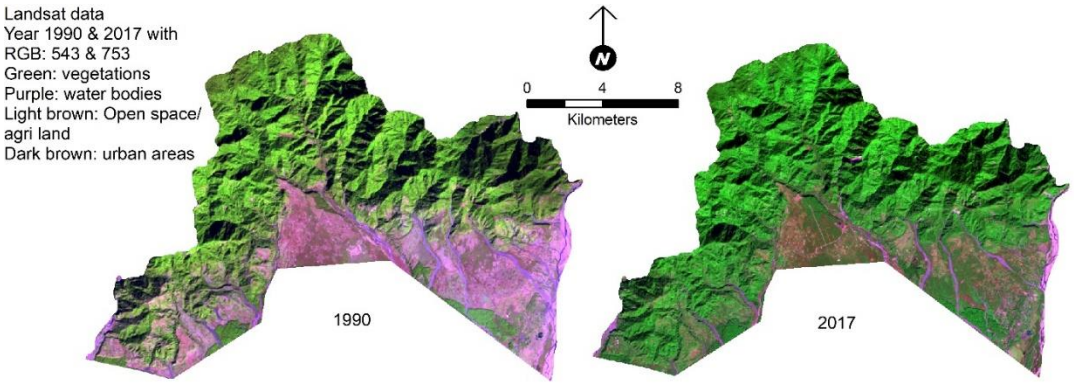

Figure 6 Satellite Images covering Gelephu city Area 1990 and 2017

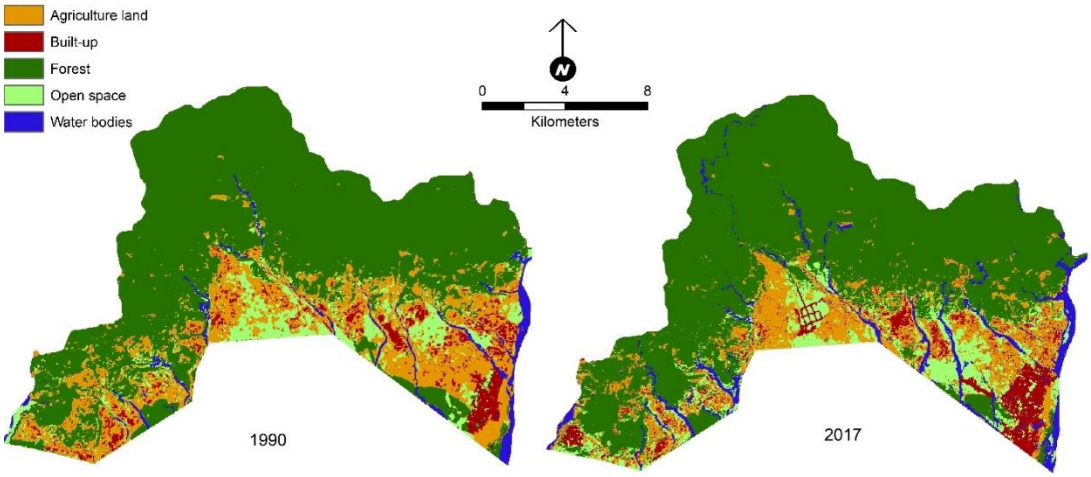

Figure 7 Classified Images 1990 and 2017

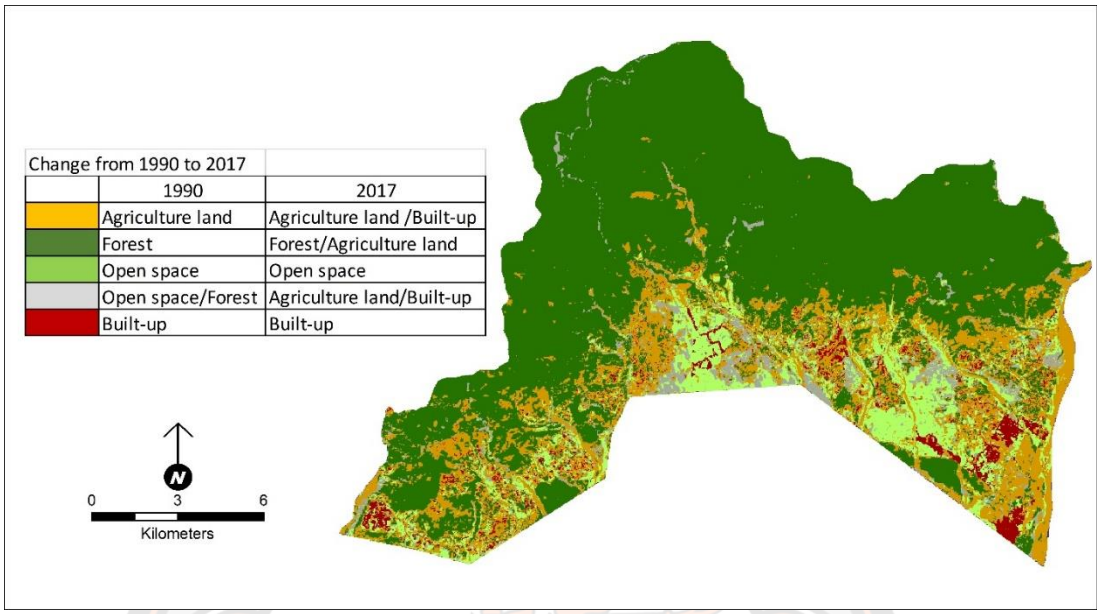

Figure 8 Land use/cover changes between 1990 and 2017

Both the classification images provides good view of land use change in the area with considerable change in more than two decades as shown in Figure 7. More change was seen in the urban area (built-up areas). In 1990, built-up areas were seen sparely located apart from the concentrated around the current city area with evidence that during the time, the area falls in the rural jurisdiction. By 2017, the urban built-up has increased much larger than ever before with dramatic expansion especially in the peri-urban region where the area has been identified as economic zone in the central part of the study area.

The Figure 8 and Table 6 visualize the actual changes in land use/cover from 1990 to 2017. Urban built-up area increased from 11 sq.km to 14 sq.km approximately, while the forest, open space and water bodies in 2017 increased about 11 sq.km approximately in total from 1990. Only agriculture land was decreased drastically from about 53 sq.km to 38 sq.km in 2017 which is about 28%. Agriculture land was a predominant land use changes in the region. Decrease of this land class attributed the increase of other land classes such as open spaces, built-up, and forest areas. The increase in forest area could be due to the concentration of urban built-up

in the specific location through municipal local area planning and conversion of open space into the forest area with less agriculture farming. Furthermore, it appears that agriculture land has changed into another Land use/cover type such as increase of water bodies. Climate change being one of the major factor for land conversion globally, river course changes every year due to major floods and the major change observed were due to the flood plain areas which was included in the water body class. In general, these land use/cover data explicitly stated that the increase in built-up and open space areas resulted in decrease in agriculture land. Its change could be the indication of a trend which may affect to the urban sustainability and regional economic development in large.

Table 6 Land use/cover changes in the study area

Land use	Approximate area* (Sq Km)				Changes Sq Km	Rate of Changes** %
	1990	%	2017	%		
Agriculture land	53.01	21.72	37.98	15.57	-15.03	-28.36
Open space	20.42	8.36	24.11	9.88	3.69	+18.09
Water bodies	7.89	3.23	12.89	5.28	5.00	+63.30
Forest	151.39	62.02	154.63	63.38	3.24	+2.14
Built-up	11.39	4.67	14.35	5.88	2.96	+25.97
	244	**100**	**244**	**100**		

*Areas are calculated based on 30m resolution

** + = increase and - = decrease

LULC classification Accuracy assessment

The accuracy of LULC change along with the overall accuracy and the Kappa coefficient was summarized in Table 4.2 & Table 4.3 respectively. The overall accuracy of the classification image of 1990 and 2017 was 88.4% and 90.80%, and the Kappa coefficient was 0.805 and 0.837. The overall accuracy is calculated based on the number of correct pixels in the classification compared to the growth truth or

reference data point with respect to the total number of pixels (see Equation 1). Similarly, the Kappa coefficient is a ratio representing difference between observed and expected sets of data. The kappa coefficient of 0.8, represents that there is an 80% probability that the result from the classification matches as per the actual reference data used for validation. Other accuracies derived from the confusion matrix are producer's and user's accuracy. It was observed that the producer's accuracies of all the classes were consistently high, ranging from 57% to 98% in both the classification image. Similarly, the user's accuracies for all the classes were precisely high, ranging from 60% to 97% except water bodies and built-up in 1990 which shows 100 percent correctly classified. The above Producer's accuracy and User's accuracy was computed based on the equation no. (2) & (3).

Table 7 Confusion matrix for 1990

Classes	**Reference Data**						**User's Accuracy (%)**
	Agriculture land	**Open space**	**Water bodies**	**Forest**	**Built-up**	**Total**	
Agriculture land	**34**	8	4	1	7	54	62.96
Open space	0	**20**	0	1	0	21	95.24
Water bodies	0	0	**10**	0	0	10	100.00
Forest	1	5	2	**147**	0	155	94.84
Built-up	0	0	0	0	**10**	10	100.00
Total	35	33	16	149	17	**250**	**Overall Accuracy *88.40%***
Producer's Accuracy (%)	97.14	60.61	62.50	98.66	58.82		**Kappa coefficient *0.805***

Table 8 Confusion matrix for 2017

Classes	Reference Data						User's Accuracy (%)
	Agriculture land	**Forest**	**Water bodies**	**Open space**	**Built-up**	**Total**	
Agriculture land	**28**	1	1	2	7	39	71.79
Forest	0	**154**	2	1	1	158	97.47
Water bodies	0	0	**12**	0	1	13	92.31
Open space	2	2	0	**21**	0	25	84.00
Built-up	2	0	0	1	**12**	15	80.00
Total	32	157	15	25	21	**250**	**Overall Accuracy *90.80%***
Producer's Accuracy (%)	87.50	98.09	80.00	84.00	57.14		**Kappa coefficient *0.837***

Anderson et al, (1976) suggested that the minimum level of image interpretation accuracy in the identification of land use and land cover classes from the remote sense data should be at least 85 percent. (Anderson et al., 1976). This indicates that the accuracy of the land use map classified for this study is relatively higher as expected. The high accuracy of the classification was confirmed by the accuracy assessment, which indicated low commission error in both classification image 1990 and 2017. Especially the open space, built-up, and water bodies. The error of commission are in relation to the classification results which refers the sites that are misclassified to other class that in fact do not belong to it. (See Table 9). On the other hand, these land classes had high omission error (relatively low producer's accuracy), which it refers to the reference sites that were left out from the correct class in the actual classified map.

Table 9 Commission & Omission error

Year	1990		2017	
Class	**Commission error (%)**	**Omission error (%)**	**Commission error (%)**	**Omission error (%)**
Agriculture land	37	3	28	12
Open space	5	39	3	2
Water bodies	0	38	8	20
Forest	5	1	16	16
Built-up	0	41	2	43

Model calibration results

The result was obtained through the calibration of historical urban extent data in three phases as described in the previous chapter. The input 120 meter spatial resolution with (219 x 153) rows and columns was used. The coefficient for coarse calibration is shown in Table 10 and the results are examined to determine the goodness of fit for each of the parameter sets obtained from the coarse calibration. All the five control coefficients were set start and stop values from 0 to 100 with a step value of 25. Throughout the calibration process, the LeeSallee metric is used as goodness of fit metric to narrow down the model parameter set. The output statistics obtained from the calibration was sorted by descending order using the LeeSallee metric. The highest six scoring values and respective coefficients values were selected which will be then used to form the input parameter ranges in the next calibration phase. (See Table 11)

Table 10 Input coefficients for Coarse (120m) calibration

Coefficient range	Coefficients				
	Diffusion	**Breed**	**Spread**	**Slope**	**Road gravity**
_start	0	0	0	0	0
_step	25	25	25	25	25
_stop	100	100	100	100	100

Table 11 Coefficient selection from coarse calibration

Run	Compare	Pop	Edges	Clusters	Leesalee	Slope	%Urban
29	0.62	0.98	0.91	0.69	0.22	1.00	0.75
34	0.62	0.98	0.91	0.69	0.22	1.00	0.75
39	0.62	0.98	0.91	0.69	0.22	1.00	0.75
44	0.62	0.98	0.91	0.69	0.22	1.00	0.75
49	0.62	0.98	0.91	0.69	0.22	1.00	0.75
25	0.62	0.98	0.90	0.70	0.22	1.00	0.75

Xmean	Ymean	Rad	Diff	Brd	Sprd	Slp	RG
0.49	0.66	0.97	1	1	25	1	100
0.49	0.66	0.97	1	1	25	25	100
0.49	0.66	0.97	1	1	25	50	100
0.49	0.66	0.97	1	1	25	75	100
0.49	0.66	0.97	1	1	25	100	100
0.42	0.41	0.97	1	1	25	1	1

For the fine calibration, the same procedure was followed. A dataset of 60 meter spatial resolution with (438 x 306) rows and columns was used in the calibration process. The coefficients selected from the coarse calibration is used to derive the input coefficients for the fine calibration as shown in the Table 12.

Table 12 Input coefficients for fine (60m) calibration

Coefficient range	Coefficients				
	Diffusion	Breed	Spread	Slope	Road gravity
_start	0	0	0	0	0
_step	5	5	5	20	20
_stop	20	20	25	100	100

Table 13 Coefficient selection from fine calibration

Run	Compare	Pop	Edges	Clusters	Leesalee	Slope	%Urban
398	0.68	1.00	0.92	0.60	0.21	0.54	0.86
404	0.68	1.00	0.92	0.60	0.21	0.54	0.86
410	0.68	1.00	0.92	0.60	0.21	0.54	0.86
416	0.68	1.00	0.92	0.60	0.21	0.54	0.86
422	0.68	1.00	0.92	0.60	0.21	0.54	0.86
428	0.68	1.00	0.92	0.60	0.21	0.54	0.86

Xmean	Ymean	Rad	Diff	Brd	Sprd	Slp	RG
0.41	0.23	1	1	5	25	1	40
0.41	0.23	1	1	5	25	20	40
0.41	0.23	1	1	5	25	40	40
0.41	0.23	1	1	5	25	60	40
0.41	0.23	1	1	5	25	80	40
0.41	0.23	1	1	5	25	100	40

The third stage is the final calibration. It was conducted in 30 meter spatial resolution with (875 x 611) rows and columns, intending to determine the best combination. The final results of the calibration process are coefficient values that best simulate historical growth for a region. Using the best coefficients derived from the fine calibration and running the SLEUTH model from historical datasets, it derives the single set of coefficients which will be used to initialize a prediction run of SLEUTH model. Table 13 shows the coefficient selection from the fine calibration to derive the input coefficient for final calibration phase. (Table 14).

Table 14 Input coefficients for final (30m) calibration

Coefficient range	Coefficients				
	Diffusion	Breed	Spread	Slope	Road gravity
_start	1	3	23	0	38
_step	1	1	1	20	1
_stop	5	7	27	100	42

Table 15 Coefficient selection from final calibration

Run	Compare	Pop	Edges	Clusters	Leesalee	Slope	%Urban
60	0.57	0.81	0.39	0.56	0.18	0.99	0.29
61	0.57	0.81	0.39	0.56	0.18	0.99	0.29
62	0.57	0.81	0.39	0.56	0.18	0.99	0.29
63	0.57	0.81	0.39	0.56	0.18	0.99	0.29
64	0.57	0.81	0.39	0.56	0.18	0.99	0.29
65	0.57	0.81	0.39	0.56	0.18	0.99	0.29

Xmean	Ymean	Rad	Diff	Brd	Sprd	Slp	RG
0.43	0.97	0.83	**1**	**5**	**23**	**1**	**38**
0.43	0.97	0.83	1	5	23	20	38
0.43	0.97	0.83	1	5	23	40	38
0.43	0.97	0.83	1	5	23	60	38
0.43	0.97	0.83	1	5	23	80	38
0.43	0.97	0.83	1	5	23	100	38

Deriving forecast coefficient

The calibration process produces initializing coefficient values that best simulate historical or past growth in the region. However, due to model self-modification, coefficient values at the initial date of a model run may be changed by the stop date. For this, the best coefficients derived from the final calibration (Table 15), were used to narrow down the input coefficient. (See Table 16). The self-modification nature of SLEUTH model produced through final calibration run for deriving the forecasting coefficients which shows the average coefficients changed in every control years. (See Table 17).

Table 16 Input coefficients for deriving the forecasting value

Coefficient range	Coefficients				
	Diffusion	Breed	Spread	Slope	Road gravity
_start	1	5	23	1	38
_step	1	1	1	1	1
_stop	1	5	23	1	38

Table 17 Output from self-modification of SLEUTH

year	area	%urban	diffus	breed	spread	slp_res	rd_grav
2000	18439.93	10.07	1.09	5.43	24.99	0.95	38.79
2010	20760.08	11.17	1.06	5.23	24.08	1.08	38.98
2017	21829.43	18.23	**0.66**	**4.96**	**14.98**	**19.79**	**38.71**

Simulation from past to present

Most of the statistics obtained in the calibration phases present high values of goodness of fit, indicating the ability of the model to represent the historical growth. It was found that the model best captured the growth characterics of the study area in the final resolution (30 meter) of input datasets. Most of the metrics were increasing with increased in spatial resolution of the input data. (See figure 9).

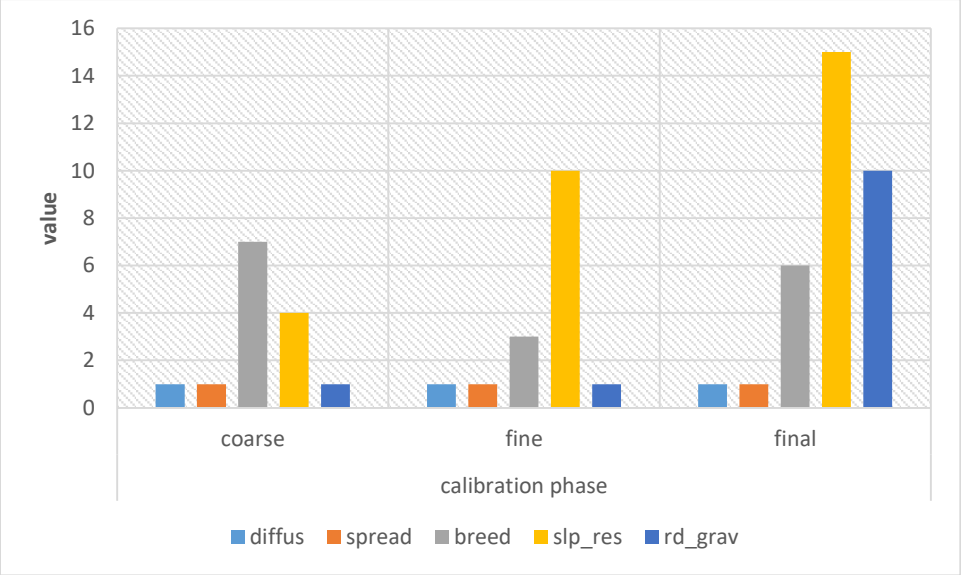

Figure 9 Change of growth coefficient

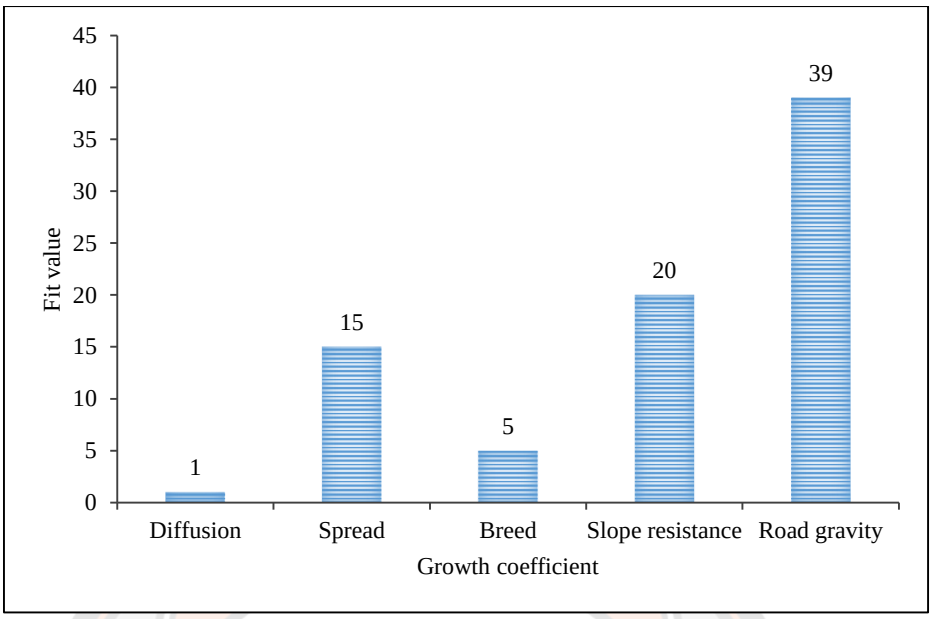

Figure 10 Best fit parameters for forecasting

Using the final calibration values, the best fit coefficient was derived for model prediction. Figure 10 shows the best fit values which defines the type of urban growth behavior which is controlled through the five growth coefficients. These coefficiets values are used to initiatize a prediction run of SLEUTH. It was observed that the urban growth in the region is highly influenced by the road gravity coefficient (39). It shows the existing road networks had played important role in attracting urban growth and development in the region.

The high value of slope resistance coefficient (20) indicates that the topography is a barrier to urban development in the region, and the increasing steeper slopes are less likely to urbanize. This is evident from the current setting of the urban area. Simillarly, the high spread coefficient (15) determines the expansion of urban centers from the existing urban areas and urban cores. However, the low diffusion and breed coefficients reflects low likelihood of dispersive growth and low probability of growth of new detached urban settlements from the existing growth. This shows the current growth is taking place mostly towards the existing urban areas and urban cores and along with transportation networks.

Model validation and Accuracy assessment

Model accuracy is an integral part of the predictive modeling especially when models are used for decision-making process (Abedini & Azizi, 2016). Using the model final calibration results, the urban growth from 1990 to 2017 was simulated and the simulation result was compared with the actual or observed 2017 urban maps obtained from the satellite image through classification. The comparison of model was done both visually and through goodness of fit metrics. It was observed that the "population" (number of urban pixels) metric yield a fit value of 0.812 and for "compare" it is 0.703 showing high correlation between modeled final urban extent to actual final urban extent. Most of the metrics of the model simulation results shows high values of fit, indicating the model's ability to represent the real growth scenario and perform the growth prediction (See Figure 11). Moreover, the visual comparison presents whether the modeled urban form fits with the actual urban form or not. (Figure 12).

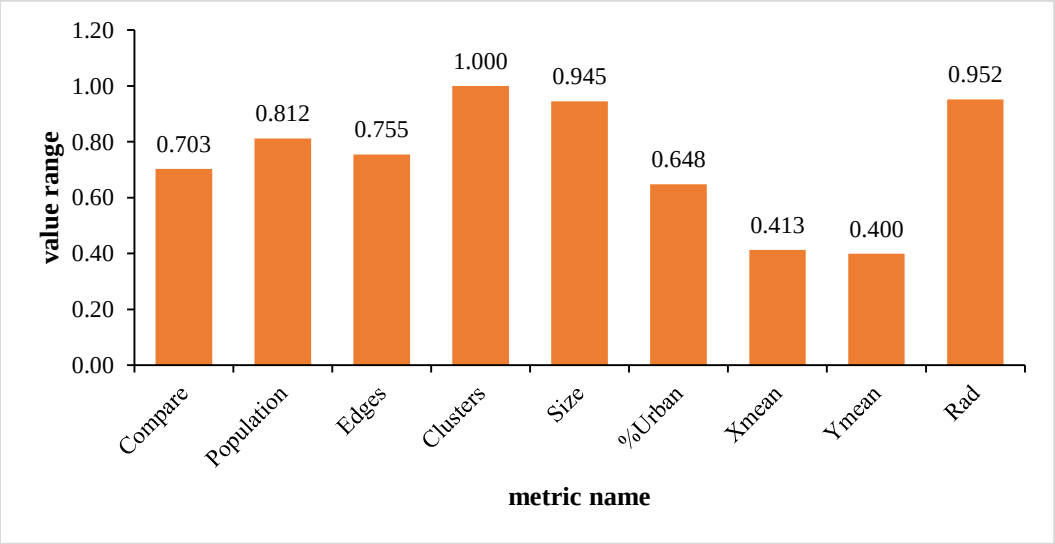

Figure 11 Spatial fit metrics generated through model simulation.

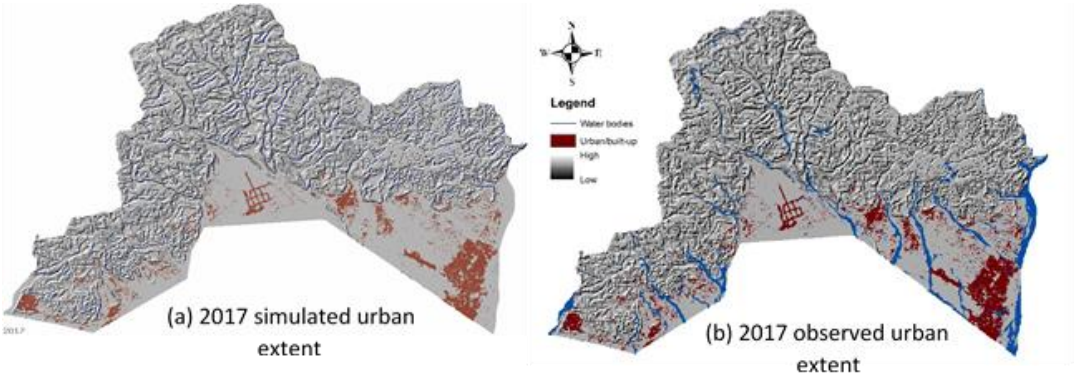

Figure 12 Visual comparison of model simulation and actual urban extent

Model prediction results

The urban growth parameters derived through model calibration process were used in the model prediction phase. The final current urban layer is used as the start "seed" year and the prediction was run for next 30 years from 2017 to 2047. The model produced an urban growth and extent for every year following the start "seed" year till to the end year. However, to highlight the urban growth changes, images were selected at an interval of ten years. It was noted that the urban exclusion layers served as one of the important input layer for the model to predict the future urban growth in different scenarios and to obtain information about future development alternatives. Detail of scenario development and level of urban growth protection were presented in previous chapter. Figure 13 illustrate the predicted future urban growth in three different management scenarios.

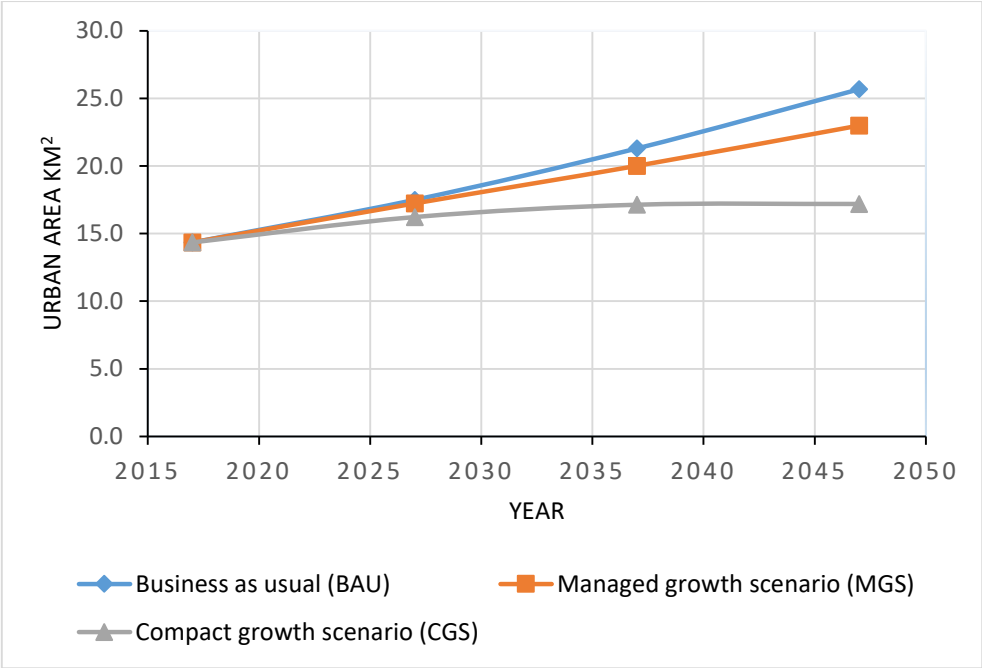

Figure 13 Comparison of urban growth for three scenarios

The results indicates that, if the historical urban growth pattern continues to be the same, approximately 26 sq.km will be added by 2047 to current area in 2017. In other hand, urban extent will be more than twice times. If the urban growth continues the Business as usual trends, the limited agricultural land along with natural environment will get consumed. The Compact growth scenario, with maximum growth protection applied in forest and open space land class (80 percent) showed the smallest increase of the urban extent in future compared to Business as usual growth and managed growth scenarios. The growth would expand approximately 17 sq.km by 2047 compared to current area in 2017. This form of urban expansion showed compact city growth with approximately saving 9 sq.km of urban land when comparing with the business as usual scenario.

The urban expansion in the second scenario will cover approximately 23 sq.km by 2047, which is 3 sq.km less then Business as usual scenario but 5 sq.km more than compact growth scenario. This scenario had defined (50 percent) protection level for forest and open space land classes. From these findings, Managed growth scenario (MGS) would be the ideal and manageable for future growth in the region

which facilitates provision of urban services by the city managers and urban planners with limited human habitat land available in the region. Hence, the MGS is preferred against other form of growth in the current study area.

The probability of urban growth scenario predictions (Figures 14 – 16) show higher dispersed development patterns for the Business as usual than the managed growth scenario with moderate protection, while compact growth with maximum protection shows highly constrained growth in the region. The output urban layers for future dates as presented above are not only shown as urban and non-urban but also with probability range of future urbanization accordingly to the scenario development. These probabilities are divided broadly into five discrete classes: 50%, 50-69%, 70-79%, 80-89%, and 90-100%.

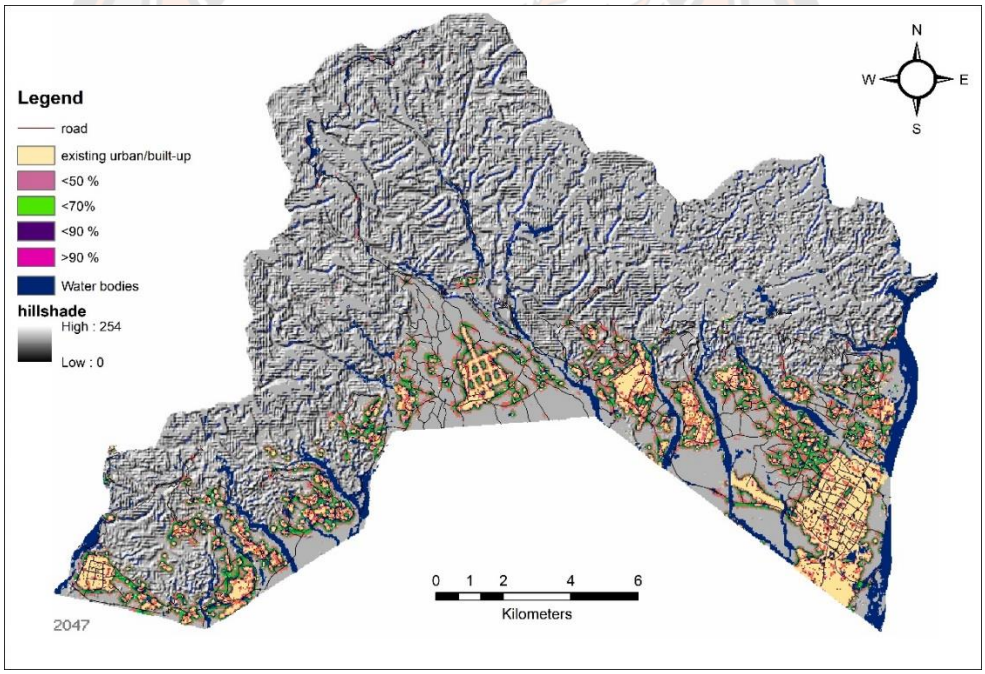

Figure 14 Probability of urban growth in Business as usual scenario

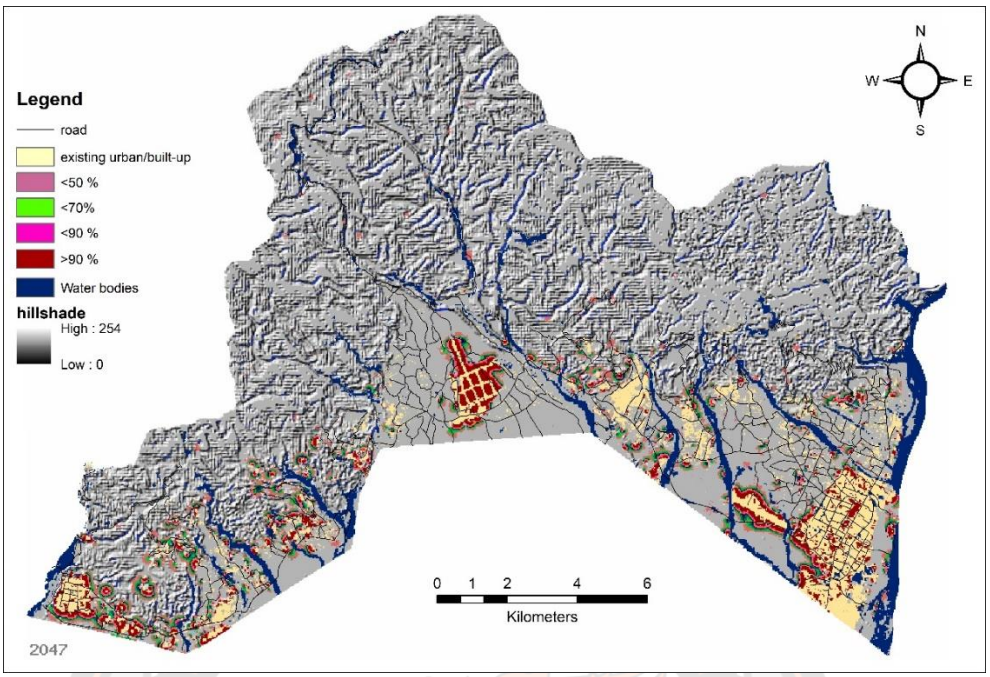

Figure 15 Probability of urban growth in Managed growth scenario

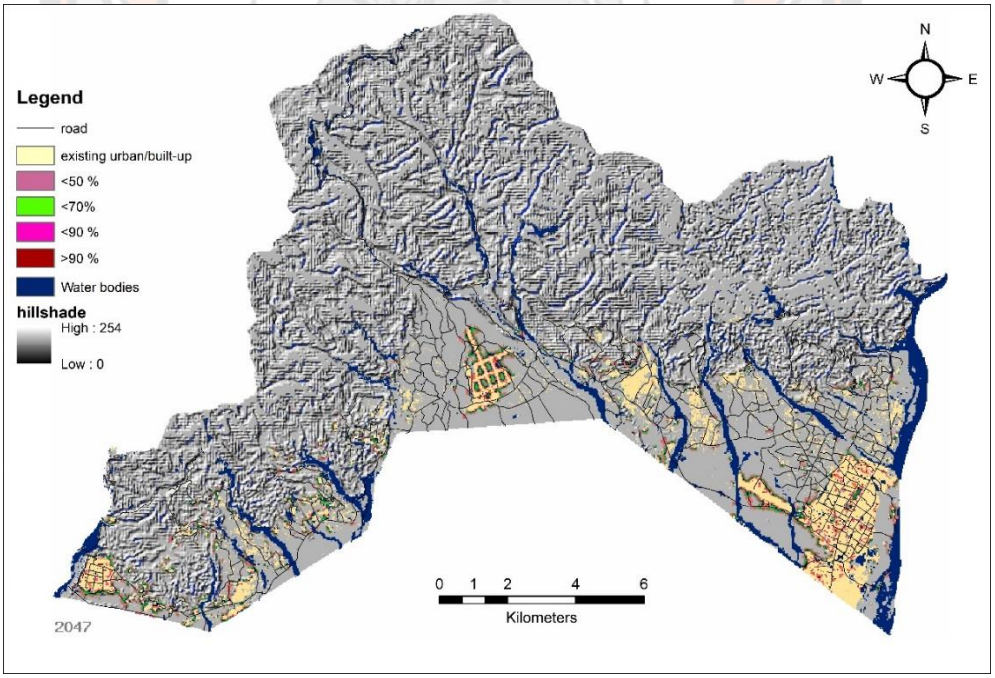

Figure 16 Probability of urban growth in Compact growth scenario

It was observed that with increase in time period, the probability of urbanization becomes high. The cells which indicates less probable to urbanize in year 2027 has high probability in year 2047. However, growth parameters differ in each growth scenarios. Gradual change of urban growth environment was clearly visible along the existing urban fringes, most notably along the existing transportation networks and in area where less growth constraints are applied. The accuracy of model prediction in 2047 needs to be interpreted in light of SLEUTH's earlier model accuracy from past to present scenario. At best that analysis can help to conclude that about more than 50 percent of the growth could be geographically correct and show high values of fit metrics. Table 18 below shows the future urban growth statistical measures selected for ten years' time period in all three scenarios to see the effect of growth parameters.

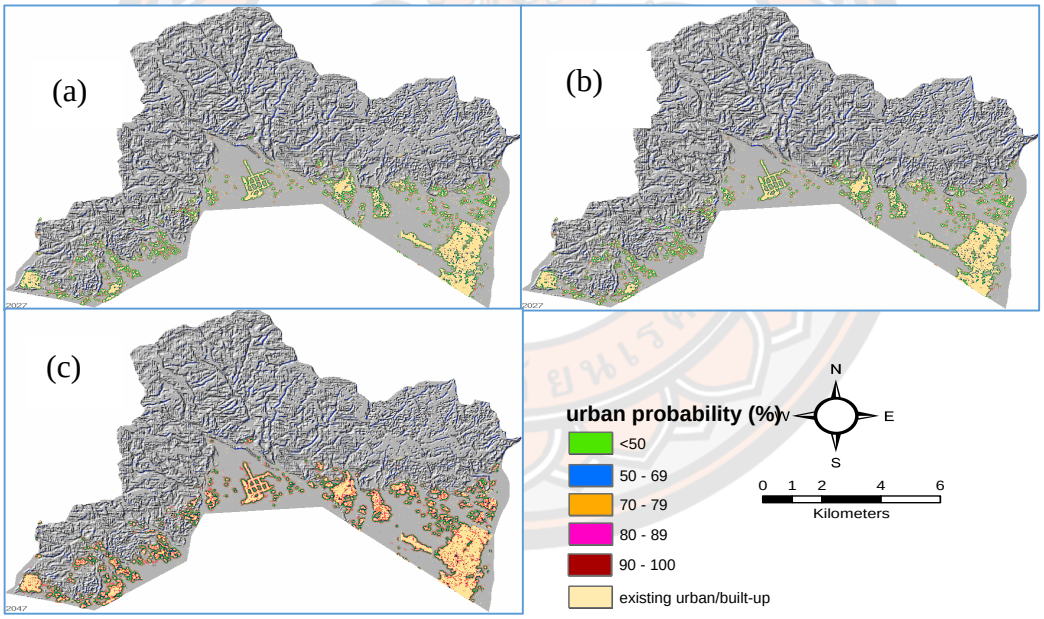

Figure 17 Modeling output results in BAU scenario

(a) 2027, (b) 2037, & (c) 2047

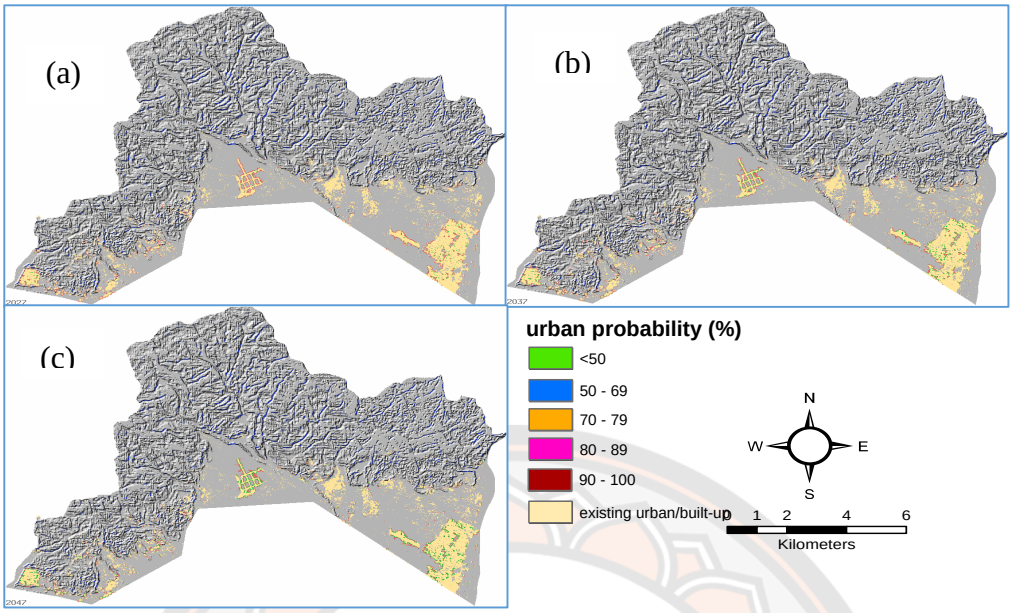

Figure 18 Modeling output results in MGS scenario

(a) 2027, (b) 2037, & (c) 2047

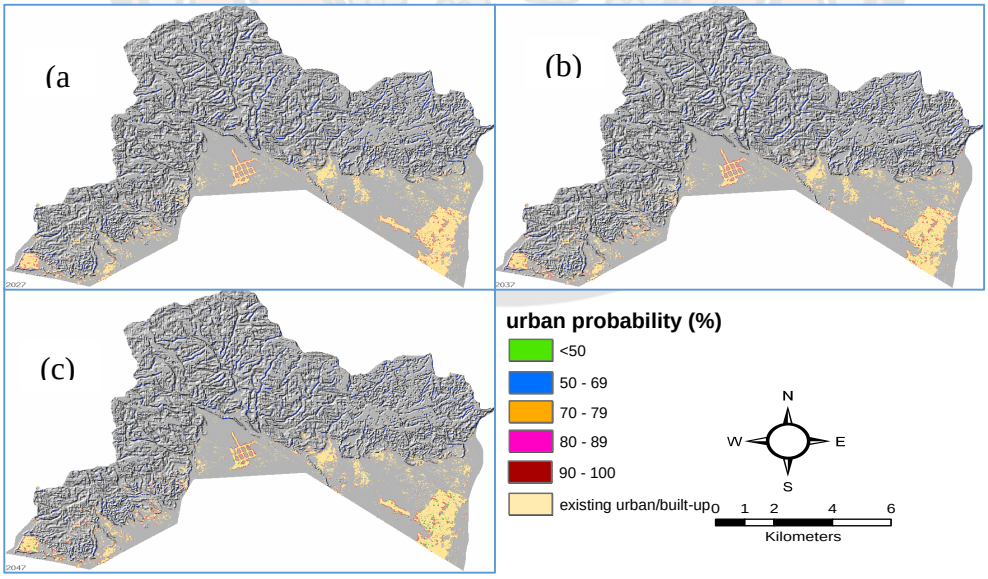

Figure 19 Modeling output results in CGS scenario

(a) 2027, (b) 2037, & (c) 2047

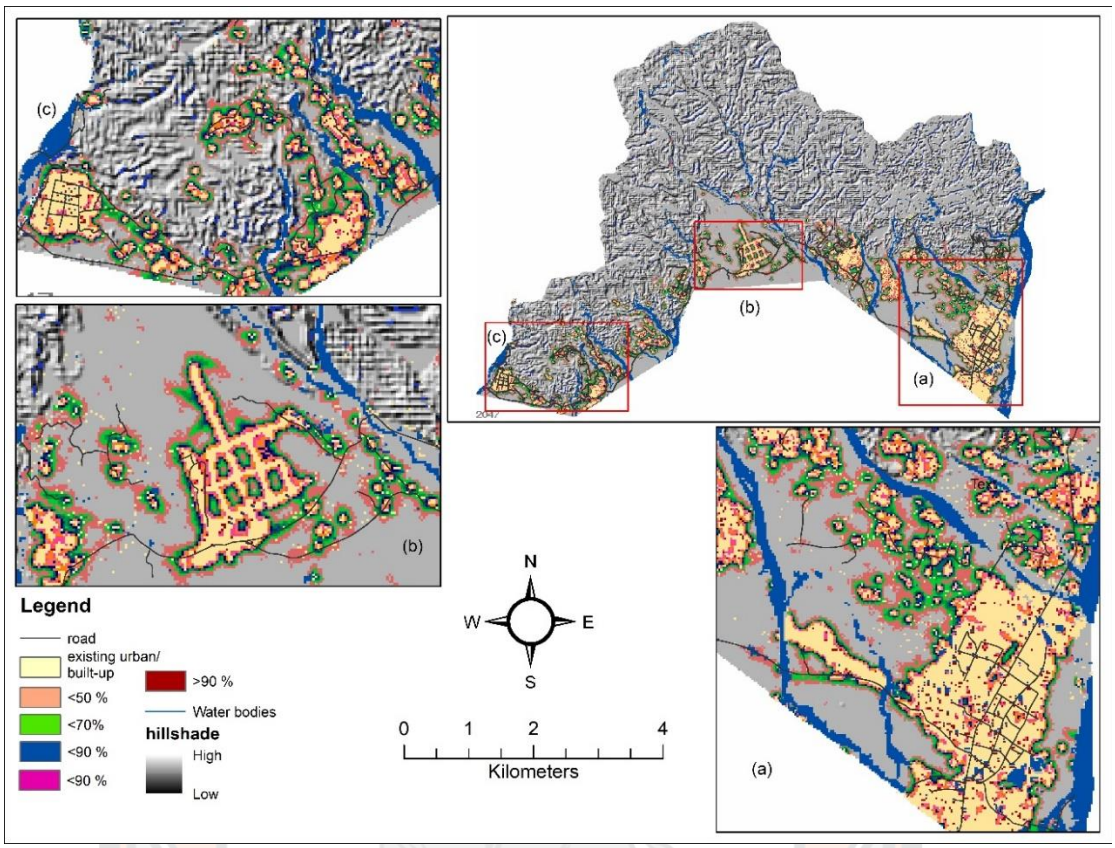

Figure 20 Output of urban growth using SLEUTH model to the year 2047

(a) Gelephu city area (right), (b) Jigmeling area (middle), future economic zone area, (c) Dzongkhag Head quarter region (left)

The results revealed that, cumulative number of urban pixels by spontaneous growth (‘sng’) parameter decreases in all three growth scenarios, indicating the decrease in new urban settlement in developed areas. However, in MGS scenario, little increase was observed from 2037 to 2047 indicating that the urban growth cell tend to randomly selects potential new urban growth cell for urbanization. (Table 18).

The cumulative organic or edge growth pixels (‘og’) is also found to be decreasing irrespective of the scenarios, indicating the less development in the existing urban growth area as compared to its neighborhood by 2047.

Table 18 Future growth statistical measures for three scenarios

Parameters	2027			2037			2047		
	BAU	**MGS**	**CGS**	**BAU**	**MGS**	**CGS**	**BAU**	**MGS**	**CGS**
sng	0.26	0.16	0.08	0.27	0.07	0.05	0.26	0.11	0.04
og	11.65	5.31	2.21	10.55	5.28	1.94	11.02	5.49	2.09
slope	17.82	17.78	17.76	33.23	33.13	33.07	48.71	48.51	48.39
rt_gravity	37.62	37.62	37.62	36.08	36.09	36.09	34.53	34.55	34.56
area	16150	16041	15979	16281	16103	16003	16411	16167	16028
%urban	15.39	15.33	15.3	15.45	15.36	15.31	15.52	15.39	15.32
grw_pix	13.37	6.11	2.38	12.13	5.91	2.19	12.77	6.15	2.33

The other interesting findings were also observed. The current urban growth which is greatly influenced by the road-gravity ('rt') coefficient, will no longer be the impending factor in future urban growth in the current study area. The rate of urban growth along the road networks gets slow down by the year 2047. This could be because we have only used the current 2017 road layer as the 'seed' layer for model prediction.

Currently, there is no future road plan data available in this study area. Had we embedded the future road layers in the model, the growth pattern would not be the same and could be the influencing factors among others as the current growth. In contrast, the slope resistance coefficient continues to acts as a barrier to urban development in future growth scenarios. It was found to be increasing due to more constraints applied especially in the compact form of urban growth. This study of SLEUTH's prediction capabilities shows a fair amount of variation in urban growth due to input data sets. However, these findings from different scenarios can be used as interpretation guides for the urban planners and decision makers that would help or contribute to the overall goal in sustainable urban development in the region.

CHAPTER V

DISCUSSION AND CONCLUSION

Urban growth change

Land use land cover dynamics clearly indicates the change of urban growth in the region. In recent decades, the urban population in the country grew approximately 196 thousand in 2005 to 275 thousand in 2017 constituting 37.8 percent of total population. It is projected that urban population will reach more than 50 percent by 2037 (National Statistics Bureau, 2018). The current study area has a total of 244 sq.km of which only 5 percent was occupied by urban settlements in 1990. However, in 2017, the urbanized area accounted for 26 percent change of the total area, a nearly quintuple increase as per the land use land cover change details (See Table 6). Such increase in urban growth is mainly due to the regional development projects such as development of local area plans, industrial estates, domestic airport, education, health, and public services among others (Ministry of Works and Human Settlement, 2010b).

The conversion of agriculture land into urban areas is a notable conversion in developing countries (Li & Yeh, 2000). The change of agriculture land into urban areas should be limited by devising effective town planning measures since the proposed development projects in the region will increase the potential of urban expansion in future. However, the area within the district head quarter towards west of Gelephu city will experience less urban expansion as compared to the area within the periphery of the Gelephu city because of their location on steep slope of hills. This verifies urbanization mostly occurs in relatively flat areas (Li et al., 2013).

Since the country is made up of mountain slopes, deep gorges and glaciers in the northern areas, flat and gentle slope areas of land are very limited which makes it difficult to secure human habitat, agriculture and infrastructure development. As we have observed from the land cover change details, urban area constitute about 14.35 sq.km, approximately 6 percent compared to the other land classes. Forest land is a dominant among other land class category. The urbanization and rural-urban

migration are the factors exerting direct pressure on urban land. According to the population projection report, 2018 of National Statistical Bureau, the Sarpang Dzongkhag will contribute the third highest share of Dzongkhag population by 2047 including the Gelephu Thromde.

Currently, the Gelephu Thromde with a population size of 9,858 and a land area of 11.5 sq.km has the lowest population density at 856 persons per sq.km compared to other Thromde areas. Thimphu with highest urban population density with 4,389 persons per sq.km, followed by Samdrup Jongkhar and Phuntsholing Thromde with 2,086 and 1,773 persons per sq.km. The urban landscape of Sarpang which was nearly absent in the 1990's has been now modifying the traditional rural landscape at a much faster rate. It was only in the late 1990's and early 2000's that the Dzongkhag began to develop that we see today though the rehabilitation program initiated by His Majesty the Fourth King of Bhutan in 1997 (National Land Commission Secretariat, 2016). The results also revealed the agglomeration of nearby villages or small towns into larger urban extent acting as a key economic links between the two main urban centers at Gelephu towards east and Dzongkhag head quarter towards west. (See Figure 17).

Model calibration and simulation

The SLEUTH model uses the past historical information on urban extent in calibrating and predicting the future urban growth. The parameters used in the model may vary from one urban area to another because every urban has its own unique properties. (Jat et al., 2017). The rigorous calibration process has resulted in identifying a set of diffusion, breed, spread, slope resistance, and road gravity growth coefficients that enable SLEUTH model to simulate the urban growth in Gelephu city over the period of 1990 to 2017.

Our results showed high road gravity and slope coefficient among other three coefficients. The growth in the region is highly influenced by the existing road where it displaces orientation of linear growth pattern along the road networks and slope acting as a barrier for the development. It is important to note that the National highway passes through this location further connecting to other Dzongkhags where

most of the development took along this highway. Such growth and high coefficients were also observed in the other research studies (Abedini & Azizi, 2016; Bihamta et al., 2014; Dadashpoor & Nateghi, 2015).

In our current study area, these two parameters represents main pattern of urban growth especially in peri-urban areas having a linear nature and edge expansion due to slope resistance and road influenced growth. It signifies that building a new transportation networks and infrastructure facilities would contribute such form of urban growth in future growth scenario. On other hand, the value of diffusion parameter and breed parameter was 1 and 5, which is low compared to other parameters indicating the low probability of spontaneous growth and breed coefficient which shows the probability of new spreading center growth pattern in the region. The value of breed coefficient is followed by the diffusion coefficients which is consistent with the findings of Pramanik & Stathakis (2015), and Osman et al. (2016).

In addition, the comparison of this research and other researches shows that LeeSallee index is much similar in the study conducted in Chiang Mai, Thailand (Sangawongse, 2006), and in Tehran metropolitan region (Dadashpoor & Nateghi, 2015), owing to the similar nature of topographic characteristics of the study area. However, the study conducted in other cities such as Pune, India (KantaKumar et al., 2011), Ajmer city in Rajasthan, India (Jat et al., 2017), and Matara city, SriLanka (Serasinghe Pathiranage et al., 2018) had reported high value of fit metrics which could be due to the use of different statistical fit metrics to narrow down the coefficient space in calibration phases.

Model Accuracy assessment

Model simulation accuracy is another concern while using the satellite mapping products as a reference data. The simulation results is definite to have some inconsistencies because of its various level of errors observed in land use/cover map. Though most of the fit metrics would obtain high value, subjectivity lies in choosing the model fit metrics to narrow down the model coefficient ranges in calibration phase.

According to Silva & Clarke (2002), achieving the high values of fit matric is challenging. In this study, we have obtained substantially high values in most of the fit matrices including the "compare" metric of 0.703 when compared with actual urban extent. The study conducted by KantaKumar et al. (2011) and Abedini & Azizi (2016), indicated the model's effectiveness to perform the prediction with a spatial fit metrics obtaining the correlation of 62% and 69% match of modeled urban cells compared with actual urban cells. A perfect spatial match would result in a value of 1, which is 100 percent.

Model prediction

The results obtained from 'what if'' scenarios could be important to public discussion since the scenarios demonstrate the potential losses of the limited resource lands that could occur if appropriate measures were not put in place (Oguz et al., 2007). However, numerous issues that need to be taken care into consideration when developing scenarios. (Xiang & Clarke, 2003). In this study, we had proposed three alternative scenarios, Business as usual (BAU), Managed growth (MGS), and Compact growth (CGS) scenarios, a concept that was also used in similar manner by other researchers (Abedini & Azizi, 2016; Oguz et al., 2007; Yang & Lo, 2003).

It was observed that the urban excluded layer proved to be an effective tool for exploring different growth scenarios. However, uncertainly lies in setting or assigning the protection values. The question arises how appropriate it can represent the changing growth if the demand for urban land increases and if protection levels are treated as same or important from other? In our case, we have assigned the exclusion probabilities based on the importance of the land use classes and also considered the existing government policy to protect the limited agriculture land available in the county. However, no best solution is available between the urban development and preservation of agriculture land which has the conflicting goals in nature.

The scenarios in reality could be more complex than what we have design to simulate. The setting of the exclusion layer was done relatively similar in previous researches. The study conducted in the Houston-Galveston-Brazoria CMSA, the

urban exclusion and protection value was divided into three levels, 100% for water areas and parks, 40% and 60% for agriculture and 60% and 80% for wetland (Oguz et al., 2007). Despite those uncertainties, SLEUTH model had provided with insights regarding the historic urban growth and future growth prospects.

Results from the exploration of three growth scenarios with different excluded maps depicts that the general characteristics of growth are common among the control coefficients for different excluded maps. The breed, spread and road gravity coefficients were found to be the major controllers of the growth in all the scenarios. It was observed that the sensitivity to local characteristics differs in each calibration stages as a result of the different excluded maps integrated into the calibration process and spatial resolution. The coefficients resulting from each of the excluded layers represent as adjustment of the model to the local characteristics.

It was observed that predicting the model with strict weighting of excluded layer did not represent the conditions in a realistic way, thus under-predicting the actual growth. In our study, CGS growth scenario resulted substantial difference between the urban prediction results compared to the BAU and MGS scenario due to the strict protection of the exclusion layer. The growth of urban pixels were prevented even in the areas which has higher urban probability. The study conducted in Adana city had observed the similar growth where use of strict weighted exclusion layers have under-predicted the urban area compared to other scenarios (Akın et al., 2014).

The SLEUTH model effectively captured the dynamics of Gelephu city in MGS scenario and it may be used as an urban planning decision support tool by the city planners to understand the urban growth dynamics to plan sustainable future growth. Though SLEUTH model may not be feasible directly for site planning and detailed planning, It may perform well in spatial planning, concept planning, and master planning and be useful for understanding the alternative future planning scenarios (Xi et al., 2009). In view of this, the municipal development planning authority should take into account the various growth scenarios which would result to the sustainable future growth in the region.

The rapid urban growth mainly depends on the city requirement, facilities availability and industrialization in the area (KantaKumar et al., 2011), posing challenge to the city urban planners as the development often outpaces the planning

processes. This can be true in our case study since the development plan has targeted the available open spaces as a potential zone for future urban development decades ago during plan preparation (Ministry of Works and Human Settlement, 2010a) which may not cater to the existing demand with the increase in the urban population over the years. In this, the model prediction results demonstrate the need to consider the different growth scenarios taking into consideration the plans and policy of the country for sustainable urban growth.

Conclusion

The increasing urban population and socio-economic development triggered the rapid change in urban landscape. Understanding the dynamics of complex urban systems and evaluating the impact of urban growth involves modeling and simulation, which require robust methodology and techniques.

The land use land cover results clearly depicts the pressure on limited agriculture land and natural environment in the region with increase in urban built-up over the past decades. About 28 percent (see Table 6) of agriculture land has been converted to other land use classes in the process of urban growth. It was seen that the urban areas have consistently increasing towards the peri-urban areas along the national highway. Results from the SLEUTH model calibration and prediction highlights different growth strategies that can be adopted by urban planner and decision makers.

The role of remote sensing and GIS in cellular automated base urban growth modeling is indispensable, particularly for preparation of input datasets, data conversion, manipulation, and growth impact assessment. The results of SLEUTH model simulations are in Graphic Interchange Format (GIF) format which is highly compatible with Geographic Information System and hence, suitable for further quantitative analysis. SLEUTH model has been widely tested in developed countries but very few studies have been conducted in developing countries especially in the mountainous region.

In developing country like Bhutan, urban modeling and growth assessment is not common in urban planning process which leads to unplanned urban growth. Due

to the complexity of the urban dynamics and the heterogeneity of the urban landscape, few limitations and uncertainties were observed in the process of model simulation and prediction. The model is sensitive to the input data sets and it does not explicitly deal with policies and socio-economic factors to define the urban growth with its predefined growth factors such as slope, and road gravity coefficients. The extraction of an accurate urban extent was a challenge due to the medium spatial resolution (30m) of Landsat images used in the study.

The SLEUTH urban growth model is calibrated and tested for the first time to a Bhutanese urban setting. The results obtained from the model are quite satisfying, although accurate growth could be achieved if we use the high spatial resolution satellite images and combination of other socio-economic growth factors. Nevertheless, the coefficient values and goodness of fit metrics derived from the model calibration and simulation demonstrated the usefulness of the SLEUTH model to simulate the urban growth in current study area. Calibration of the SLEUTH model showed a high road gravity and slope coefficients, which means that the current urban growth is highly influenced by the existing road networks and controlled by topography of the region. These two growth parameters continue to contribute in future growth scenarios especially the slope resistance, which continue to act as barrier to urban growth. The influence of road gravity coefficient seems to decrease gradually.

Three scenarios have been designed and simulated in this research. The first scenario simulated the unmanaged growth if the urban growth is allowed to continue as Business as usual trend. The second scenario projected the growth trend with moderate protection on forest and open space land class which we named as managed growth scenario. The last scenario simulated the compact form of urban growth with maximum growth protection on both the land classes, forest and open space. Results from the first scenario (BAU) indicate that current study area would lose considerable amount of agriculture and natural land, such as forest and open space with approximately consuming 12 sq.km of land in urban growth by 2047. The third scenario (CGS) resulted in much more protection compared to first and second scenarios, however, the growth would highly constraint in urban centers where vertical growth could be only the ideal solution for urban expansion where such

growth are not favored by the existing policies and by nature of topography of the region. The second growth scenario (MGS) results seems to be much better than first and third scenarios in view that this scenario not only attempt to save the limited agriculture land but will also facilitate the future growth in much sustained manner. Therefore, SLEUTH model scenarios and outputs could have an important role on urban planning and decision-making process in the region.

The scenarios used in this study represented the results only as examples that urban planners can have available for urban growth strategies. In addition, the results obtained from the SLEUTH model or any other predictive models do not match exactly in reality, but at best produce approximations. However, the results of SLEUTH modeling in this study were found to be effective to compare the consequences of different growth scenarios which could serve as a decision support tool and aid urban planners and policy makers both at regional and local levels. The study also demonstrated that the use of remote sensing, GIS, and SLEUTH urban growth model is a powerful tool to analyze the future urban growth scenarios.

Future research and Recommendations

The current study used the CA-based SLEUTH urban growth model with remote sensing and GIS technique to study the urban growth and expansion. Though the study could accomplish the primary objective to simulate the urban expansion and evaluate the urban growth factors using the SLEUTH model, we found that there is need to highlight some important points that could be consider in future research.

Firstly, how growth would response if the future road layers and the land cover deltatron module are embedded in the model simulation? In this study, we have used the same existing road layers of 2017 as a ‘seed’ layer in prediction mode since we don’t have future planned transportation data of the current study area.

Secondly, we can see how different methodology of model calibration with temporal range of control years in model simulation affect the model growth results and its accuracy?

Moreover, we could also see how different types of data such as socio-economic data and policy framework can be incorporated in the existing framework to

improve the model? Currently, the model uses six input data sets derived from satellite images and topographic maps.

Finally, use of high spatial resolution satellite images is highly recommended in order to obtain accurate model simulation results, especially in the urban setting like Bhutan.

REFERENCES

Abedini, A., & Azizi, P. (2016, December 2016). Prediction of future urban growth scenarios using SLEUTH model (Case study: Urmia city, Iran). *Int. J. Architect. Eng. Urban Plan, 26*(2), 161-172. https://doi.org/10.22068/ijaup.26.2.161

Akın, A., Clarke, K. C., & Berberoglu, S. (2014). The impact of historical exclusion on the calibration of the SLEUTH urban growth model. *International Journal of Applied Earth Observation and Geoinformation, 27*, 156-168. https://doi.org/10.1016/j.jag.2013.10.002

Al-Dail, M. A. (1998). Change Detection in Urban Areas using Satellite Data. *Journal of King Saud University - Engineering Sciences, 10*(2), 217-227. https://doi.org/10.1016/s1018-3639(18)30697-4

Al-shalabi, M., Billa, L., Pradhan, B., Mansor, S., & Al-Sharif, A. A. A. (2012). Modelling urban growth evolution and land-use changes using GIS based cellular automata and SLEUTH models: the case of Sana'a metropolitan city, Yemen. *Environmental Earth Sciences, 70*(1), 425-437. https://doi.org/10.1007/s12665-012-2137-6

Alphan, H. (2003). Land-use change and urbanization of Adana, Turkey. *Land Degradation & Development, 14*(6), 575-586. https://doi.org/10.1002/ldr.581

Anderson, J. R., Hardy, E. E., Roach, J. T., & Witmer, R. E. (1976). A Land Use and Land Cover Classification System for Use with Remote Sensor Data. *GEOLOGICAL SURVEY PROFESSIONAL PAPER 964*. https://doi.org/ I 19.16:964

Batty, M., Couclelis, H., & Eichen, M. (1997). Urban systems as cellular automata. *Environment and Planning B: Planning and Design, 24*, 159-164. (© 1997 a Pion publication printed in Great Britain)

Batty, M., Longley, P., & Fotheringham, S. (1989). Urban growth and form: scaling, fractal geometry, and diffusion-limited aggregation. *Environment and Planning A, 21*(11), 1447-1472. (© 1989 a Pion publication printed in Great Britain)

Batty, M., Xie, Y., & Sun, Z. (1999). Modeling urban dynamics through GIS-based cellular automata. *Computers, Environment and Urban Systems*(23), 205-233. https://doi.org/10.1016/S0198-9715(99)00015-0

Benenson, I. (1998). Multi-agent simulations of residential dynamics in the city.

Comput., Environ, and Urban Systems, *22*(1), 25-42. https://doi.org/S0198-9715(98)00017-9 (Printed in Great Britain)

Bihamta, N., Soffianian, A., Fakheran, S., & Gholamalifard, M. (2014). Using the SLEUTH Urban Growth Model to Simulate Future Urban Expansion of the Isfahan Metropolitan Area, Iran. *Journal of the Indian Society of Remote Sensing*, *43*(2), 407-414. https://doi.org/10.1007/s12524-014-0402-8

Chand, R. (2017). Social Ecology of Immigrant Population and Changing Urban Landscape of Thimphu, Bhutan. *Journal of Urban and Regional Studies on Contemporary India*, *4*(1), 1-12. http://home.hiroshima-u.ac.jp/hindas/index.html

Chaudhuri, G., & Clarke, K. C. (2013). The SLEUTH Land Use Change Model: A Review. *The International Journal of Environmental Resources Research*, *1*(1).

Cheng, J., & Masser, I. (2003). Urban growth pattern modeling: a case study of Wuhan city, PR China. *Landscape and Urban Planning*, *62*(4), 199-217. https://doi.org/10.1016/s0169-2046(02)00150-0

Chimi, C., Tenzin, J., & Cheki, T. (2017). Assessment of Land Use/Cover Change and Urban Expansion Using Remote Sensing and GIS: A Case Study in Phuentsholing Municipality, Chukha, Bhutan. *International Journal of Energy and Environmental Science*, 127-135. https://doi.org/10.11648/j.ijees.20170206.12

Clarke, K. C., & Gaydos, L. J. (1998, Oct-Nov). Loose-coupling a cellular automaton model and GIS: long-term urban growth prediction for San Francisco and Washington/Baltimore. *Int J Geogr Inf Sci*, *12*(7), 699-714. https://doi.org/10.1080/136588198241617

Clarke, K. C., Hoppen, S., & Gaydos, L. (1997). A self-modifying cellular automaton model of historical urbanization in the San Francisco Bay area. *Environment and Planning B: Planning and Design*, *24*, 247-261.

Congalton, R. G. (1991). A Review of Assessing the Accuracy of Classifications of Remotely Sensed Data. *REMOTE SENS. ENVIRON.*

Congalton, R. G. (1998). *Considerations and techniques for assessing the accuracy of remotely sensed data* 12th Canadian Symposium on Remote Sensing Geoscience and Remote Sensing Symposium, Canada.

The Constitution of the Kingdom of Bhutan. (2008). http://www.nab.gov.bt/en/business/constitution_of_bhutan

Couclelis, H. (1997). From cellular automata to urban models: new principles for model development and implementation. *Environment and Planning B: Planning and Design*, *24*, 165-174.

Dadashpoor, H., & Nateghi, M. (2015). Simulating spatial pattern of urban growth using GIS-based SLEUTH model: a case study of eastern corridor of Tehran metropolitan region, Iran. *Environment, Development and Sustainability*, *19*(2), 527-547. https://doi.org/10.1007/s10668-015-9744-9

Dietzel, C., & Clarke, K. (2006). The effect of disaggregating land use categories in cellular automata during model calibration and forecasting. *Computers, Environment and Urban Systems*, *30*(1), 78-101. https://doi.org/10.1016/j.compenvurbsys.2005.04.001

Dietzel, C., & Clarke, K. C. (2007). Toward Optimal Calibration of the SLEUTH Land Use Change Model. *© 2007 The Authors. Journal compilation © 2007 Blackwell Publishing Ltd, Transactions in GIS*, *11*(1), 29–45.

Ding , Y.-C., & Zhang, Y.-K. (2007). The simulation of urban growth applying SLEUTH CA model to the Yilan Delta in Taiwan. *Jurnal Alam Bina, Jilid 09*(01).

Erasu, D. (2017). Remote Sensing-Based Urban Land Use/Land Cover Change Detection and Monitoring. *Journal of Remote Sensing & GIS*, *06*(02). https://doi.org/10.4172/2469-4134.1000196

Fan, F., Weng, Q., & Wang, Y. (2007). Land Use and Land Cover Change in Guangzhou, China, from 1998 to 2003, Based on Landsat TM /ETM+ Imagery [Full Research Paper]. *Sensors*, *7*, 1323-1342.

Firdaus, R. (2014). *Assessing Land Use and Land Cover Change toward Sustainability in Humid Tropical Watersheds, Indonesia* Hiroshima University].

Foody, G. M. (2002). Status of land cover classification accuracy assessment. *Remote Sensing of Environment*, *80*, 185–201.

Gelephu Thromde. (2019, August 2). *Background history*. http://www.gcc.bt/background-history

Giri, N., & Singh, O. P. (2013). Urban growth and water quality in Thimphu, Bhutan. *Journal of Urban and Environmental Engineering, 7*(1), 082-095. https://doi.org/10.4090/juee.2013.v7n1.082095

Gosai, M. A. (2009). *Land Use Change in Thimphu, Bhutan from 1990 – 2007: Effects of Cultural, Political, and Economic Frameworks.* North Carolina at Greensboro].

Hägerstrand, T. (1965). A Monte Carlo Approach to Diffusion. *European Journal of Sociology, 6*(01), 43-67. https://doi.org/10.1017/S0003975600001132

Huanga, J., Zhang, J., & Lu, X. X. (2008). Applying SLEUTH for simulating and assessing urban growth scenario based in Time series TM images: Referencing to a case study of Chongqing, China. *The International Archives of the Photogrammetry, Remote Sensing and Spatial Information Sciences, XXXVII*(B2).

Jantz, C. A., Goetz, S. J., & Shelley, M. K. (2003). Using the SLEUTH urban growth model to simulate the impats of future policy scenarios on urban land use in the Baltomire -Washington metropolitan area. *Environmental and Planing B: Planning and Design, 30*, 251-271. https://doi.org/10.1068/b2983

Jat, M. K., Choudhary, M., & Saxena, A. (2017). Application of geo-spatial techniques and cellular automata for modelling urban growth of a heterogeneous urban fringe. *The Egyptian Journal of Remote Sensing and Space Science, 20*(2), 223-241. https://doi.org/10.1016/j.ejrs.2017.02.002

KantaKumar, N. L., Sawant, N. G., & Kumar, S. (2011). Forecasting urban growth based on GIS, RS and SLEUTH model in Pune metropolitan area. *INTERNATIONAL JOURNAL OF GEOMATICS AND GEOSCIENCES, 2*(2), 568-579.

Lambin, E. F., Geist, H. J., & Lepers, E. (2003). Dynamics Of land-Use Andland-Coverchange Intropicalregions. *Annual Review of Environment and Resources, 28*(1), 205-241. https://doi.org/10.1146/annurev.energy.28.050302.105459

Leao, S., Bishop, I., & Evans, D. (2004). Simulating Urban Growth in a Developing Nation's Region Using a Cellular Automata-Based Model. *Journal of Urban Planning and Development, 130*(3), 145-158. https://doi.org/10.1061/(asce)0733-9488(2004)130:3(145)

Li, C. (2014). *Monitoring and analysis of urban growth process using Remote Sensing, GIS and Cellular Automata modeling: A case study of Xuzhou city, China* [dissertation, TU Dortmund University].

Li, L., Sato, Y., & Zhu, H. (2003). Simulating spatial urban expansion based on a physical process. *Landscape and Urban Planning*, *64*(1-2), 67-76. https://doi.org/10.1016/s0169-2046(02)00201-3

Li, X., & Yeh, A. G.-O. (2000). Modelling sustainable urban development by the integration of constrained cellular automata and GIS. *International Journal of Geographical Information Science*, *14*(2), 131-152. https://doi.org/10.1080/136588100240886

Li, X., Zhou, W., & Ouyang, Z. (2013). Forty years of urban expansion in Beijing: What is the relative importance of physical, socioeconomic, and neighborhood factors? *Applied Geography*, *38*, 1-10. https://doi.org/10.1016/j.apgeog.2012.11.004

Liu, B., Huang, B., & Zhang, W. (2017). *Spatio-Temporal Analysis and Optimization of Land Use/Cover Change*. CRC Press/Balkema Schipholweg 107C, 2316 XC Leiden, The Netherlands www.crcpress.com – www.taylorandfrancis.com.

Lu, D., & Weng, Q. (2007). A survey of image classification methods and techniques for improving classification performance. *International Journal of Remote Sensing*, *28*(5), 823-870. https://doi.org/10.1080/01431160600746456

Maithani, S. (2011). Cellular Automata Based Model of Urban Spatial Growth. *Journal of the Indian Society of Remote Sensing*, *38*(4), 604-610. https://doi.org/10.1007/s12524-010-0053-3

Masser, I. (2001). Managing our urban future: The role of remote sensing and geographic information systems. *Habitat International*, *25*, 503–512. https://doi.org/S0197 - 3 975(01)00021-2 ((c)2001 Elsevier Science Ltd. All rights reserved.)

Meyer, W. B., & Turner, B. L. (1996). Land-use/land-cover change: challenges for geographers. *Geo Journal*, *39*(3), 237-240.

Ministry of Works and Human Settlement. (2010a). *Sarpang Structure Plan 2010-2035 Final Report – Volume 01*. https://www.mowhs.gov.bt/wp-content/uploads/2012/03/Final-Structure-Plan-Vol-01-new.pdf

Ministry of Works and Human Settlement. (2010b). *Sarpang Structure Plan 2010-2035*

Final Report – Volume 02. http://www.mowhs.gov.bt/wp-content/uploads/2012/03/Final-Structure-Plan-Vol-02-new.pdf

Ministry of Works and Human Settlement. (2016). *National Report, The 3rd UN Conference on Housing and Sustainable Urban Development, Ministry of Works and Human Settlement, Royal Government of Bhutan.* [National Report]. M. o. W. a. H. Settlement. http://habitat3.org/wp-content/uploads/Bhutan_Habitat-III-National-Report.pdf

Ministry of Works and Human Settlement. (2019). *The Project for Formulation of Comprehensive Development Plan for Bhutan 2030, Existing Conditions and Development Issues*.

National Land Commission Secretariat. (2016). *National rehab program*. https://www.nlcs.gov.bt/?page_id=50

National Statistics Bureau. (2017). *2017 Population & Housing Census of Bhutan, National Report*. http://www.nsb.gov.bt/publication/publications.php?id=2

National Statistics Bureau. (2018). *Population Projections Bhutan 2017-2047, National Statiscal Bureau*. http://www.nsb.gov.bt/publication/publications.php?id=2

Oana, P. L., Harutyun, S., Brendan, W., & Sheila, C. (2011). *Scenarios and Indicators Supporting Urban Regional Planning* Spatial Thinking and Geographical Information Sciences

Oguz, H., Klein, A. G., & Srinivasan, R. (2007). Using the Sleuth Urban Growth Model to Simulate the Impacts of Future Policy Scenarios on Urban Land Use in the Houston-Galveston-Brazoria CMSA. *Research Journal of Social Sciences*(2), 72-82. https://www.researchgate.net/publication/266610961 (© 2007, INSInet Publication)

Osman, T., Divigalpitiya, P., & Arima, T. (2016). Using the SLEUTH urban growth model to simulate the impacts of future policy scenarios on land use in the Giza Governorate, Greater Cairo Metropolitan region. *International Journal of Urban Sciences, 20*(3), 407-426. https://doi.org/10.1080/12265934.2016.1216327

Pijanowskia, B. C., Brownb, D. G., Shellitoc, B. A., & Manikd, G. A. (2002). Using neural networks and GIS to forecast land use changes: a Land Transformation Model. *Computers, Environment and Urban Systems, 26*(6), 553-575. (Elsevier Science Ltd. All rights reserved.)

Project gigalopolis. (2003). *Data input*. http://www.ncgia.ucsb.edu/projects/gig/About/dtInput.htm

Qi, L. (2012). *Urban land expansion model based on SLEUTH, a case study in Dongguan city, China* (Publication Number INES nr 270) Lund University].

Rafiee, R., Mahiny, A. S., Khorasani, N., Darvishsefat, A. A., & Danekar, A. (2009). Simulating urban growth in Mashad City, Iran through the SLEUTH model (UGM). *Cities*, *26*(1), 19-26. https://doi.org/10.1016/j.cities.2008.11.005

Rongqun, Z., & Daolin, Z. (2011). Study of land cover classification based on knowledge rules using high-resolution remote sensing images. *Expert Systems with Applications*, *38*(4), 3647-3652. https://doi.org/10.1016/j.eswa.2010.09.019

Roy, T. B., & Saha, S. (2011). A study on factors related to urban growth of a municipal corporation and emerging challenges: A case of Siliguri Municipal Corporation, West Bengal, India. *Journal of Geography and Regional Planning, 4*(14), 683-694.

Sakieh, Y., Amiri, B. J., Danekar, A., Feghhi, J., & Dezhkam, S. (2014). Simulating urban expansion and scenario prediction using a cellular automata urban growth model, SLEUTH, through a case study of Karaj City, Iran. *Journal of Housing and the Built Environment*, *30*(4), 591-611. https://doi.org/10.1007/s10901-014-9432-3

Sangawongse, S. (2006). Land -Use/Land- Cover Dynamics In Chiang Mai : Appraisal from Remote Sensing, GIS and Modelling Approaches. *CMU. Journal, 5(2),* 243-254.

Sebastain, M., Jayaraman, V., & Chandrasekher, M. G. (1998). Facilities management using remote sensing data in a GIS environemnt. *43*(9-10), 487-491.

Serasinghe Pathiranage, I. S., Lakshmi N., K., & Sivanantharajah, S. (2018). Remote Sensing Data and SLEUTH Urban Growth Model: As Decision Support Tools for Urban Planning. *Chinese Geographical Science*, *28*(2), 274-286. https://doi.org/10.1007/s11769-018-0946-6

Shalaby, A., & Tateishi, R. (2007). Remote sensing and GIS for mapping and monitoring land cover and land-use changes in the Northwestern coastal zone of Egypt. *Applied Geography*, *27*(1), 28-41. https://doi.org/10.1016/j.apgeog.2006.09.004

Silva, E. A., & Clarke, K. C. (2002). Calibration of the SLEUTH urban growth model for Lisbon and Porto, Portugal. *Computers, Environment and Urban Systems*, 525–552.

Silva, E. A., & Clarke, K. C. (2005). Complexity, emergence and cellular urban models: lessons learned from applying SLEUTH to two Portuguese metropolitan areas. *European Planning Studies, 13*(1), 93-115. https://doi.org/10.1080/0965431042000312424

Singh, A. (1989). Review Article Digital change detection techniques using remotely-sensed data. *International Journal of Remote Sensing, 10*(6), 989-1003. https://doi.org/10.1080/01431168908903939

Stehman, S. V., & Czaplewski, R. L. (1998). Design and Analysis for Thematic Map Accuracy Assessment. *Remote Sensing of Environment, 64*(3), 331-344. https://doi.org/10.1016/s0034-4257(98)00010-8

Tobler, W. R. (1970). A Computer Movie Simulating Urban Growth in the Detroit Region. *Economic Geography, 46*, 234-240. http://www.jstor.org/stable/143141

Torrens, P. M. (2000). How cellular models of urban systems work: (1.THEORY). *Centre for Advanced Spatial Analysis, University College London*(28). http://www.casa.ucl.ac.uk/working_papers.htm

Torrens, P. M., & O'Sullivan, D. (2001). Cellular automata and urban simulation: where do we go from here? *Environmental and Planing B: Planning and Design, 28*, 163-168. https://doi.org/DOI:10.1068/b2802ed (2001 a Pion publication printed in Great Britain)

Treitz, P., & Rogan, J. (2004). Remote sensing for mapping and monitoring land-cover and land-use change—an introduction. *Progress in Planning, 61*(4), 269-279. https://doi.org/10.1016/s0305-9006(03)00064-3

United Nations. (2014). *Department of Economic and Social Affair, Population Division. World Urbanization Prospects:The 2014 Revisions, Highlights (ST/ESA/SER.A/352).* U. Nations. https://www.un.org/en/development/desa/publications/2014-revision-world-urbanization-prospects.html

United Nations. (2018). *Revision of World Urbanization Prospects*. https://www.un.org/development/desa/publications/2018-revision-of-world-urbanization-prospects.html

Veldkamp, A., & Lambin, E. F. (2001). Predicting land-use change. *Agriculture, Ecosystems and Environment, 85*, 1–6.

Walcott, S. (2009). Urbanization in Bhutan. *Geographical Review, 99*(1), 81-93. https://www.researchgate.net/publication/287003909

Watkiss, B. M. (2008). *The SLEUTH urban growth models as forecasting and decision-making tool* Stellenbosch University]. Copyright ©2007 Stellenbosch University.

White, R., & Engelen, G. (1993). Cellular automata and fractal urban form: a cellular modelling approach to the evolution of urban land-use patterns. *Environment and Planning A, 25*, 1175-1199.

Wilson, E. H., Hurd, J. D., Civco, D. L., Prisloe, M. P., & Arnold, C. (2003). Development of a geospatial model to quantify, describe and map urban growth. *Remote Sensing of Environment, 86*(3), 275-285. https://doi.org/10.1016/s0034-4257(03)00074-9

Xi, F., He, H., Hu, Y., Wu, X., Bu, R., Chang, Y., Liu, M., & Yu, J. (2009). *Simulate urban growth based on RS, GIS, and SLEUTH model in Shenyang-Fushun metropolitan area northeastern China* Urban Remote Sensing Event, 2009 Joint, https://doi.org/10.1109/URS.2009.5137630

Xiang, W.-N., & Clarke, K. C. (2003). The Use of Scenarios in Land-Use Planning. *Environment and Planning B: Planning and Design, 30*(6), 885-909. https://doi.org/10.1068/b2945

Yang, X., & Lo, C. P. (2003). Modelling urban growth and landscape changes in the Atlanta metropolitan area. *International Journal of Geographical Information Science, 17*(5), 463-488. https://doi.org/10.1080/1365881031000086965

Yangzom, K., Kalota, D., & Raj, M. (2017). A Temporal Study of the Urban Expansion of Thimphu City using Geo-Information Techniques. *International Journal of Economic Research, 14*(November 20). www.serialsjournals.com

Zhu, B., Zhu, X., Zhang, R., & Zhao, X. (2019). Study of Multiple Land Use Planning Based on the Coordinated Development of Wetland Farmland: A Case Study of Fuyuan City, China. *Sustainability, 11*(1), 271. https://doi.org/10.3390/su11010271

APPENDIX

APPENDIX A: Source code for Model calibration

1. SLEUTH's scenario file (coarse calibration)

```
# FILE: 'scenario file' for SLEUTH land cover transition model
#       (UGM  v3.0)
#       Comments start with #
#
#   I. Path Name Variables
#  II. Running Status (Echo)
# III. Output ASCII Files
#  IV. Log File Preferences
#   V. Working Grids
#  VI. Random Number Seed
# VII. Monte Carlo Iteration
#VIII. Coefficients
#      A. Coefficients and Growth Types
#      B. Modes and Coefficient Settings
#  IX. Prediction Date Range
#   X. Input Images
#  XI. Output Images
# XII. Colortable Settings
#      A. Date_Color
#      B. Non-Landuse Colortable
#      C. Land Cover Colortable
#      D. Growth Type Images
#      E. Deltatron Images
#XIII. Self Modification Parameters

# I.PATH NAME VARIABLES
#   INPUT_DIR: relative or absolute path where input image files and
#              (if modeling land cover) 'landuse.classes' file are
#              located.
#   OUTPUT_DIR: relative or absolute path where all output files will
#               be located.
#   WHIRLGIF_BINARY: relative path to 'whirlgif' gif animation program.
#                    These must be compiled before execution.
```

```
INPUT_DIR=../Input/demo_data30/
OUTPUT_DIR=../Output/demo_output/
WHIRLGIF_BINARY=../Whirlgif/whirlgif
# II. RUNNING STATUS (ECHO)
#  Status of model run, monte carlo iteration, and year will be
#  printed to the screen during model execution.
ECHO(YES/NO)=yes

# III. Output Files
# INDICATE TYPES OF ASCII DATA FILES TO BE WRITTEN TO
OUTPUT_DIRECTORY.
#
#   COEFF_FILE: contains coefficient values for every run, monte carlo
#             iteration and year.
#   AVG_FILE: contains measured values of simulated data averaged over
#           monte carlo iterations for every run and control year.
#   STD_DEV_FILE: contains standard diviation of averaged values
#              in the AVG_FILE.
#   MEMORY_MAP: logs memory map to file 'memory.log'
#   LOGGING: will create a 'LOG_#' file where # signifies the processor
#           number that created the file if running code in parallel.
#           Otherwise, # will be 0. Contents of the LOG file may be
#           described below.
WRITE_COEFF_FILE(YES/NO)=no
WRITE_AVG_FILE(YES/NO)=no
WRITE_STD_DEV_FILE(YES/NO)=no
WRITE_MEMORY_MAP(YES/NO)=YES
LOGGING(YES/NO)=YES

# IV. Log File Preferences
# INDICATE CONTENT OF LOG_# FILE (IF LOGGING == ON).
#   LANDCLASS_SUMMARY: (if landuse is being modeled) summary of input
#                  from 'landuse.classes' file
#   SLOPE_WEIGHTS(YES/NO): annual slope weight values as effected
#                     by slope_coeff
#   READS(YES/NO)= notes if a file is read in
#   WRITES(YES/NO)= notes if a file is written
#   COLORTABLES(YES/NO)= rgb lookup tables for all colortables generated
#   PROCESSING_STATUS(0:off/1:low verbosity/2:high verbosity)=
#   TRANSITION_MATRIX(YES/NO)= pixel count and annual probability of
#                        land class transitions
```

```
#     URBANIZATION_ATTEMPTS(YES/NO)= number of times an attempt to urbanize
#                                   a pixel occurred
#   INITIAL_COEFFICIENTS(YES/NO)= initial coefficient values for
#                                 each monte carlo
#   BASE_STATISTICS(YES/NO)= measurements of urban control year data
#   DEBUG(YES/NO)= data dump of igrid object and grid pointers
#   TIMINGS(0:off/1:low verbosity/2:high verbosity)= time spent within
#    each module. If running in parallel, LOG_0 will contain timing for
#    complete job.
LOG_LANDCLASS_SUMMARY(YES/NO)=yes
LOG_SLOPE_WEIGHTS(YES/NO)=no
LOG_READS(YES/NO)=no
LOG_WRITES(YES/NO)=no
LOG_COLORTABLES(YES/NO)=no
LOG_PROCESSING_STATUS(0:off/1:low verbosity/2:high verbosity)=1
LOG_TRANSITION_MATRIX(YES/NO)=yes
LOG_URBANIZATION_ATTEMPTS(YES/NO)=no
LOG_INITIAL_COEFFICIENTS(YES/NO)=no
LOG_BASE_STATISTICS(YES/NO)=yes
LOG_DEBUG(YES/NO)= no
LOG_TIMINGS(0:off/1:low verbosity/2:high verbosity)=1

# V. WORKING GRIDS
# The number of working grids needed from memory during model execution is
# designated up front. This number may change depending upon modes. If
# NUM_WORKING_GRIDS needs to be increased, the execution will be exited
# and an error message will be written to the screen and to 'ERROR_LOG'
# in the OUTPUT_DIRECTORY. If the number may be decreased an optimal
# number will be written to the end of the LOG_0 file.
NUM_WORKING_GRIDS=2

# VI. RANDOM NUMBER SEED
# This number initializes the random number generator. This seed will be
# used to initialize each model run.
RANDOM_SEED=1

# VII. MONTE CARLO ITERATIONS
# Each model run may be completed in a monte carlo fashion.
#  For CALIBRATION or TEST mode measurements of simulated data will be
#  taken for years of known data, and averaged over the number of monte
```

```
#  carlo iterations. These averages are written to the AVG_FILE, and
#  the associated standard diviation is written to the STD_DEV_FILE.
#  The averaged values are compared to the known data, and a Pearson
#  correlation coefficient measure is calculated and written to the
#  control_stats.log file. The input per run may be associated across
#  files using the 'index' number in the files' first column.
#
MONTE_CARLO_ITERATIONS=4

# VIII. COEFFICIENTS
# The coefficients effect how the growth rules are applied to the data.
# Setting requirements:
#    *_START values >= *_STOP values
#    *_STEP values > 0
#   if no coefficient increment is desired:
#    *_START == *_STOP
#    *_STEP == 1
# For additional information about how these values affect simulated
# land cover change see our publications and PROJECT GIGALOPOLIS
#  site: (www.ncgia.ucsb.edu/project/gig/About/abGrowth.htm).
#  A. COEFFICIENTS AND GROWTH TYPES
#    DIFFUSION: affects SPONTANEOUS GROWTH and search distance along the
#              road network as part of ROAD INFLUENCED GROWTH.
#    BREED: NEW SPREADING CENTER probability and affects number of ROAD
#           INFLUENCED GROWTH attempts.
#    SPREAD: the probabilty of ORGANIC GROWTH from established urban
#            pixels occuring.
#    SLOPE_RESISTANCE: affects the influence of slope to urbanization. As
#                      value increases, the ability to urbanize
#                      ever steepening slopes decreases.
#    ROAD_GRAVITY: affects the outward distance from a selected pixel for
#                  which a road pixel will be searched for as part of
#                  ROAD INFLUENCED GROWTH.
#
#  B. MODES AND COEFFICIENT SETTINGS
#    TEST: TEST mode will perform a single run through the historical
#          data using the CALIBRATION_*_START values to initialize
#          growth, complete the MONTE_CARLO_ITERATIONS, and then conclude
#          execution. GIF images of the simulated urban growth will be
#          written to the OUTPUT_DIRECTORY.
#    CALIBRATE: CALIBRATE will perform monte carlo runs through the
```

```
#               historical data using every combination of the
#               coefficient values indicated. The CALIBRATION_*_START
#               coefficient values will initialize the first run. A
#               coefficient will then be increased by its *_STEP value,
#               and another run performed. This will be repeated for all
#               possible permutations of given ranges and increments.
#     PREDICTION: PREDICTION will perform a single run, in monte carlo
#                fashion, using the PREDICTION_*_BEST_FIT values
#                for initialization.
CALIBRATION_DIFFUSION_START= 0
CALIBRATION_DIFFUSION_STEP=  25
CALIBRATION_DIFFUSION_STOP=  100

CALIBRATION_BREED_START=     0
CALIBRATION_BREED_STEP=      25
CALIBRATION_BREED_STOP=      100

CALIBRATION_SPREAD_START=    0
CALIBRATION_SPREAD_STEP=     25
CALIBRATION_SPREAD_STOP=     100

CALIBRATION_SLOPE_START=     0
CALIBRATION_SLOPE_STEP=      25
CALIBRATION_SLOPE_STOP=      100

CALIBRATION_ROAD_START=      0
CALIBRATION_ROAD_STEP=       25
CALIBRATION_ROAD_STOP=       100

PREDICTION_DIFFUSION_BEST_FIT=  20
PREDICTION_BREED_BEST_FIT=  20
PREDICTION_SPREAD_BEST_FIT=  20
PREDICTION_SLOPE_BEST_FIT=  20
PREDICTION_ROAD_BEST_FIT=  20

# IX. PREDICTION DATE RANGE
# The urban and road images used to initialize growth during
# prediction are those with dates equal to, or greater than,
# the PREDICTION_START_DATE. If the PREDICTION_START_DATE is greater
# than any of the urban dates, the last urban file on the list will be
# used. Similarly, if the PREDICTION_START_DATE is greater
```

```
# than any of the road dates, the last road file on the list will be
# used. The prediction run will terminate at PREDICTION_STOP_DATE.
#
PREDICTION_START_DATE=1990
PREDICTION_STOP_DATE=2017

# X. INPUT IMAGES
# The model expects grayscale, GIF image files with file name
# format as described below. For more information see our
# PROJECT GIGALOPOLIS web site:
# (www.ncgia.ucsb.edu/project/gig/About/dtInput.htm).
#
# IF LAND COVER IS NOT BEING MODELED: Remove or comment out
# the LANDUSE_DATA data input flags below.
#
#   < >  = user selected fields
#  < > = optional fields
#
# Urban data GIFs
#  format:  <location>.urban.<date>.<user info>.gif
#
#
URBAN_DATA= demo.urban.1990.gif
URBAN_DATA= demo.urban.2000.gif
URBAN_DATA= demo.urban.2010.gif
URBAN_DATA= demo.urban.2017.gif
#
# Road data GIFs
#  format:  <location>.roads.<date>.<user info>.gif
#
ROAD_DATA= demo.roads.1990.gif
ROAD_DATA= demo.roads.2017.gif
#
# Landuse data GIFs
#  format:  <location>.landuse.<date>.<user info>.gif
#
#LANDUSE_DATA= demo.landuse.1990.gif
#LANDUSE_DATA= demo.landuse.2017.gif
#
# Excluded data GIF
#  format:  <location>.excluded.<user info>.gif
```

```
#
EXCLUDED_DATA= demo.excluded.gif
#
# Slope data GIF
#  format:  <location>.slope.<user info>.gif
#
SLOPE_DATA= demo.slope.gif
#
# Background data GIF
#  format:   <location>.hillshade.<user info>.gif
#
#BACKGROUND_DATA= demo.hillshade.gif
BACKGROUND_DATA= demo.hillshade.gif

# XI. OUTPUT IMAGES
#   WRITE_COLOR_KEY_IMAGES: Creates image maps of each colortable.
#                File name format: 'key_type_COLORMAP'
#                where type represents the colortable.
#   ECHO_IMAGE_FILES: Creates GIF of each input file used in that job.
#              File names format: 'echo_of_input_filename'
#              where input_filename represents the input name.
#   ANIMATION: if whirlgif has been compiled, and the WHIRLGIF_BINARY
#           path has been defined, animated gifs begining with the
#           file name 'animated' will be created in PREDICT mode.
WRITE_COLOR_KEY_IMAGES(YES/NO)=no
ECHO_IMAGE_FILES(YES/NO)=no
ANIMATION(YES/NO)= no

# XII. COLORTABLE SETTINGS
#  A. DATE COLOR SETTING
#     The date will automatically be placed in the lower left corner
#     of output images. DATE_COLOR may be designated in with red, green,
#     and blue values (format: <red_value, green_value, blue_value> )
#     or with hexadecimal begining with '0X' (format: <0X######> ).
#default DATE_COLOR= 0XFFFFFF white
DATE_COLOR=     0XFFFFFF #white

#  B. URBAN (NON-LANDUSE) COLORTABLE SETTINGS
#     1. URBAN MODE OUTPUTS
#        TEST mode: Annual images of simulated urban growth will be
#                created using SEED_COLOR to indicate urbanized areas.
```

```
#       CALIBRATE mode: Images will not be created.
#       PREDICT mode: Annual probability images of simulated urban
#                growth will be created using the PROBABILITY
#                _COLORTABLE. The initializing urban data will be
#                indicated by SEED_COLOR.
#
#    2. COLORTABLE SETTINGS
#        SEED_COLOR: initializing and extrapolated historic urban extent

#        WATER_COLOR: BACKGROUND_DATA is used as a backdrop for

#                simulated urban growth. If pixels in this file
#                contain the value zero (0), they will be filled
#                with the color value in WATER_COLOR. In this way,
#                major water bodies in a study area may be included
#                in output images.
#SEED_COLOR= 0XFFFF00 #yellow
SEED_COLOR=  249, 209, 110 #pale yellow
#WATER_COLOR=  0X0000FF # blue
WATER_COLOR=  20, 52, 214 # royal blue

#    3. PROBABILITY COLORTABLE FOR URBAN GROWTH
#       For PREDICTION, annual probability images of urban growth
#       will be created using the monte carlo iterations. In these
#       images, the higher the value the more likely urbanizaion is.
#       In order to interpret these 'continuous' values more easily
#       they may be color classified by range.
#
#       If 'hex' is not present then the range is transparent.
#       The transparent range must be the first on the list.
#       The max number of entries is 100.
#        PROBABILITY_COLOR: a color value in hexadecimal that indicates
#                        a probability range.
#          low/upper: indicate the boundaries of the range.
#
#               low,  upper,   hex,  (Optional Name)
PROBABILITY_COLOR=   0,    1,        , #transparent
PROBABILITY_COLOR=   1,    10, 0X00ff33, #green
PROBABILITY_COLOR=   10,   20, 0X00cc33, #
PROBABILITY_COLOR=   20,   30, 0X009933, #
```

```
PROBABILITY_COLOR=   30,   40, 0X006666, #blue
PROBABILITY_COLOR=   40,   50, 0X003366, #
PROBABILITY_COLOR=   50,   60, 0X000066, #
PROBABILITY_COLOR=   60,   70, 0XFF6A6A, #lt orange
PROBABILITY_COLOR=   70,   80, 0Xff7F00, #dark orange
PROBABILITY_COLOR=   80,   90, 0Xff3E96, #violetred
PROBABILITY_COLOR=   90,  100, 0Xff0033, #dark red

#  C. LAND COVER COLORTABLE
#  Land cover input images should be in grayscale GIF image format.
#  The 'pix' value indicates a land class grayscale pixel value in
#  the image. If desired, the model will create color classified
#  land cover output. The output colortable is designated by the
#  'hex/rgb' values.
#    pix: input land class pixel value
#    name: text string indicating land class
#    flag: special case land classes
#          URB - urban class (area is included in urban input data
#                and will not be transitioned by deltatron)
#          UNC - unclass (NODATA areas in image)
#          EXC - excluded (land class will be ignored by deltatron)
#    hex/rgb: hexidecimal or rgb (red, green, blue) output colors
#
#             pix, name,     flag,   hex/rgb, #comment
LANDUSE_CLASS=  0,  Unclass , UNC   , 0X000000
LANDUSE_CLASS=  1,  Urban   , URB   , 0X8b2323 #dark red
LANDUSE_CLASS=  2,  Agric   ,       , 0Xffec8b #pale yellow
LANDUSE_CLASS=  3,  Range   ,       , 0Xee9a49 #tan
LANDUSE_CLASS=  4,  Forest  ,       , 0X006400
LANDUSE_CLASS=  5,  Water   , EXC   , 0X104e8b
LANDUSE_CLASS=  6,  Wetland ,       , 0X483d8b
LANDUSE_CLASS=  7,  Barren  ,       , 0Xeec591

#  D. GROWTH TYPE IMAGE OUTPUT CONTROL AND COLORTABLE
#
#  From here you can control the output of the Z grid
#  (urban growth) just after it is returned from the spr_spread()
#  function. In this way it is possible to see the different types
#  of growth that have occured for a particular growth cycle.
#
#  VIEW_GROWTH_TYPES(YES/NO) provides an on/off
```

```
#  toggle to control whether the images are generated.
#
#  GROWTH_TYPE_PRINT_WINDOW provides a print window
#  to control the amount of images created.
#  format:  <start_run>,<end_run>,<start_monte_carlo>,
#         <end_monte_carlo>,<start_year>,<end_year>
#  for example:
#  GROWTH_TYPE_PRINT_WINDOW=run1,run2,mc1,mc2,year1,year2
#  so images are only created when
#  run1<= current run <=run2 AND
#  mc1 <= current monte carlo <= mc2 AND
#  year1 <= currrent year <= year2
#
#  0 == first
VIEW_GROWTH_TYPES(YES/NO)=NO
GROWTH_TYPE_PRINT_WINDOW=0,0,0,0,1995,2020
PHASE0G_GROWTH_COLOR=  0xff0000 # seed urban area
PHASE1G_GROWTH_COLOR=  0X00ff00 # diffusion growth
PHASE2G_GROWTH_COLOR=  0X0000ff # NOT USED
PHASE3G_GROWTH_COLOR=  0Xffff00 # breed growth
PHASE4G_GROWTH_COLOR=  0Xffffff # spread growth
PHASE5G_GROWTH_COLOR=  0X00ffff # road influenced growth

#*************************************************************
#
#  E. DELTATRON AGING SECTION
#
#  From here you can control the output of the deltatron grid
#  just before they are aged
#
#  VIEW_DELTATRON_AGING(YES/NO) provides an on/off
#  toggle to control whether the images are generated.
#
#  DELTATRON_PRINT_WINDOW provides a print window
#  to control the amount of images created.
#  format:  <start_run>,<end_run>,<start_monte_carlo>,
#         <end_monte_carlo>,<start_year>,<end_year>
#  for example:
#  DELTATRON_PRINT_WINDOW=run1,run2,mc1,mc2,year1,year2
#  so images are only created when
#  run1<= current run <=run2 AND
```

```
#  mc1 <= current monte carlo <= mc2 AND
#  year1 <= currrent year <= year2
#
#  0 == first
VIEW_DELTATRON_AGING(YES/NO)=NO
DELTATRON_PRINT_WINDOW=0,0,0,0,1930,2020
DELTATRON_COLOR=  0x000000 # index 0 No or dead deltatron
DELTATRON_COLOR=  0X00FF00 # index 1 age = 1 year
DELTATRON_COLOR=  0X00D200 # index 2 age = 2 year
DELTATRON_COLOR=  0X00AA00 # index 3 age = 3 year
DELTATRON_COLOR=  0X008200 # index 4 age = 4 year
DELTATRON_COLOR=  0X005A00 # index 5 age = 5 year

# XIII. SELF-MODIFICATION PARAMETERS
#       SLEUTH is a self-modifying cellular automata. For more
#       information see our PROJECT GIGALOPOLIS web site
#       (www.ncgia.ucsb.edu/project/gig/About/abGrowth.htm)
#       and publications (and/or grep 'self modification' in code).
ROAD_GRAV_SENSITIVITY=0.01
SLOPE_SENSITIVITY=0.1
CRITICAL_LOW=0.97
CRITICAL_HIGH=1.3
#CRITICAL_LOW=0.0
#CRITICAL_HIGH=10000000000000.0
CRITICAL_SLOPE=21.0
BOOM=1.01
BUST=0.09
```

2. <u>SLEUTH's scenario file (fine calibration)</u>

```
# FILE: 'scenario file' for SLEUTH land cover transition model
#       (UGM  v3.0)
#       Comments start with #
#
#   I. Path Name Variables
#  II. Running Status (Echo)
# III. Output ASCII Files
#  IV. Log File Preferences
#   V. Working Grids
#  VI. Random Number Seed
```

```
# VII. Monte Carlo Iteration
#VIII. Coefficients
#      A. Coefficients and Growth Types
#      B. Modes and Coefficient Settings
#  IX. Prediction Date Range
#   X. Input Images
#  XI. Output Images
# XII. Colortable Settings
#      A. Date_Color
#      B. Non-Landuse Colortable
#      C. Land Cover Colortable
#      D. Growth Type Images
#      E. Deltatron Images
#XIII. Self Modification Parameters

# I.PATH NAME VARIABLES
#   INPUT_DIR: relative or absolute path where input image files and
#              (if modeling land cover) 'landuse.classes' file are
#              located.
#   OUTPUT_DIR: relative or absolute path where all output files will
#               be located.
#   WHIRLGIF_BINARY: relative path to 'whirlgif' gif animation program.
#                    These must be compiled before execution.
INPUT_DIR=../Input/final_data60/
OUTPUT_DIR=../Output/data60_cal/
WHIRLGIF_BINARY=../Whirlgif/whirlgif

# II. RUNNING STATUS (ECHO)
#  Status of model run, monte carlo iteration, and year will be
#  printed to the screen during model execution.
ECHO(YES/NO)=yes

# III. Output Files
#  INDICATE TYPES OF ASCII DATA FILES TO BE WRITTEN TO
OUTPUT_DIRECTORY.
#
#   COEFF_FILE: contains coefficient values for every run, monte carlo
#               iteration and year.
#   AVG_FILE: contains measured values of simulated data averaged over
#             monte carlo iterations for every run and control year.
#   STD_DEV_FILE: contains standard deviation of averaged values
```

```
#              in the AVG_FILE.
#   MEMORY_MAP: logs memory map to file 'memory.log'
#   LOGGING: will create a 'LOG_#' file where # signifies the processor
#          number that created the file if running code in parallel.
#          Otherwise, # will be 0. Contents of the LOG file may be
#          described below.
WRITE_COEFF_FILE(YES/NO)=no
WRITE_AVG_FILE(YES/NO)=no
WRITE_STD_DEV_FILE(YES/NO)=no
WRITE_MEMORY_MAP(YES/NO)=no
LOGGING(YES/NO)=YES

# IV. Log File Preferences
# INDICATE CONTENT OF LOG_# FILE (IF LOGGING == ON).
#   LANDCLASS_SUMMARY: (if landuse is being modeled) summary of input
#                  from 'landuse.classes' file
#   SLOPE_WEIGHTS(YES/NO): annual slope weight values as effected
#                  by slope_coeff
#   READS(YES/NO)= notes if a file is read in
#   WRITES(YES/NO)= notes if a file is written
#   COLORTABLES(YES/NO)= rgb lookup tables for all colortables generated
#   PROCESSING_STATUS(0:off/1:low verbosity/2:high verbosity)=
#   TRANSITION_MATRIX(YES/NO)= pixel count and annual probability of
#                  land class transitions
#     URBANIZATION_ATTEMPTS(YES/NO)= number of times an attempt to
urbanize
#                  a pixel occurred
#   INITIAL_COEFFICIENTS(YES/NO)= initial coefficient values for
#                  each monte carlo
#   BASE_STATISTICS(YES/NO)= measurements of urban control year data
#   DEBUG(YES/NO)= data dump of igrid object and grid pointers
#   TIMINGS(0:off/1:low verbosity/2:high verbosity)= time spent within
#    each module. If running in parallel, LOG_0 will contain timing for
#    complete job.
LOG_LANDCLASS_SUMMARY(YES/NO)=yes
LOG_SLOPE_WEIGHTS(YES/NO)=no
LOG_READS(YES/NO)=no
LOG_WRITES(YES/NO)=no
LOG_COLORTABLES(YES/NO)=no
LOG_PROCESSING_STATUS(0:off/1:low verbosity/2:high verbosity)=1
LOG_TRANSITION_MATRIX(YES/NO)=no
```

```
LOG_URBANIZATION_ATTEMPTS(YES/NO)=no
LOG_INITIAL_COEFFICIENTS(YES/NO)=no
LOG_BASE_STATISTICS(YES/NO)=yes
LOG_DEBUG(YES/NO)= no
LOG_TIMINGS(0:off/1:low verbosity/2:high verbosity)=1

# V. WORKING GRIDS
# The number of working grids needed from memory during model execution is

# designated up front. This number may change depending upon modes. If
# NUM_WORKING_GRIDS needs to be increased, the execution will be exited
# and an error message will be written to the screen and to 'ERROR_LOG'
# in the OUTPUT_DIRECTORY. If the number may be decreased an optimal
# number will be written to the end of the LOG_0 file.
NUM_WORKING_GRIDS=4

# VI. RANDOM NUMBER SEED
# This number initializes the random number generator. This seed will be
# used to initialize each model run.
RANDOM_SEED=1

# VII. MONTE CARLO ITERATIONS
# Each model run may be completed in a monte carlo fashion.
#  For CALIBRATION or TEST mode measurements of simulated data will be
#  taken for years of known data, and averaged over the number of monte
#  carlo iterations. These averages are written to the AVG_FILE, and
#  the associated standard diviation is written to the STD_DEV_FILE.
#  The averaged values are compared to the known data, and a Pearson
#  correlation coefficient measure is calculated and written to the
#  control_stats.log file. The input per run may be associated across
#  files using the 'index' number in the files' first column.
#
MONTE_CARLO_ITERATIONS=8

# VIII. COEFFICIENTS
# The coefficients effect how the growth rules are applied to the data.
# Setting requirements:
#    *_START values >= *_STOP values
#    *_STEP values > 0
#   if no coefficient increment is desired:
#    *_START == *_STOP
```

```
#    *_STEP == 1
# For additional information about how these values affect simulated
# land cover change see our publications and PROJECT GIGALOPOLIS
#  site: (www.ncgia.ucsb.edu/project/gig/About/abGrowth.htm).
#  A. COEFFICIENTS AND GROWTH TYPES
#    DIFFUSION: affects SPONTANEOUS GROWTH and search distance along the
#            road network as part of ROAD INFLUENCED GROWTH.
#    BREED: NEW SPREADING CENTER probability and affects number of ROAD
#          INFLUENCED GROWTH attempts.
#    SPREAD: the probabilty of ORGANIC GROWTH from established urban
#           pixels occuring.
#    SLOPE_RESISTANCE: affects the influence of slope to urbanization. As
#                   value increases, the ability to urbanize
#                   ever steepening slopes decreases.
#    ROAD_GRAVITY: affects the outward distance from a selected pixel for
#                which a road pixel will be searched for as part of
#                ROAD INFLUENCED GROWTH.
#
#  B. MODES AND COEFFICIENT SETTINGS
#    TEST: TEST mode will perform a single run through the historical
#         data using the CALIBRATION_*_START values to initialize
#         growth, complete the MONTE_CARLO_ITERATIONS, and then conclude
#         execution. GIF images of the simulated urban growth will be
#         written to the OUTPUT_DIRECTORY.
#    CALIBRATE: CALIBRATE will perform monte carlo runs through the
#              historical data using every combination of the
#              coefficient values indicated. The CALIBRATION_*_START
#              coefficient values will initialize the first run. A
#              coefficient will then be increased by its *_STEP value,
#              and another run performed. This will be repeated for all
#              possible permutations of given ranges and increments.
#    PREDICTION: PREDICTION will perform a single run, in monte carlo
#               fashion, using the PREDICTION_*_BEST_FIT values
#               for initialization.

CALIBRATION_DIFFUSION_START= 0
CALIBRATION_DIFFUSION_STEP=  5
CALIBRATION_DIFFUSION_STOP=  20

CALIBRATION_BREED_START=     0
CALIBRATION_BREED_STEP=      15
```

```
CALIBRATION_BREED_STOP=      75

CALIBRATION_SPREAD_START=    0
CALIBRATION_SPREAD_STEP=     5
CALIBRATION_SPREAD_STOP=     20

CALIBRATION_SLOPE_START=     0
CALIBRATION_SLOPE_STEP=      20
CALIBRATION_SLOPE_STOP=      100

CALIBRATION_ROAD_START=      0
CALIBRATION_ROAD_STEP=       15
CALIBRATION_ROAD_STOP=       75

PREDICTION_DIFFUSION_BEST_FIT=  20
PREDICTION_BREED_BEST_FIT=  20
PREDICTION_SPREAD_BEST_FIT=  20
PREDICTION_SLOPE_BEST_FIT=  20
PREDICTION_ROAD_BEST_FIT=  20

# IX. PREDICTION DATE RANGE
# The urban and road images used to initialize growth during
# prediction are those with dates equal to, or greater than,
# the PREDICTION_START_DATE. If the PREDICTION_START_DATE is greater
# than any of the urban dates, the last urban file on the list will be
# used. Similarly, if the PREDICTION_START_DATE is greater
# than any of the road dates, the last road file on the list will be
# used. The prediction run will terminate at PREDICTION_STOP_DATE.
#
PREDICTION_START_DATE=1990
PREDICTION_STOP_DATE=2017

# X. INPUT IMAGES
# The model expects grayscale, GIF image files with file name
# format as described below. For more information see our
# PROJECT GIGALOPOLIS web site:
# (www.ncgia.ucsb.edu/project/gig/About/dtInput.htm).
#
# IF LAND COVER IS NOT BEING MODELED: Remove or comment out
# the LANDUSE_DATA data input flags below.
#
```

```
#    < >  = user selected fields
#   < > = optional fields
#
# Urban data GIFs
#  format:  <location>.urban.<date>.<user info>.gif
#
#
URBAN_DATA= data60.urban.1990.gif
URBAN_DATA= data60.urban.2000.gif
URBAN_DATA= data60.urban.2010.gif
URBAN_DATA= data60.urban.2017.gif
#
# Road data GIFs
#  format:  <location>.roads.<date>.<user info>.gif
#
ROAD_DATA= data60.roads.1990.gif
ROAD_DATA= data60.roads.2017.gif
#
# Landuse data GIFs
#  format:  <location>.landuse.<date>.<user info>.gif
#
#LANDUSE_DATA= data60.landuse.1990.gif
#LANDUSE_DATA= data60.landuse.2017.gif
#
# Excluded data GIF
#  format:  <location>.excluded.<user info>.gif
#
EXCLUDED_DATA= data60.excluded.gif
#
# Slope data GIF
#  format:  <location>.slope.<user info>.gif
#
SLOPE_DATA= data60.slope.gif
#
# Background data GIF
#  format:   <location>.hillshade.<user info>.gif
#
BACKGROUND_DATA= data60.hillshade.gif

# XI. OUTPUT IMAGES
#   WRITE_COLOR_KEY_IMAGES: Creates image maps of each colortable.
```

```
#                   File name format: 'key_type_COLORMAP'
#                   where type represents the colortable.
#  ECHO_IMAGE_FILES: Creates GIF of each input file used in that job.
#               File names format: 'echo_of_input_filename'
#               where input_filename represents the input name.
#  ANIMATION: if whirlgif has been compiled, and the WHIRLGIF_BINARY
#          path has been defined, animated gifs begining with the
#          file name 'animated' will be created in PREDICT mode.
WRITE_COLOR_KEY_IMAGES(YES/NO)=no
ECHO_IMAGE_FILES(YES/NO)=no
ANIMATION(YES/NO)= no

# XII. COLORTABLE SETTINGS
#  A. DATE COLOR SETTING
#    The date will automatically be placed in the lower left corner
#    of output images. DATE_COLOR may be designated in with red, green,
#    and blue values (format: <red_value, green_value, blue_value> )
#    or with hexadecimal begining with '0X' (format: <0X######> ).
#default DATE_COLOR= 0XFFFFFF white
DATE_COLOR=     0XFFFFFF #white

#  B. URBAN (NON-LANDUSE) COLORTABLE SETTINGS
#    1. URBAN MODE OUTPUTS
#       TEST mode: Annual images of simulated urban growth will be
#              created using SEED_COLOR to indicate urbanized areas.

#       CALIBRATE mode: Images will not be created.
#       PREDICT mode: Annual probability images of simulated urban
#                growth will be created using the PROBABILITY
#                _COLORTABLE. The initializing urban data will be
#                indicated by SEED_COLOR.
#
#    2. COLORTABLE SETTINGS
#        SEED_COLOR: initializing and extrapolated historic urban extent

#       WATER_COLOR: BACKGROUND_DATA is used as a backdrop for

#                simulated urban growth. If pixels in this file
#                contain the value zero (0), they will be filled
#                with the color value in WATER_COLOR. In this way,
#                major water bodies in a study area may be included
```

```
#                   in output images.
#SEED_COLOR= 0XFFFF00 #yellow
SEED_COLOR=  249, 209, 110 #pale yellow
#WATER_COLOR=  0X0000FF # blue
WATER_COLOR=  20, 52, 214 # royal blue

#    3. PROBABILITY COLORTABLE FOR URBAN GROWTH
#      For PREDICTION, annual probability images of urban growth
#      will be created using the monte carlo iterations. In these
#      images, the higher the value the more likely urbanizaion is.
#      In order to interpret these 'continuous' values more easily
#      they may be color classified by range.
#
#      If 'hex' is not present then the range is transparent.
#      The transparent range must be the first on the list.
#      The max number of entries is 100.
#        PROBABILITY_COLOR: a color value in hexadecimal that indicates
#                  a probability range.
#         low/upper: indicate the boundaries of the range.
#
#             low,  upper,   hex,  (Optional Name)
PROBABILITY_COLOR=   0,    50,        , #transparent
PROBABILITY_COLOR=   50,   60, 0X005A00, #0, 90,0 dark green
PROBABILITY_COLOR=   60,   70, 0X008200, #0,130,0
PROBABILITY_COLOR=   70,   80, 0X00AA00, #0,170,0
PROBABILITY_COLOR=   80,   90, 0X00D200, #0,210,0
PROBABILITY_COLOR=   90,   95, 0X00FF00, #0,255,0 light green
PROBABILITY_COLOR=   95,  100, 0X8B0000, #dark red

#  C. LAND COVER COLORTABLE
#  Land cover input images should be in grayscale GIF image format.
#  The 'pix' value indicates a land class grayscale pixel value in
#  the image. If desired, the model will create color classified
#  land cover output. The output colortable is designated by the
#  'hex/rgb' values.
#   pix: input land class pixel value
#   name: text string indicating land class
#   flag: special case land classes
#        URB - urban class (area is included in urban input data
#             and will not be transitioned by deltatron)
#        UNC - unclass (NODATA areas in image)
```

```
#         EXC - excluded (land class will be ignored by deltatron)
#    hex/rgb: hexidecimal or rgb (red, green, blue) output colors
#
#             pix, name,     flag,   hex/rgb, #comment
LANDUSE_CLASS=  0,  Unclass , UNC   , 0X000000
LANDUSE_CLASS=  1,  Urban   , URB   , 0X8b2323 #dark red
LANDUSE_CLASS=  2,  Agric   ,       , 0Xffec8b #pale yellow
LANDUSE_CLASS=  3,  Range   ,       , 0Xee9a49 #tan
LANDUSE_CLASS=  4,  Forest  ,       , 0X006400
LANDUSE_CLASS=  5,  Water   , EXC   , 0X104e8b
LANDUSE_CLASS=  6,  Wetland ,       , 0X483d8b
LANDUSE_CLASS=  7,  Barren  ,       , 0Xeec591

#  D. GROWTH TYPE IMAGE OUTPUT CONTROL AND COLORTABLE
#
#  From here you can control the output of the Z grid
#  (urban growth) just after it is returned from the spr_spread()
#  function. In this way it is possible to see the different types
#  of growth that have occured for a particular growth cycle.
#
#  VIEW_GROWTH_TYPES(YES/NO) provides an on/off
#  toggle to control whether the images are generated.
#
#  GROWTH_TYPE_PRINT_WINDOW provides a print window
#  to control the amount of images created.
#  format:  <start_run>,<end_run>,<start_monte_carlo>,
#           <end_monte_carlo>,<start_year>,<end_year>
#  for example:
#  GROWTH_TYPE_PRINT_WINDOW=run1,run2,mc1,mc2,year1,year2
#  so images are only created when
#  run1<= current run <=run2 AND
#  mc1 <= current monte carlo <= mc2 AND
#  year1 <= currrent year <= year2
#
#  0 == first
VIEW_GROWTH_TYPES(YES/NO)=NO
GROWTH_TYPE_PRINT_WINDOW=0,0,0,0,1995,2020
PHASE0G_GROWTH_COLOR=  0xff0000 # seed urban area
PHASE1G_GROWTH_COLOR=  0X00ff00 # diffusion growth
PHASE2G_GROWTH_COLOR=  0X0000ff # NOT USED
PHASE3G_GROWTH_COLOR=  0Xffff00 # breed growth
```

```
PHASE4G_GROWTH_COLOR=  0Xffffff # spread growth
PHASE5G_GROWTH_COLOR=  0X00ffff # road influenced growth

#*************************************************************
#
#  E. DELTATRON AGING SECTION
#
#  From here you can control the output of the deltatron grid
#  just before they are aged
#
#  VIEW_DELTATRON_AGING(YES/NO) provides an on/off
#  toggle to control whether the images are generated.
#
#  DELTATRON_PRINT_WINDOW provides a print window
#  to control the amount of images created.
#  format:  <start_run>,<end_run>,<start_monte_carlo>,
#           <end_monte_carlo>,<start_year>,<end_year>
#  for example:
#  DELTATRON_PRINT_WINDOW=run1,run2,mc1,mc2,year1,year2
#  so images are only created when
#  run1<= current run <=run2 AND
#  mc1 <= current monte carlo <= mc2 AND
#  year1 <= currrent year <= year2
#
#  0 == first
VIEW_DELTATRON_AGING(YES/NO)=NO
DELTATRON_PRINT_WINDOW=0,0,0,0,1930,2020
DELTATRON_COLOR=  0x000000 # index 0 No or dead deltatron
DELTATRON_COLOR=  0X00FF00 # index 1 age = 1 year
DELTATRON_COLOR=  0X00D200 # index 2 age = 2 year
DELTATRON_COLOR=  0X00AA00 # index 3 age = 3 year
DELTATRON_COLOR=  0X008200 # index 4 age = 4 year
DELTATRON_COLOR=  0X005A00 # index 5 age = 5 year

# XIII. SELF-MODIFICATION PARAMETERS
#      SLEUTH is a self-modifying cellular automata. For more
#      information see our PROJECT GIGALOPOLIS web site
#      (www.ncgia.ucsb.edu/project/gig/About/abGrowth.htm)
#      and publications (and/or grep 'self modification' in code).
ROAD_GRAV_SENSITIVITY=0.01
SLOPE_SENSITIVITY=0.1
```

```
CRITICAL_LOW=0.97
CRITICAL_HIGH=1.3
#CRITICAL_LOW=0.0
#CRITICAL_HIGH=10000000000000.0
CRITICAL_SLOPE=21.0
BOOM=1.01
BUST=0.9
```

3. SLEUTH's scenario file (final calibration)

```
# FILE: 'scenario file' for SLEUTH land cover transition model
#       (UGM  v3.0)
#       Comments start with #
#
#   I. Path Name Variables
#  II. Running Status (Echo)
# III. Output ASCII Files
#  IV. Log File Preferences
#   V. Working Grids
#  VI. Random Number Seed
# VII. Monte Carlo Iteration
#VIII. Coefficients
#      A. Coefficients and Growth Types
#      B. Modes and Coefficient Settings
#  IX. Prediction Date Range
#   X. Input Images
#  XI. Output Images
# XII. Colortable Settings
#      A. Date_Color
#      B. Non-Landuse Colortable
#      C. Land Cover Colortable
#      D. Growth Type Images
#      E. Deltatron Images
#XIII. Self Modification Parameters

# I.PATH NAME VARIABLES
#   INPUT_DIR: relative or absolute path where input image files and
#              (if modeling land cover) 'landuse.classes' file are
#              located.
#   OUTPUT_DIR: relative or absolute path where all output files will
```

```
#             be located.
#   WHIRLGIF_BINARY: relative path to 'whirlgif' gif animation program.
#                 These must be compiled before execution.
INPUT_DIR=../Input/final_data30/
OUTPUT_DIR=../Output/data30_cal/
WHIRLGIF_BINARY=../Whirlgif/whirlgif

# II. RUNNING STATUS (ECHO)
#  Status of model run, monte carlo iteration, and year will be
#  printed to the screen during model execution.
ECHO(YES/NO)=yes

# III. Output Files
#  INDICATE TYPES OF ASCII DATA FILES TO BE WRITTEN TO
OUTPUT_DIRECTORY.
#
#   COEFF_FILE: contains coefficient values for every run, monte carlo
#             iteration and year.
#   AVG_FILE: contains measured values of simulated data averaged over
#           monte carlo iterations for every run and control year.
#   STD_DEV_FILE: contains standard deviation of averaged values
#               in the AVG_FILE.
#   MEMORY_MAP: logs memory map to file 'memory.log'
#   LOGGING: will create a 'LOG_#' file where # signifies the processor
#           number that created the file if running code in parallel.
#           Otherwise, # will be 0. Contents of the LOG file may be
#           described below.
WRITE_COEFF_FILE(YES/NO)=no
WRITE_AVG_FILE(YES/NO)=no
WRITE_STD_DEV_FILE(YES/NO)=no
WRITE_MEMORY_MAP(YES/NO)=no
LOGGING(YES/NO)=YES

# IV. Log File Preferences
# INDICATE CONTENT OF LOG_# FILE (IF LOGGING == ON).
#   LANDCLASS_SUMMARY: (if landuse is being modeled) summary of input
#                   from 'landuse.classes' file
#   SLOPE_WEIGHTS(YES/NO): annual slope weight values as effected
#                       by slope_coeff
#   READS(YES/NO)= notes if a file is read in
#   WRITES(YES/NO)= notes if a file is written
```

```
#   COLORTABLES(YES/NO)= rgb lookup tables for all colortables generated
#   PROCESSING_STATUS(0:off/1:low verbosity/2:high verbosity)=
#   TRANSITION_MATRIX(YES/NO)= pixel count and annual probability of
#                       land class transitions
#     URBANIZATION_ATTEMPTS(YES/NO)= number of times an attempt to urbanize
#                           a pixel occurred
#   INITIAL_COEFFICIENTS(YES/NO)= initial coefficient values for
#                           each monte carlo
#   BASE_STATISTICS(YES/NO)= measurements of urban control year data
#   DEBUG(YES/NO)= data dump of igrid object and grid pointers
#   TIMINGS(0:off/1:low verbosity/2:high verbosity)= time spent within
#    each module. If running in parallel, LOG_0 will contain timing for
#    complete job.
LOG_LANDCLASS_SUMMARY(YES/NO)=yes
LOG_SLOPE_WEIGHTS(YES/NO)=no
LOG_READS(YES/NO)=no
LOG_WRITES(YES/NO)=no
LOG_COLORTABLES(YES/NO)=no
LOG_PROCESSING_STATUS(0:off/1:low verbosity/2:high verbosity)=1
LOG_TRANSITION_MATRIX(YES/NO)=no
LOG_URBANIZATION_ATTEMPTS(YES/NO)=no
LOG_INITIAL_COEFFICIENTS(YES/NO)=no
LOG_BASE_STATISTICS(YES/NO)=yes
LOG_DEBUG(YES/NO)= no
LOG_TIMINGS(0:off/1:low verbosity/2:high verbosity)=1

# V. WORKING GRIDS
# The number of working grids needed from memory during model execution is

# designated up front. This number may change depending upon modes. If
# NUM_WORKING_GRIDS needs to be increased, the execution will be exited
# and an error message will be written to the screen and to 'ERROR_LOG'
# in the OUTPUT_DIRECTORY. If the number may be decreased an optimal
# number will be written to the end of the LOG_0 file.
NUM_WORKING_GRIDS=4

# VI. RANDOM NUMBER SEED
# This number initializes the random number generator. This seed will be
# used to initialize each model run.
RANDOM_SEED=1
```

```
# VII. MONTE CARLO ITERATIONS
# Each model run may be completed in a monte carlo fashion.
#  For CALIBRATION or TEST mode measurements of simulated data will be
#  taken for years of known data, and averaged over the number of monte
#  carlo iterations. These averages are written to the AVG_FILE, and
#  the associated standard diviation is written to the STD_DEV_FILE.
#  The averaged values are compared to the known data, and a Pearson
#  correlation coefficient measure is calculated and written to the
#  control_stats.log file. The input per run may be associated across
#  files using the 'index' number in the files' first column.
#
MONTE_CARLO_ITERATIONS=10

# VIII. COEFFICIENTS
# The coefficients effect how the growth rules are applied to the data.
# Setting requirements:
#    *_START values >= *_STOP values
#    *_STEP values > 0
#   if no coefficient increment is desired:
#    *_START == *_STOP
#    *_STEP == 1
# For additional information about how these values affect simulated
# land cover change see our publications and PROJECT GIGALOPOLIS
#  site: (www.ncgia.ucsb.edu/project/gig/About/abGrowth.htm).
#  A. COEFFICIENTS AND GROWTH TYPES
#    DIFFUSION: affects SPONTANEOUS GROWTH and search distance along the
#              road network as part of ROAD INFLUENCED GROWTH.
#    BREED: NEW SPREADING CENTER probability and affects number of ROAD
#           INFLUENCED GROWTH attempts.
#    SPREAD: the probabilty of ORGANIC GROWTH from established urban
#            pixels occuring.
#    SLOPE_RESISTANCE: affects the influence of slope to urbanization. As
#                      value increases, the ability to urbanize
#                      ever steepening slopes decreases.
#    ROAD_GRAVITY: affects the outward distance from a selected pixel for
#                  which a road pixel will be searched for as part of
#                  ROAD INFLUENCED GROWTH.
#
#  B. MODES AND COEFFICIENT SETTINGS
#    TEST: TEST mode will perform a single run through the historical
```

```
#         data using the CALIBRATION_*_START values to initialize
#         growth, complete the MONTE_CARLO_ITERATIONS, and then conclude
#         execution. GIF images of the simulated urban growth will be
#         written to the OUTPUT_DIRECTORY.
#    CALIBRATE: CALIBRATE will perform monte carlo runs through the
#              historical data using every combination of the
#              coefficient values indicated. The CALIBRATION_*_START
#              coefficient values will initialize the first run. A
#              coefficient will then be increased by its *_STEP value,
#              and another run performed. This will be repeated for all
#              possible permutations of given ranges and increments.
#    PREDICTION: PREDICTION will perform a single run, in monte carlo
#               fashion, using the PREDICTION_*_BEST_FIT values
#               for initialization.

CALIBRATION_DIFFUSION_START= 1
CALIBRATION_DIFFUSION_STEP=  1
CALIBRATION_DIFFUSION_STOP=  5

CALIBRATION_BREED_START=     43
CALIBRATION_BREED_STEP=      1
CALIBRATION_BREED_STOP=      47

CALIBRATION_SPREAD_START=    1
CALIBRATION_SPREAD_STEP=     1
CALIBRATION_SPREAD_STOP=     5

CALIBRATION_SLOPE_START=     0
CALIBRATION_SLOPE_STEP=      25
CALIBRATION_SLOPE_STOP=      100

CALIBRATION_ROAD_START=      0
CALIBRATION_ROAD_STEP=       6
CALIBRATION_ROAD_STOP=       30

PREDICTION_DIFFUSION_BEST_FIT=  20
PREDICTION_BREED_BEST_FIT=  20
PREDICTION_SPREAD_BEST_FIT=  20
PREDICTION_SLOPE_BEST_FIT=  20
PREDICTION_ROAD_BEST_FIT=  20
```

```
# IX. PREDICTION DATE RANGE
# The urban and road images used to initialize growth during
# prediction are those with dates equal to, or greater than,
# the PREDICTION_START_DATE. If the PREDICTION_START_DATE is greater
# than any of the urban dates, the last urban file on the list will be
# used. Similarly, if the PREDICTION_START_DATE is greater
# than any of the road dates, the last road file on the list will be
# used. The prediction run will terminate at PREDICTION_STOP_DATE.
#
PREDICTION_START_DATE=1990
PREDICTION_STOP_DATE=2017

# X. INPUT IMAGES
# The model expects grayscale, GIF image files with file name
# format as described below. For more information see our
# PROJECT GIGALOPOLIS web site:
# (www.ncgia.ucsb.edu/project/gig/About/dtInput.htm).
#
# IF LAND COVER IS NOT BEING MODELED: Remove or comment out
# the LANDUSE_DATA data input flags below.
#
#   < >  = user selected fields
#  < > = optional fields
#
# Urban data GIFs
#  format:  <location>.urban.<date>.<user info>.gif
#
#
URBAN_DATA= data30.urban.1990.gif
URBAN_DATA= data30.urban.2000.gif
URBAN_DATA= data30.urban.2010.gif
URBAN_DATA= data30.urban.2017.gif
#
# Road data GIFs
#  format:  <location>.roads.<date>.<user info>.gif
#
ROAD_DATA= data30.roads.1990.gif
ROAD_DATA= data30.roads.2017.gif
#
# Landuse data GIFs
#  format:  <location>.landuse.<date>.<user info>.gif
```

```
#
#LANDUSE_DATA= data30.landuse.1990.gif
#LANDUSE_DATA= data30.landuse.2017.gif
#
# Excluded data GIF
#  format:  <location>.excluded.<user info>.gif
#
EXCLUDED_DATA= data30.excluded.gif
#
# Slope data GIF
#  format:  <location>.slope.<user info>.gif
#
SLOPE_DATA= data30.slope.gif
#
# Background data GIF
#  format:   <location>.hillshade.<user info>.gif
#
BACKGROUND_DATA= data30.hillshade.gif

# XI. OUTPUT IMAGES
#   WRITE_COLOR_KEY_IMAGES: Creates image maps of each colortable.
#                   File name format: 'key_type_COLORMAP'
#                   where type represents the colortable.
#   ECHO_IMAGE_FILES: Creates GIF of each input file used in that job.
#                 File names format: 'echo_of_input_filename'
#                 where input_filename represents the input name.
#   ANIMATION: if whirlgif has been compiled, and the WHIRLGIF_BINARY
#            path has been defined, animated gifs begining with the
#            file name 'animated' will be created in PREDICT mode.
WRITE_COLOR_KEY_IMAGES(YES/NO)=no
ECHO_IMAGE_FILES(YES/NO)=no
ANIMATION(YES/NO)= no

# XII. COLORTABLE SETTINGS
#  A. DATE COLOR SETTING
#     The date will automatically be placed in the lower left corner
#     of output images. DATE_COLOR may be designated in with red, green,
#     and blue values (format: <red_value, green_value, blue_value> )
#     or with hexadecimal begining with '0X' (format: <0X######> ).
#default DATE_COLOR= 0XFFFFFF white
DATE_COLOR=     0XFFFFFF #white
```

```
#  B. URBAN (NON-LANDUSE) COLORTABLE SETTINGS
#    1. URBAN MODE OUTPUTS
#       TEST mode: Annual images of simulated urban growth will be
#                  created using SEED_COLOR to indicate urbanized areas.

#       CALIBRATE mode: Images will not be created.
#       PREDICT mode: Annual probability images of simulated urban
#                  growth will be created using the PROBABILITY
#                  _COLORTABLE. The initializing urban data will be
#                  indicated by SEED_COLOR.
#
#    2. COLORTABLE SETTINGS
#       SEED_COLOR: initializing and extrapolated historic urban extent

#       WATER_COLOR: BACKGROUND_DATA is used as a backdrop for

#                  simulated urban growth. If pixels in this file
#                  contain the value zero (0), they will be filled
#                  with the color value in WATER_COLOR. In this way,
#                  major water bodies in a study area may be included
#                  in output images.
#SEED_COLOR= 0XFFFF00 #yellow
SEED_COLOR=  249, 209, 110 #pale yellow
#WATER_COLOR=  0X0000FF # blue
WATER_COLOR=  20, 52, 214 # royal blue

#    3. PROBABILITY COLORTABLE FOR URBAN GROWTH
#      For PREDICTION, annual probability images of urban growth
#      will be created using the monte carlo iterations. In these
#      images, the higher the value the more likely urbanizaion is.
#      In order to interpret these 'continuous' values more easily
#      they may be color classified by range.
#
#      If 'hex' is not present then the range is transparent.
#      The transparent range must be the first on the list.
#      The max number of entries is 100.
#       PROBABILITY_COLOR: a color value in hexadecimal that indicates
#                       a probability range.
#         low/upper: indicate the boundaries of the range.
#
```

```
#               low,  upper,   hex,  (Optional Name)
PROBABILITY_COLOR=   0,    50,        , #transparent
PROBABILITY_COLOR=   50,   60, 0X005A00, #0, 90,0 dark green
PROBABILITY_COLOR=   60,   70, 0X008200, #0,130,0
PROBABILITY_COLOR=   70,   80, 0X00AA00, #0,170,0
PROBABILITY_COLOR=   80,   90, 0X00D200, #0,210,0
PROBABILITY_COLOR=   90,   95, 0X00FF00, #0,255,0 light green
PROBABILITY_COLOR=   95,  100, 0X8B0000, #dark red

#  C. LAND COVER COLORTABLE
#  Land cover input images should be in grayscale GIF image format.
#  The 'pix' value indicates a land class grayscale pixel value in
#  the image. If desired, the model will create color classified
#  land cover output. The output colortable is designated by the
#  'hex/rgb' values.
#    pix: input land class pixel value
#    name: text string indicating land class
#    flag: special case land classes
#         URB - urban class (area is included in urban input data
#               and will not be transitioned by deltatron)
#         UNC - unclass (NODATA areas in image)
#         EXC - excluded (land class will be ignored by deltatron)
#    hex/rgb: hexidecimal or rgb (red, green, blue) output colors
#
#            pix, name,     flag,   hex/rgb, #comment
LANDUSE_CLASS=  0,  Unclass , UNC   , 0X000000
LANDUSE_CLASS=  1,  Urban   , URB   , 0X8b2323 #dark red
LANDUSE_CLASS=  2,  Agric   ,       , 0Xffec8b #pale yellow
LANDUSE_CLASS=  3,  Range   ,       , 0Xee9a49 #tan
LANDUSE_CLASS=  4,  Forest  ,       , 0X006400
LANDUSE_CLASS=  5,  Water   , EXC   , 0X104e8b
LANDUSE_CLASS=  6,  Wetland ,       , 0X483d8b
LANDUSE_CLASS=  7,  Barren  ,       , 0Xeec591

#  D. GROWTH TYPE IMAGE OUTPUT CONTROL AND COLORTABLE
#
#  From here you can control the output of the Z grid
#  (urban growth) just after it is returned from the spr_spread()
#  function. In this way it is possible to see the different types
#  of growth that have occured for a particular growth cycle.
#
```

```
#  VIEW_GROWTH_TYPES(YES/NO) provides an on/off
#  toggle to control whether the images are generated.
#
#  GROWTH_TYPE_PRINT_WINDOW provides a print window
#  to control the amount of images created.
#  format:  <start_run>,<end_run>,<start_monte_carlo>,
#         <end_monte_carlo>,<start_year>,<end_year>
#  for example:
#  GROWTH_TYPE_PRINT_WINDOW=run1,run2,mc1,mc2,year1,year2
#  so images are only created when
#  run1<= current run <=run2 AND
#  mc1 <= current monte carlo <= mc2 AND
#  year1 <= currrent year <= year2
#
#  0 == first
VIEW_GROWTH_TYPES(YES/NO)=NO
GROWTH_TYPE_PRINT_WINDOW=0,0,0,0,1995,2020
PHASE0G_GROWTH_COLOR=  0xff0000 # seed urban area
PHASE1G_GROWTH_COLOR=  0X00ff00 # diffusion growth
PHASE2G_GROWTH_COLOR=  0X0000ff # NOT USED
PHASE3G_GROWTH_COLOR=  0Xffff00 # breed growth
PHASE4G_GROWTH_COLOR=  0Xffffff # spread growth
PHASE5G_GROWTH_COLOR=  0X00ffff # road influenced growth

#*************************************************************
#
#  E. DELTATRON AGING SECTION
#
#  From here you can control the output of the deltatron grid
#  just before they are aged
#
#  VIEW_DELTATRON_AGING(YES/NO) provides an on/off
#  toggle to control whether the images are generated.
#
#  DELTATRON_PRINT_WINDOW provides a print window
#  to control the amount of images created.
#  format:  <start_run>,<end_run>,<start_monte_carlo>,
#         <end_monte_carlo>,<start_year>,<end_year>
#  for example:
#  DELTATRON_PRINT_WINDOW=run1,run2,mc1,mc2,year1,year2
#  so images are only created when
```

```
#  run1<= current run <=run2 AND
#  mc1 <= current monte carlo <= mc2 AND
#  year1 <= currrent year <= year2
#
#  0 == first
VIEW_DELTATRON_AGING(YES/NO)=NO
DELTATRON_PRINT_WINDOW=0,0,0,0,1930,2020
DELTATRON_COLOR=  0x000000 # index 0 No or dead deltatron
DELTATRON_COLOR=  0X00FF00 # index 1 age = 1 year
DELTATRON_COLOR=  0X00D200 # index 2 age = 2 year
DELTATRON_COLOR=  0X00AA00 # index 3 age = 3 year
DELTATRON_COLOR=  0X008200 # index 4 age = 4 year
DELTATRON_COLOR=  0X005A00 # index 5 age = 5 year

# XIII. SELF-MODIFICATION PARAMETERS
#       SLEUTH is a self-modifying cellular automata. For more
#       information see our PROJECT GIGALOPOLIS web site
#       (www.ncgia.ucsb.edu/project/gig/About/abGrowth.htm)
#       and publications (and/or grep 'self modification' in code).
ROAD_GRAV_SENSITIVITY=0.01
SLOPE_SENSITIVITY=0.1
CRITICAL_LOW=0.97
CRITICAL_HIGH=1.3
#CRITICAL_LOW=0.0
#CRITICAL_HIGH=10000000000000.0
CRITICAL_SLOPE=21.0
BOOM=1.01
BUST=0.9
```

APPENDIX B: SLEUTH installation and Implementation

SLEUTH is a Linux program and will not run as a program in Windows, so we need Cygwin, a Linux emulator, to be able to run SLEUTH model.

Step 1: Installation of Cygwin

- Go to the link https://cygwin.com/install.html to download the required Cygwin package versions and follow the installation notes.
- Some useful Cygwin commands to run the SLEUTH model
  - cd = Change directory (cd d:\ SLEUTH3.0beta_p01_linux)
  - cd.. = To move up one directory.
  - cd gd = Access to the growth model.
  - make clean = To clean the specific file directories.
  - make= Prepare the specific directory for model run.
  - cd Scenarios = This command will prompt to the Scenario files.
  - ls = To list all the scenario files.
  - .. /grow.exe (Test/Calibrate/Predict) = To run the model in different modes. **(**Example: ../grow.exe **test** scenario.demo30_test)

Step 2: Installation of SLEUTH model

- Download the SLEUTH files form http://www.ncgia.ucsb.edu/projects/gig/Dnload/download.htm
- You will find different types of SLEUTH model versions. Select the (SLEUTH3.0beta_p01 LINUX released 6/2005) libraries for Linux or Cygwin.
- Select the directory (C: / or D :/) to save the SLEUTH file package. (Example: D:\SLEUTH3.0beta_p01_linux)
- SLEUTH3.0beta_p01_linux\
  - Input\ This is where the input data is located.
  - Output\ This is where output from the SLEUTH calibration or predictions is save.

- Scenarios\ This is where SLEUTH stores the different scenario files.
- GD\ This is a folder for a program called GD that handles GIF image files
- Whirlgif\ This is a folder for a program called Whirlgif that handles GIF image files
- Other files with extension .o, .h, .c are the SLEUTH's program files required to run the model.

Step 3: Edit scenario files

Make sure that you are in the scenario file folder. Open the scenario file using the text editor (Notepad ++) that can save the output in UNIX or Linux format. Do not use word, Notepad, or WordPad to edit the scenario file. The scenario file is a simple text file where you can set the parameters to run the model. Though the structure may look complicated, we need to make only couple of changes to the scenario file. Need to check the following sections in the scenario file:

- **Section I: Path Name Variables**

  Make sure to specify the correct input and output directory names for different inputs and output files. (Example: If input file name is Test & Output file name is Test_output), we can set as;

  INPUT_DIR=../Input/Test/

  OUTPUT_DIR=../Output/Test_output/

- **Section VII: Monte Carlo Iteration**

  Each model run may be completed in a Monte Carlo iteration as per the calibration mode. We need to set this iteration for every model calibration and in prediction. Ideally, higher value of 100 Monte Carlo iteration is set for the model prediction. (See: http://www.ncgia.ucsb.edu/projects/gig/).

- **Section IX: Prediction date range**

  Need to set the prediction start date and stop date as our prediction range dates. (Example as shown below)

  PREDICTION_START_DATE=1990

  PREDICTION_STOP_DATE=2017

- **Section X: Input images**

  In this section, we have to input the correct naming format of the input data files in (gif) format which was created during data preparation. (Example as shown below);

  URBAN_DATA= demo30.urban.1990.gif

  ROAD_DATA= demo.roads.1990.gif

- **Section XIII: Self-modification parameters**

  Here we can set the critical slope value. By default the SLEUTH model take 21 as a critical slope value.

Example datasets (30m) – 875 x 611 (rows x columns)

demo30.excluded.gif

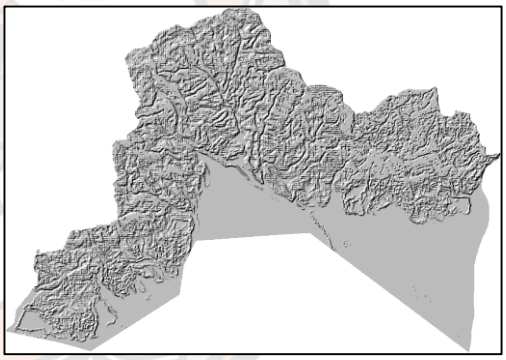

demo30.hillshade.gif

demo30.urban.1990.gif

demo30.urban.2000.gif

demo30.urban.2010.gif

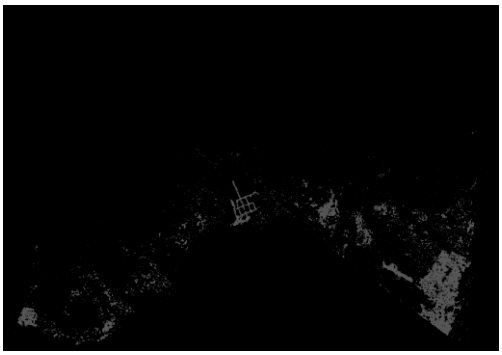

demo30.urban.1990.gif

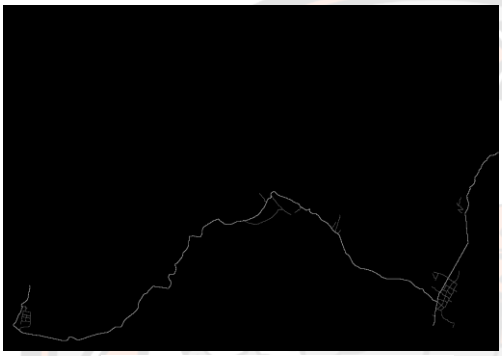

demo30.roads.1990.gif

demo30.roads.2017.gif

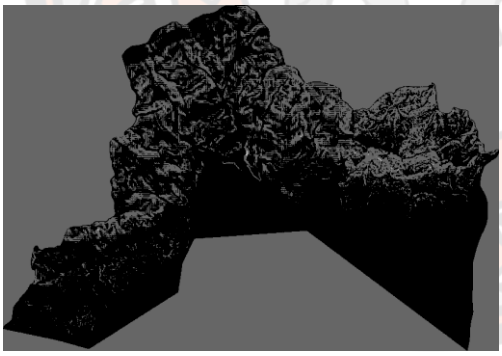

demo30.slope.gif